AN INSTRUMENTATION SYSTEM FOR THERAPEUTIC PREPULSE DELIVERY

AN INSTRUMENTATION SYSTEM FOR THERAPEUTIC PREPULSE DELIVERY

By

MICHAEL P. WILLAND, B.ENG

A Thesis

Submitted to the School of Graduate Studies

in Partial Fulfillment of the Requirements

for the Degree

Master of Applied Science

MASTER OF APPLIED SCIENCE (2008) McMaster University

(Biomedical Engineering) Hamilton, Ontario

TITLE: An Instrumentation System for Therapeutic Prepulse Delivery

AUTHOR: Michael P. Willand, B.Eng. (McMaster University)

SUPERVISOR: Dr. H. de Bruin

NUMBER OF PAGES:x, 107

Abstract

High amplitude electrical muscle stimulation has been known to cause pain and discomfort among those receiving long duration stimulation treatments to build muscle strength. Recently, the use of prepulses in sensory tactile stimulation has been shown to increase the pain threshold in human subjects. The use of prepulses in surface motor point stimulation has not been tested or published in the literature. However, typical electrical stimulator cannot output a prepulse and have limited recording capabilities.

This thesis presents the design and prototype of a novel muscle stimulator that can output any type of prepulse shape and duration. The system is fully computer controlled and provides muscle action potential recordings through a custom built electromyography amplifier. The system was tested with a series of single subject pilot studies that also looked at the merits of using ramped and rectangular prepulses during surface motor point stimulation.

The results show that both ramped and rectangular prepulses are effective at augmenting the M-wave response. By keeping the stimulus amplitude fixed, the prepulses elicited M-waves responses that had much larger peak to peak amplitudes than those elicited with the control stimulus (no prepulse). Those studies used a single stimulus to elicit a response. A pulse train experiment was also conducted. Clinically, pulse trains are used in a rehabilatory setting to build muscle strength. The pulse train experiment also showed that both ramped and rectangular prepulses are effective at augmenting the M-wave response. By lowering stimulus amplitude requirements, pain associated with high

amplitude stimulation may be reduced. Further studies that include multiple subjects should be carried out to evaluate the full merit of using prepulses for muscle stimulation.

Acknowledgements

Table of Contents

List of Figures

Chapter 1: Introduction

The use of electrical stimulation to build muscle has been in practice for decades. However, most patients complain about the discomfort associated with stimulation (Balogun, 1986). The main cause of this pain is the high amplitude stimulus used to elicit muscle contractions which also stimulates sensory axons. Also, when stimulating electrically, the motor nerve fibers are recruited in an opposite manner than when recruited physiologically (Henneman, Somjen, & Carpenter, 1965). That is, large fibers are recruited first when stimulating electrically (Fang & Mortimer, 1991a). In addition, when stimulating using surface electrodes, nerves closer to the electrode are depolarized first and these are cutaneous nerves that relay sensory information (Poletto & Van Doren, 2002).

In the last 20 years a number of studies have shown that reversing the order of neuron recruitment is possible when stimulating nerves electrically (Baratta et al., 1989; Deurloo, Holsheimer, & Bergveld, 2001; Fang & Mortimer, 1991b; Grill & Mortimer, 1997; Hennings, Arendt-Nielsen, & Andersen, 2005; Poletto & Van Doren, 2002; van Bolhuis, Holsheimer, & Savelberg, 2001). Most of these studies were carried out on the nerve itself using cuff electrodes which requires invasive surgery. However, two studies were carried out using surface stimulation. In one, only sensory fibers were stimulated and the researchers showed that they could inhibit the afferent pain fibers and increase the pain threshold (Poletto & Van Doren, 2002). In the other study, very long duration ramped stimuli were used to reverse the order of motor unit recruitment (Hennings, Arendt-

Nielsen, & Andersen, 2005). Both of these studies had in common the usage of depolarizing prepulses to either increase the pain threshold or reverse the order of neuron recruitment. We wanted to take these ideas and apply them to peripheral nerve stimulation to observe what effects prepulses would have on muscle recruitment.

The easiest way to test the usage of prepulses is to use a commercial muscle stimulator. However, typical stimulators are not able to deliver long duration ramped or rectangular prepulses and hence a new stimulator had to be designed and prototyped. Previous stimulator designs have been created for prepulse delivery, however, they were not suitable for our needs and further reinforced the fact that a new design was necessary (Poletto & Van Doren, 1999). What is also important is to have a recording or quantitative measure of the stimulating outcome. Certain clinical machines are built with electromyography (EMG) amplifiers which record the resulting muscle action potential (M-wave). Without relying on any commercial product and to keep the size of the design small, we set out to design and build an EMG amplifier.

As with any medical device, safety is very important. Most of all, isolation from the AC outlet is crucial. With this important fact, isolation of the stimulator needed to be factored into the design. As well, the stimulator output has to be isolated from the EMG amplifier input to avoid stimulus artifact and potential electronic damage.

This thesis outlines the design, development, and prototyping of a novel muscle stimulator that can deliver prepulses and record M-waves. A short pilot study was also conducted to look at the effects prepulses have on peripheral nerve stimulation. Varying prepulse durations and stimulus amplitudes were delivered and M-wave recordings were

made during each trial. A small investigation into pulse train stimulation was also carried out.

The chapters of the thesis are organized in the following manner: Chapter 2 provides background information on muscle structure and motor units. It also briefly covers electrical muscle stimulation and various methods used to achieve the reversal of the order of neuron recruitment. Chapter 3 describes the hardware development process from the design requirements to the design implementation. In Chapter 4, the results from the hardware testing of the stimulator are shown. As well, results from a small pilot study that was carried out is presented. Finally, Chapter 5 concludes the thesis by summarizing the work that was accomplished and provides a number of future directions and studies that can be carried out with this stimulator.

Chapter 2: Background

The purpose of this chapter is to outline the physiology of muscle from the microscopic level of individual muscle fibrils to the macroscopic level of muscle groups contracting. Furthermore, artificial contraction, or electrical stimulation of muscle, will be explained and therapeutic uses explored. As this thesis provides only a brief overview of the structure and physiology of muscle, more detail can be found by consulting a standard physiology text (Guyton & Hall, 2006).

2.1 Structure of Muscle

Three types of muscle exist in the human body: smooth, cardiac, and skeletal muscle. These muscle types primarily differ in terms of their morphology, location in the body, method of control and contractile mechanism. For this thesis, only skeletal muscle will be discussed as this type of muscle forms the structural basis of voluntary muscles and accounts for all major body movements.

2.1.1 Skeletal Muscle

Skeletal muscle is made up of thousands of smaller units called muscle fibers (Figure 2-1). Each fiber, also known as a myocyte, is multinucleated and contains bundles of filaments called myofibrils. These myofibrils are composed of longitudinally connected units called sarcomeres which are made of filaments that form the basis for muscle contraction. The filaments are further categorized into thick and thin. The thick filaments, called myosin, and the thin filaments, called actin, are arranged in an overlapping fashion

to allow a sliding movement when activated (Figure 2-2). During activation of a muscle, the thick filaments, or myosin heads, attach to the thin filaments and move along them, progressively pulling the thin filaments towards the center of the sarcomere or M line. When millions of these myofibrils shorten, they produce a summative effect and hence the macroscopic contraction that we see (Tortora & Grabowski, 2003).

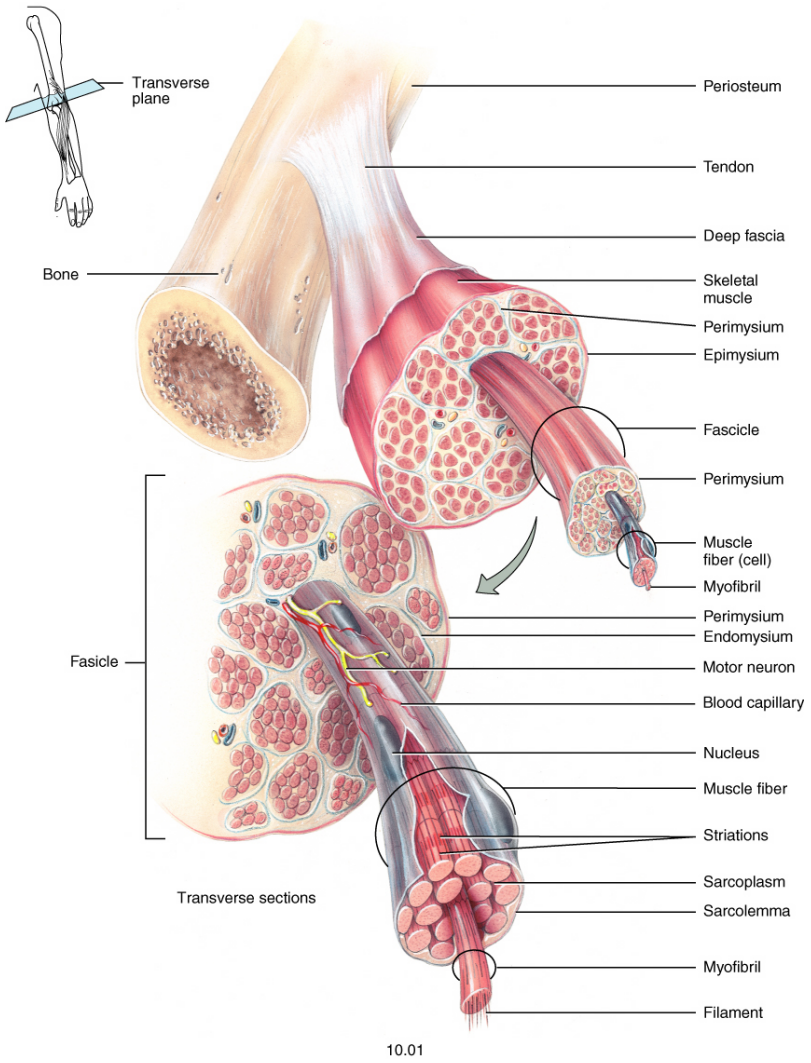

Figure 2-1 - Organization of skeletal muscle (Tortora & Grabowski, 2003)

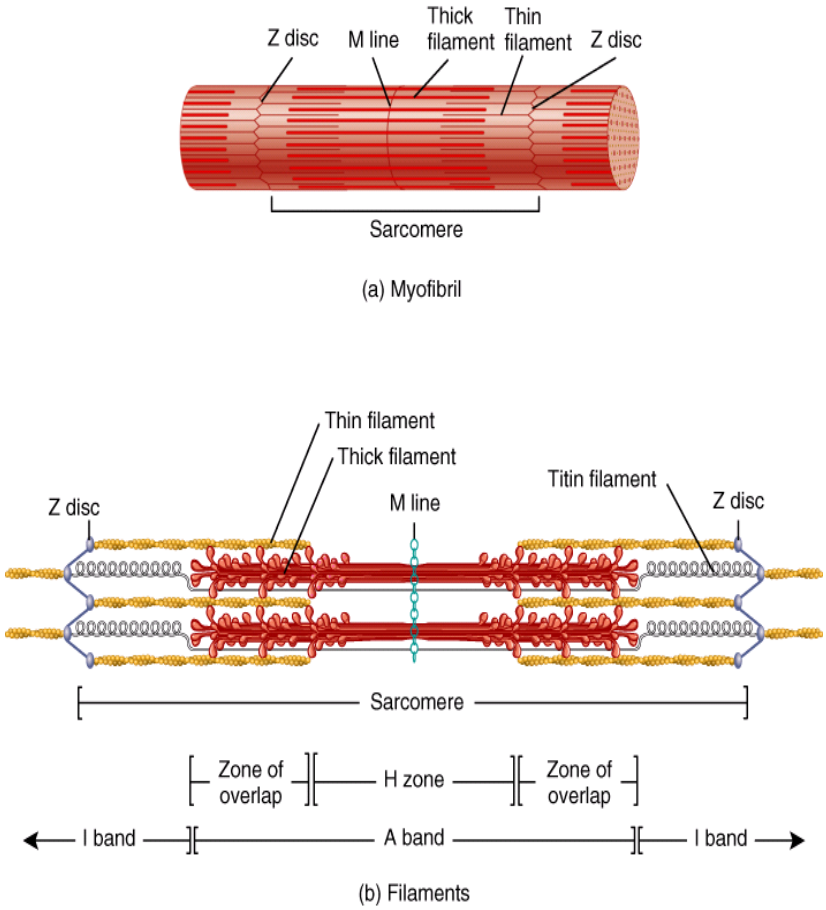

Figure 2-2 - The myofibril shown in a). A detailed illustration of the sarcomere shown in b). (Tortora & Grabowski, 2003)

2.1.2 The Motor Unit

Each motor neuron connects to a few or many muscle fibers, and it is this collective grouping that defines the motor unit. On average, a single motor neuron makes contact with approximately 150 muscle fibers that all contract simultaneously. The varying number of innervated muscle fibers largely depends on the function of the muscle. For example, motor units in the larynx only have as few as 2 to 3 muscle fibers associated with them. Motor units controlling eye movements have approximately 10 to 20 fibers,

and motor units in large muscles, such as the biceps, have as many as 2000 to 3000 fibers (Tortora & Grabowski, 2003). As the complexity or precision of the muscle action increases, the number of muscle fibers associated with each motor unit decreases. On the contrary, the larger the number of fibers associated with each motor unit, the greater the force that unit can produce. The muscle fibers in each unit are not only associated with that particular motor unit but also overlap to other units in bundles of 3 to 15 fibers. This allows separate motor units to contract in a collaborative effort rather than in an individualistic manner (Guyton & Hall, 2006).

Motor units and muscles in general can also be classified by their energy source. Muscles with a smaller amount of motor units, such as ocular muscles, tend to require rapid movements and primarily consist of fast-glycolytic (type-II) muscle fibers. These fibers are also innervated by large motor neurons. Type-II fibers contain an extensive sarcoplasmic reticulum to initiate rapid release of calcium ions for a fast contraction. Energy in these fibers is primarily supplied by glycolytic enzymes. This allows for very fast energy transfer rather than relying on mitochondria, myoglobin, and an extensive blood supply. This also makes the muscle appear white when observed under a microscope. Muscles with a large amount of motor units, such as the soleus muscle, are classified as Type-I, or slow-oxidative fibers. This muscle type has a much slower contraction time and is more fatigue resistant. The soleus in this case is used as a stabilizing muscle for the body against gravity. Type-II fibers are innervated by smaller motor neurons, have an extensive blood supply, and contain large amounts of mitochondria to continuously supply the muscle with energy. The fibers also contain a

protein called myoglobin. This protein binds and stores oxygen, greatly improving the speed of oxygen transport to the mitochondria. Myoglobin also accounts for the red colour of Type-II fibers. Figure 2-3 shows a comparison of the different contraction times for fast, slow, and a mixture of oxidative fibers.

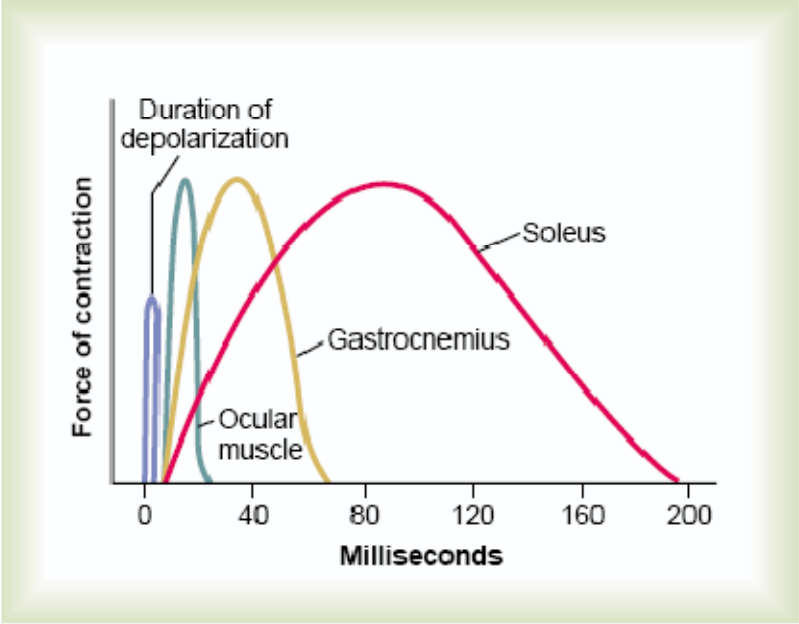

Figure 2-3 – Comparison of contraction times for fast fibers (ocular muscle), slow fibers (soleus), and fibers in between containing a mixture of both fast and slow fibers (gastrocnemius) (Guyton & Hall, 2006).

2.1.3 The Fiber Action Potential

A normal skeletal muscle contraction does not occur spontaneously. A signal, usually derived from the brain or spinal cord, is needed to activate the muscle and initiate a contraction. This signal is called the action potential. The action potential travels down a motor nerve axon until it reaches its endpoint, the neuromuscular junction. It is akin to an electrical signal travelling down a wire until it reaches its desired destination. At the

neuromuscular junction, the action potential is converted into a chemical signal via the use of neurotransmitters. These neurotransmitters are released from the end of the motor nerve axon, called the synaptic end bulb. The neurotransmitters are released into an area called the synaptic cleft and proceed to the other boundary called the motor end plate. The motor end plate, which is part of the muscle fiber, contains receptors on its surface to convert the chemical signal back into an electrical signal to allow the muscle to contract. This new electrical signal, or action potential, is rapidly spread throughout the muscle fiber by intricate pathways called T tubules. These tubules then pass the signal onto the contractile filaments. The T tubules are of critical importance since without them the action potential would not be able to produce a summative contraction (Tortora & Grabowski, 2003). Figure 2-4 illustrates the entire process.

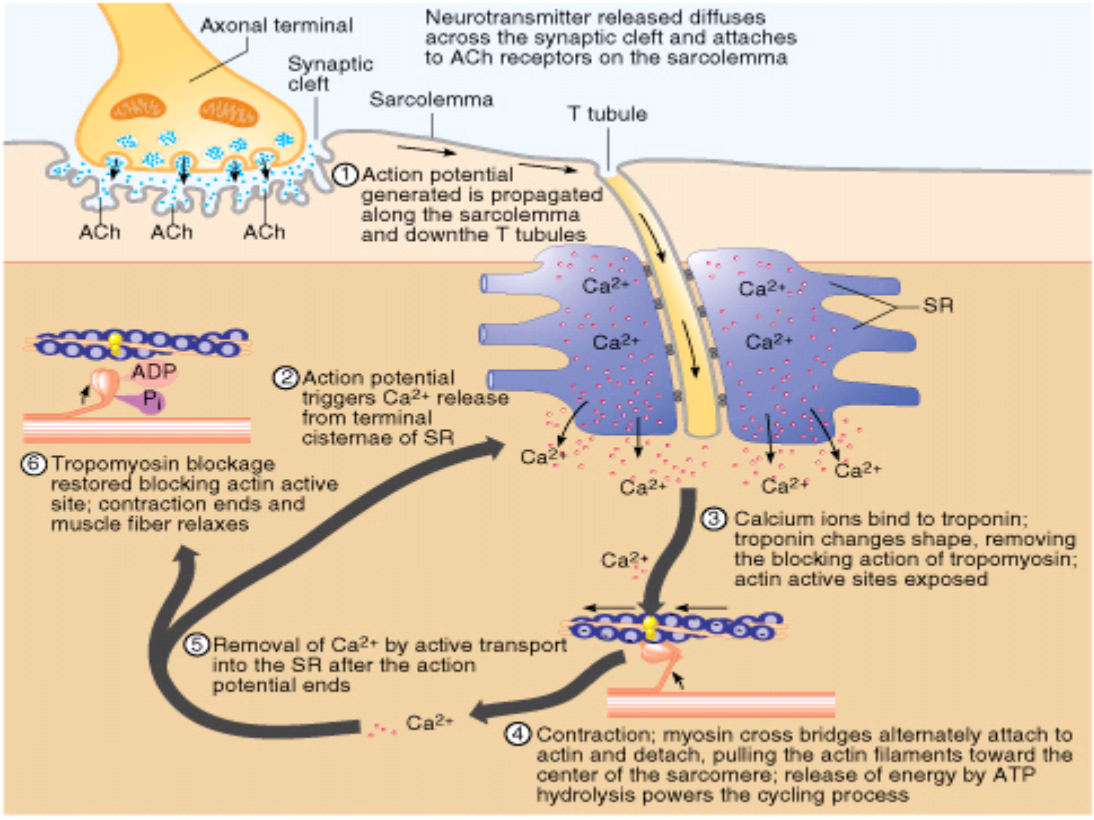

Figure 2-4 - The muscle contraction from start to finish (Tortora & Grabowski, 2003).

2.2 Muscle Force Production

When a single impulse from a motor neuron propagates to its neuromuscular junction, it causes a single muscle fiber action potential in all the muscle fibers with which it forms synapses. The resultant contraction from a single action potential produces a much smaller force, called a twitch, than the maximum force that the fiber is capable of producing. This is because the total force that the fiber can produce is directly related to the frequency of incoming action potentials. If we look at the contraction of an entire

muscle, the total force it can produce depends on the number of fibers contracting simultaneously (Tortora & Grabowski, 2003).

2.2.1 Twitch to Tetanic Contractions

Twitch contractions arise from a single action potential activating its motor unit. When the central nervous system outputs a weak signal to contract a muscle, the smaller motor units react first, producing a small twitch. As the signal becomes stronger, larger motor units are activated and thus an increase in force is observed - but this is still a twitch contraction. This phenomenon is known as the size principle, and it occurs because smaller motor units are driven by smaller motor neurons. In the spinal cord, smaller motor neurons are more excitable than larger ones and hence become activated earlier. However, the size principle only accounts for one of two summative effects that produce stronger muscle contractions. The second summative effect is called tetanization.

Tetanization is the effect of a muscle being rapidly stimulated. When a subsequent action potential arrives at the muscle, a new contraction occurs before the previous one has finished, thus increasing the strength of the contraction slightly. During a single twitch contraction, the series elastic components of the muscle dissipate most of the twitch force. These elastic components are found primarily in the tendons. Figure 2-5 shows that as the frequency of incoming stimuli increases, the contractions start to fuse and the entire muscle seems to undergo a smooth contraction. It is also evident that after a certain frequency, in this figure approximately 50-60 stimuli a second (Hz), the strength of the contraction does not increase further. This happens because enough calcium ions

are maintained in the muscle allowing a full contractile state to be maintained without any relaxation between the stimuli (Guyton & Hall, 2006).

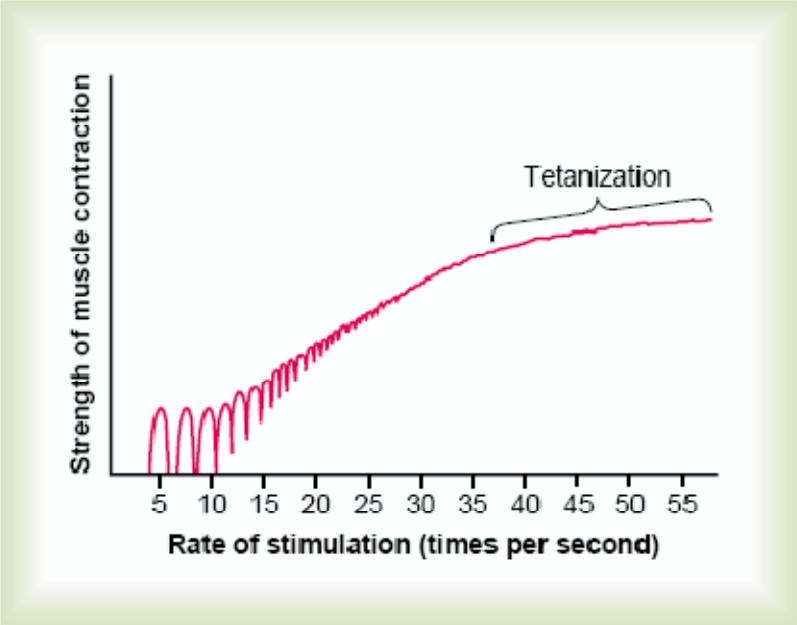

Figure 2-5 – Frequency summation and tetanization (Guyton & Hall, 2006)

The frequency that tetanization occurs depends on the type of muscle that is being stimulated. Postural muscles generally have longer twitch contraction times, from 40 to 200 milliseconds (ms). The individual motor units in postural muscles start to fuse at approximately 6 - 8 Hz. On the contrary, muscles used for movement which requires more speed or force, have much shorter twitch times, on the order of less than 35 ms to begin fusion (Nelson et al., 1999).

2.2.2 Regulation of Muscle Force

Typically, not all motor units are stimulated to contract simultaneously. When some motor units are contracting, others are relaxed. In isometric or slow contractions, motor

units are recruited asynchronously producing a smooth constant force at the tendon, resulting in individual motor unit firing rates much less than that required for tetanus. This allows a muscle to be active much longer by delaying fatigue and even allowing alternate contracting motor units to take over from one another. Activation of motor units occurs in a fixed pattern. Low force, slow and fatigue resistant units are activated first. These are called type S motor units. When demand for more force or for a quicker contraction is required, type F motor units are activated. What is interesting, is that when muscle is stimulated electrically – as discussed in the next section – type F motor units are recruited first followed by type S motor units (Nelson et al., 1999).

2.3 Electrical Stimulation of Muscle and Nerves

Electric stimulation of motor nerves is not a new idea. It has been used as a medical treatment over 2000 years ago when one of the first Roman physicians, Scribonius Largus, recommended the use of torpedo fish, which provide electric shocks, to treat such minor ailments as headaches and joint pain. It was not until 1791 when Luigi Galvani stimulated the nerve of a frog to contract its muscle that research into electrotherapy and its medical application took off (McNeal, 1977). Since then, numerous applications have been discovered for electrically stimulating tissue, some of which include: building muscle tissue (Banerjee, Caulfield, Crowe, & Clark, 2005), waking comatose patients (Cooper, Jane, Alves, & Cooper, 1999), allowing quadriplegics to use their hands (Prochazka, Gauthier, Wieler, & Kenwell, 1997), and improving blood supply to various tissues of the body (Dobsak et al., 2006).

Electrical stimulation of nerves typically targets the peripheral nervous system that includes both afferent sensory axons and efferent motor axons. The basic premise behind peripheral nerve stimulation is to create an electric field that will depolarize the nerve cell membranes. If the depolarization reaches a certain level, called the threshold, an action potential is generated that travels in both directions, towards the muscle, and towards the spinal cord. Similarly, when stimulating muscle directly, the depolarization occurs at the neuronal branches that end at the neuromuscular junction where the action potential directly spreads throughout the muscle. Larger axons have smaller thresholds than smaller axons when equidistant from the stimulus source. This is why when stimulating electrically, large diameter fibers tend to be recruited before small diameter fibers, the opposite of what happens physiologically (Nelson et al., 1999).

2.3.1 Stimulation Wave Shapes

The shape, duration, and frequency of the stimulus waveform play an important role in electrical stimulation. The response that a stimulus elicits is directly controlled by these parameters. Different wave shapes, shown in Figure 2-6, are used for a variety of electrotherapeutic applications.

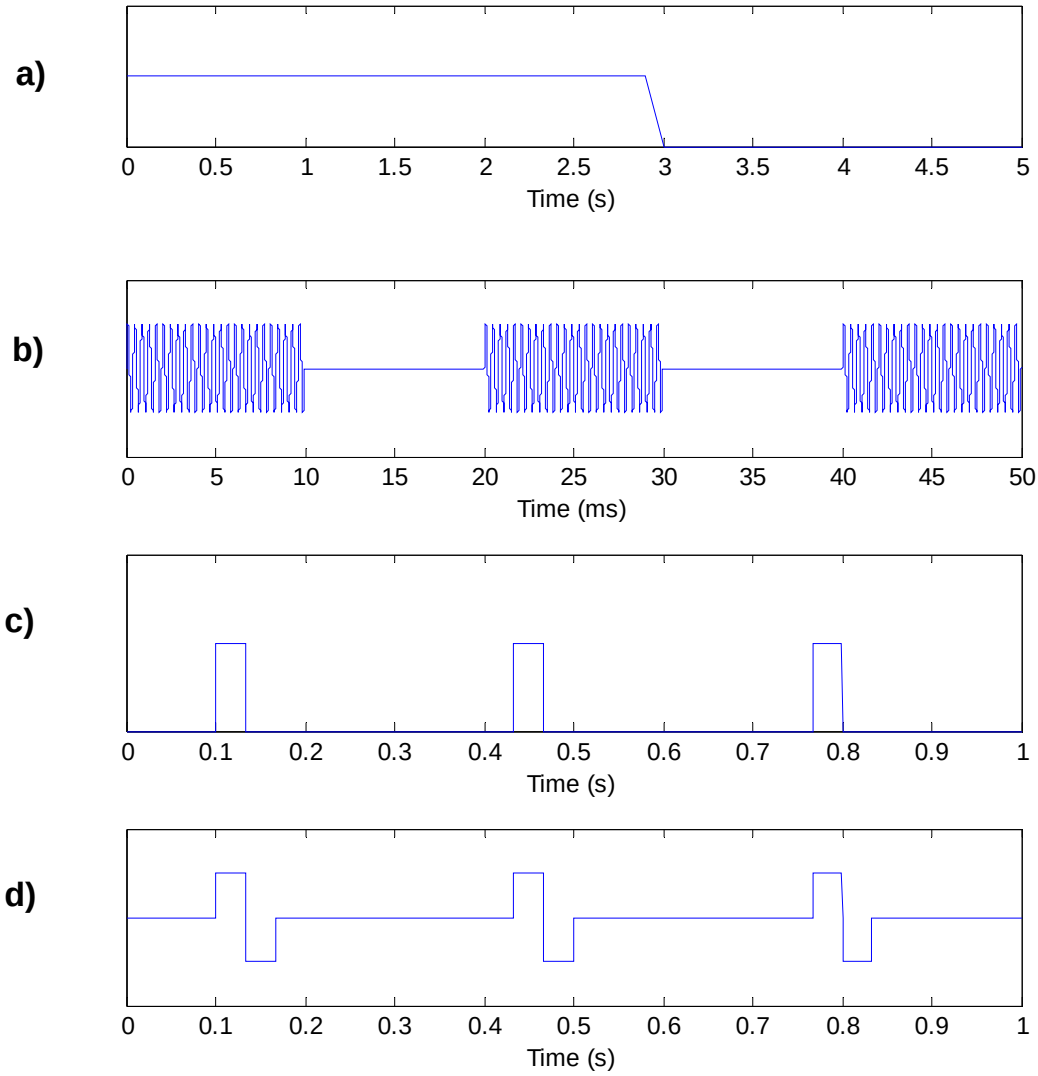

Figure 2-6 – A variety of stimulus waveforms. DC current shown in a), Russian current (2500 Hz bursts) shown in b), monophasic pulsed DC current shown in c), and biphasic pulsed DC current shown in d).

These waveforms can be placed into two categories, monophasic and biphasic, as shown in Figure 2-7.

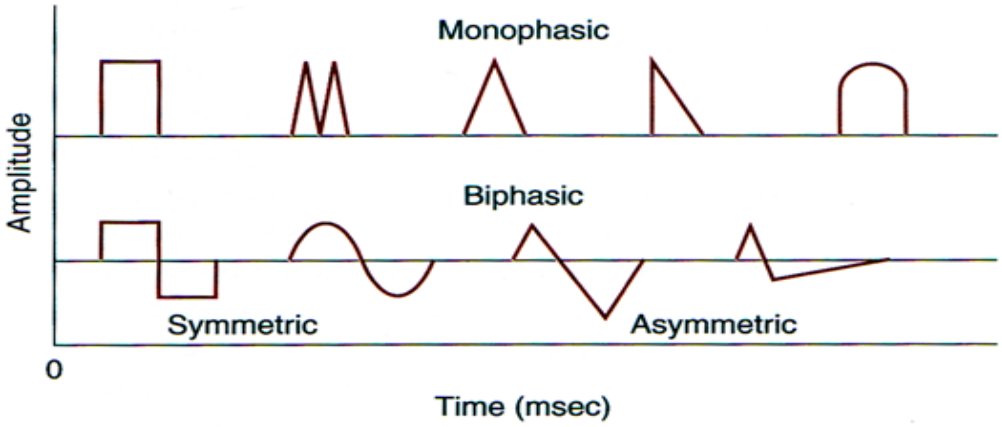

Figure 2-7 – Monophasic and biphasic pulses (Nelson, Hayes, & Currier, 1999).

DC waveforms, shown in Figure 2-6 a), where no change in polarity occurs, are used for treatment of excessive sweating or subcutaneous drug delivery. High frequency wave forms on the order of 2500 to 5000 Hz pulsed at 50 times per second or more are classified as Russian currents, shown in Figure 2-6 b). Russian currents have been used for regaining muscle force, improving joint range of motion and reducing chronic edema. Pulsed DC, or rectangular wave pulses, shown in Figure 2-6 c) and d), are typically used clinically to elicit muscle contractions. Their primary benefit over Russian currents is that significantly less current amplitude is needed to elicit the same level of contraction, making the stimulation more comfortable (Nelson et al., 1999).

In most applications of electrical nerve or muscle stimulation, the pulse duration, frequency, and amplitude are what control the level of muscular contraction. The amount of charge contained in each pulse depolarizes the nerve membrane and it is this value that

directly affects the production of a muscular twitch or contraction. Long duration pulses have a much higher charge level, and hence require lower amplitudes for contraction production but produce electrochemical effects, such as burning or electrode corrosion, at the electrode skin interface (Ward, 1980). In order to reduce these effects, an opposite polarity pulse is delivered to produce a zero net charge. This is especially used in nerve cuff stimulation to avoid charge buildup at the electrodes. The frequency of stimulation controls the contraction strength by combining successive twitch contractions into one fused long contraction. A frequency too low will cause a jerky movement of the stimulated muscle. The maximum effective frequency of stimulation is approximately 30-40 Hz. Pulses at higher frequencies than these would not have an effect on the depolarization of the membrane since the muscle fibers are fully fused and can produce no more force (Peckham & Knutson, 2005).

2.3.2 Pain Associated with Electrical Stimulation

When stimulating any type of peripheral nerve, recruitment or activation of various types of nerve fibers takes place. Because a nerve bundle contains both sensory and motor fibers, regular electrical stimulation of nerves would result in action potentials propagating in all the stimulated axons, both sensory and motor. Therefore, when the goal of electrical stimulation is to contract a muscle, painful or uncomfortable sensations usually accompany the stimulus (Nelson et al., 1999). However, various factors are involved in the perception of pain when stimulating nerves. A study published by Delitto et al (Delitto, Strube, Shulman, & Minor, 1992), states that perception of amplitudes, individual coping styles, and whether or not a muscle contraction was evoked, all play

important roles in pain and discomfort. The size of the electrode is also important. Smaller electrodes present a much higher resistance to a stimulator than larger electrodes do, and hence a higher voltage is needed for smaller electrodes to elicit the same level of contraction than when using a larger electrode (Alon, Kantor, & Ho, 1994).

2.3.3 Reversing the Order of Motor Unit Recruitment

Some interesting work has been published on the effect of reversing the order of neuron or motor unit recruitment when stimulating nerves electrically (Grill & Mortimer, 1997; Hennings, Arendt-Nielsen, & Andersen, 2005; Hennings, Arendt-Nielsen, Christensen, & Andersen, 2005; van Bolhuis et al., 2001). These studies showed that along with the reversal order in terms of size, neurons located distal from the electrode were recruited before neurons located close to the electrode. The strategies employed in these papers may be used to avoid recruitment of small pain fibers close to the electrode, thus limiting perceived pain associated with stimulation. There are a few techniques used to reverse the order of recruitment: direct current blocking and high frequency stimulation, anodal block and subthreshold prepulses.

Direct current blocking (Sassen & Zimmermann, 1973) and high-frequency stimulation (Baratta et al., 1989) both involve the use of a stimulating electrode pair and a blocking electrode pair. The idea behind this method is to have the blocking electrode pair, distal, or a short distance away from the stimulating pair. By delivering either a long DC stimulus or a burst of high frequency waves, different motor units can be blocked. Figure 2-8 shows the standard setup for both the stimulating electrode (FR) and the blocking electrode (R).

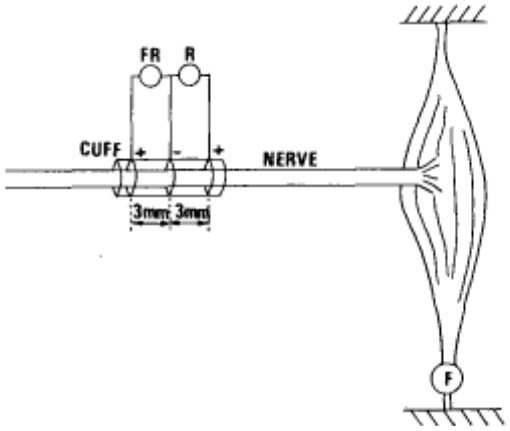

Figure 2-8 - Typical setup for tripolar cuff stimulation. FR is the stimulating electrode. R is the blocking electrode (Baratta, Ichie, Hwang, & Solomonow, 1989).

To control the recruitment, a depolarizing stimulus at suprathreshold amplitudes was used and its rate was also controlled, this constituted the firing rate stimulus. The recruitment or blocking stimulus consisted of a high frequency (600 Hz) amplitude modulated waveform. Initially, the recruitment stimulus is at suprathreshold amplitudes and no neurons are recruited. As the amplitude is decreased, smaller diameter neurons are recruited first. By ramping down the recruitment stimulus an orderly activation of neurons can take place. The use of high frequency stimulation waveforms was shown by Tanner to block muscle contraction (Tanner, 1962). Figure 2-9 shows the stimulus parameters employed by Baratta et al as described above.

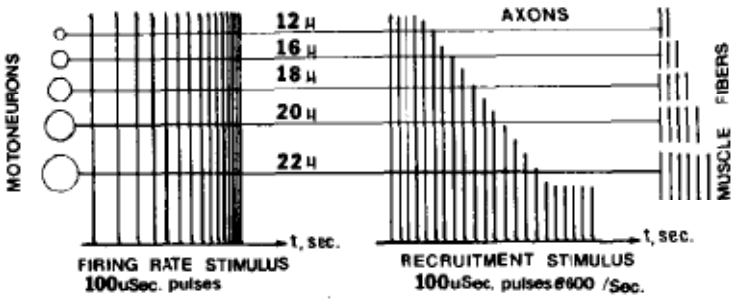

Figure 2-9 - Stimulating waveform, left, and blocking waveform, right (Baratta et al., 1989).

Anodal blocking is very similar to DC current and high frequency blocking. It involves hyperpolarization of the membrane to stop a propagating action potential but in this case, anodal blocking only utilizes a single tripolar cuff electrode (Fang & Mortimer, 1991a). Figure 2-10 shows the setup used for anodal blocking. The two anodes or positive terminals are connected and create an inward bound electric field when the stimulus is delivered.

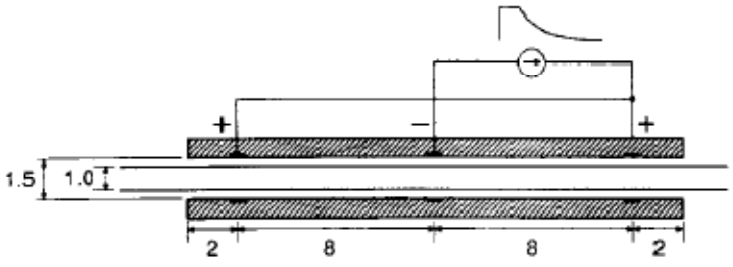

Figure 2-10 – Single tripolar cuff electrode. Dimensions are in millimeters. Quasitrapezoidal waveform intialliy hyperpolarizes the anodes (+) and the exponential decline allows smaller nerves to be recruited first. Waveform is shown on top of the electrode (Fang & Mortimer, 1991b).

The use of a quasitrapezoidal shaped stimulus pulse allows for the reversal of recruitment. This wave shape once again takes advantage of the fact that larger neurons have much lower firing thresholds and hence the initial high amplitude portion of the stimulus hyperpolarizes the membranes. This hyperpolarization is followed by an exponential trailing phase similar to the modulated high frequency wave form used by Baratta. The exponential phase is what selectively recruits smaller before larger neurons.

The techniques outlined above have been proven to selectively block neurons of various diameters, but the negative aspects of these methods are that they are highly invasive. The use of cuff electrodes requires surgery and is suitable for functional electrical stimulation (FES) of paralyzed muscle, but not for general muscle strengthening.

The last method to be discussed is the use of subthreshold prepulses. In this method, a long duration pulse, with an amplitude below firing threshold, precedes a short duration stimulus pulse. Published results have shown, both in theory and in practice, that the use of a subthreshold prepulse can inactivate fibers lying close to the electrode while maintaining excitability of nerve fibers distant from the stimulating electrode (Deurloo et al., 2001; Grill & Mortimer, 1997; Hennings, Arendt-Nielsen, & Andersen, 2005; van Bolhuis et al., 2001). It was hypothesized that fibers closest to the electrode had their sodium channels inactivated by the prepulse, putting the fibers into a refractory state (Grill & Mortimer, 1997). Subthreshold prepulses have also been used to increase the pain threshold in humans when stimulating sensory fibers in the distal periphery (Poletto & Van Doren, 2002). However, the results presented in this thesis show that prepulses

place the fibers much closer to their firing threshold and a subsequent short duration stimulus pulse can elicit the firing of the neuron. The amplitude of the stimulus pulse needed to elicit an action potential is much lower when preceded by a prepulse than when delivered on its own.

2.3.4 Strengthening Muscles using Electrical Stimulation

The use of electrical stimulation to build muscle strength is not new, and is an effective method for those individuals who have weak or atrophied muscle (Neder et al., 2002). It has also been shown to improve strength and aerobic capacity in normal individuals who do not have an active lifestyle (Banerjee et al., 2005). There are two protocols used for strengthening: stimulation of the peripheral nerve or stimulation of the muscle itself. The latter method is used more often as activation of both sensory and motor nerves takes place when stimulating in the periphery. However, when stimulating the muscle directly, the stimulating current dissipates, and only some of the motor axons are activated and not all muscle fibers will be recruited. Consequently, the maximum induced force is approximately 30-50% of an individual's maximum voluntary contraction (Lieber, Silva, & Daniel, 1996). Overall, when muscle is strongly stimulated electrically over a number of weeks, it provides many positive results, such as: an increase in muscle strength, fiber hypertrophy, and an increase in muscle cross-sectional diameter (Laufer, Ries, Leininger, & Alon, 2001; McMiken, Todd-Smith, & Thompson, 1983; Quittan et al., 1999).

Two methods exist to quantify the level of contraction: the muscle action potential or M-wave response, and mechanical force measurements (Nelson, Hayes, & Currier, 1999).

Mechanical force measurements are accomplished by placing a dynamometer or force transducer near the end of the joint. By varying the stimulation amplitude, a different force level can be produced and hence the level of contraction can be quantified.

The M-wave response is measured by placing electrodes directly on the muscle and observing the action potential following an electrical stimulus. Once all motor units are recruited the M-wave response is considered to be at a maximum level. Studies have shown that to build muscle strength using electrical stimulation, the intensity of the stimulus should elicit a contraction with at least 30 to 50 percent of the maximum force elicited by a voluntary contraction (Currier & Mann, 1983; Laughman, Youdas, Garrett, & Chao, 1983; Selkowitz, 1985).

Chapter 3: System Development

Clinical electrical stimulation devices have been around for quite some time. Devices specifically for stimulating nerves to elicit muscle contractions or obtain nerve conduction velocities are plentiful and typically found in physiotherapy and neurology clinics. However, these devices are very specifically designed in terms of what they can do. Some devices cannot change the shape of their pulses or only output a fixed set of pulse durations. Others do not include any means for observing the muscle response, either using a force transducer or looking at the M-wave. Most of all, these devices are proprietary and not open to modification.

In order to look at methods to decrease pain using prepulse inhibition techniques, we had to design and build a new stimulator that can output long duration prepulses and short but high intensity stimulus pulses. The stimulator also incorporates an electromyography (EMG) amplifier to observe muscle action potentials (M-waves). It also features extensive isolation without the need for a large isolation transformer, thus making the device smaller and more portable.

Custom written software has been designed to control the stimulator in both a pulse train and single stimulus fashion, and record and save M-wave responses.

This chapter outlines the design requirements, the approach we took to meet our requirements, and test results for our prototype.

3.1 System Design Requirements

A number of design requirements were needed before proceeding to the prototyping stage. These are high level requirements for our system to ensure flexible human testing and different research objectives.

1. Ability to output a pre stimulus pulse of various durations (at least 5 ms, maximum 500 ms) and amplitudes.
2. Ability to change the shape of the pre stimulus waveform.
3. Ability to select either pulse train output or single stimulus output and be able to control settings (amplitude, train frequency) of each.
4. Ability to monitor the level of stimulation using M-wave responses.
5. Ensure adequate isolation exists between patient and stimulator and between recording equipment and stimulator.
6. Ensure design is modular in the case future upgrades or changes need to be made
7. Ensure design is portable

3.1.1 Prepulse Output Requirements

The need to output a prepulse is essential in order to test the hypothesis of pain reduction during electrical stimulation. As mentioned in the previous chapter, subthreshold prepulses have been used to increase the pain threshold in humans when stimulating sensory fibers (Poletto & Van Doren, 2002). However, the shape of the prepulse has been debated (Hennings, Arendt-Nielsen, & Andersen, 2005), and we chose to implement both rectangular and ramped prepulses. The duration of the prepulse for

maximal inhibition is also highly debated and not well established. Various durations, from 5 ms up to 500 ms, have been used to change the order of motor unit recruitment (Grill & Mortimer, 1997; Hennings, Arendt-Nielsen, & Andersen, 2005; van Bolhuis et al., 2001). The reason for these various durations is that the amplitudes used in each study varied. For long duration prepulses, very low amplitudes were used. For shorter duration prepulses much higher amplitudes were used. This follows the strength duration curve, where longer but lower amplitude stimuli can elicit the same axonal excitation that shorter but higher amplitude stimuli can. In order to test the various parameters used, we designed our stimulator to output prepulses ranging from zero to a maximum of 1 second.

3.1.2 Stimulus Control Requirements

The control of the stimulus output would be handled by software routines written in LabVIEW. These routines would control the various parameters such as prepulse and stimulus amplitudes and durations, train or single stimulus settings and wave shapes.

3.1.3 M-Wave Recording Requirements

To observe the M-waves elicited by electrical stimulation, two approaches can be taken. The first, is to use an existing commercial EMG amplifier. The second is to design our own amplifier. While using an existing amplifier is an easy solution, these amplifiers are usually part of a larger system, both in size and complexity, and have general purpose filters. To meet our last requirement, portable design, we would have to design our own amplifier.

The normal EMG signal frequency range is from approximately 10 Hz to 4 KHz but when using surface electrodes to measure the response, the signal rarely has frequency components above 500 Hz (Kamen & Caldwell, 1996). Given these numbers, we would band limit our amplifier to approximately 500 Hz.

Typical EMG amplifiers have variable gain controls and this is something that we kept in mind. With EMG signals being in the microvolt to millivolt range, we decided on having the following gains: 250, 500, 1000, 1500, and 2000. This would span a much larger range than is required for EMG signals but gives us flexibility in the case that higher gains are required.

3.1.4 Isolation Requirements

The purpose of isolation is to ensure that there are no common current paths or loops. Methods of isolation include the use of light, radio waves, and magnet coupling (Prutchi & Norris, 2005). Our system needs to be isolated on a number of fronts. First, the stimulator must be isolated from the patient. We satisfy this requirement by using DC/DC converters with built in isolation to provide the high stimulation voltage. We also need to protect our recording equipment and isolate the EMG amplifier from the stimulator. To isolate the EMG amplifier, the use of mini DC/DC converters to supply power to the circuit will be used. However, if the output of the EMG amplifier is directly connected to a computer for recording, it would reference the EMG circuit to ground since the computer itself is not isolated. To accommodate for this, an isolation amplifier is placed on the output of the EMG amplifier circuit. The control stimulus is also isolated from the computer via the use of an opto-isolator circuit.

3.2 Hardware Design Implementation

Before an overall system design could be developed, the stimulator output type had to be chosen to be either of the constant voltage or constant current variety.

Constant voltage stimulators are very easy to implement as they are primarily based on transformer circuit designs. Figure 3-1 shows a typical transformer output circuit used for low rate, high energy stimulations such as cardiac defibrillation.

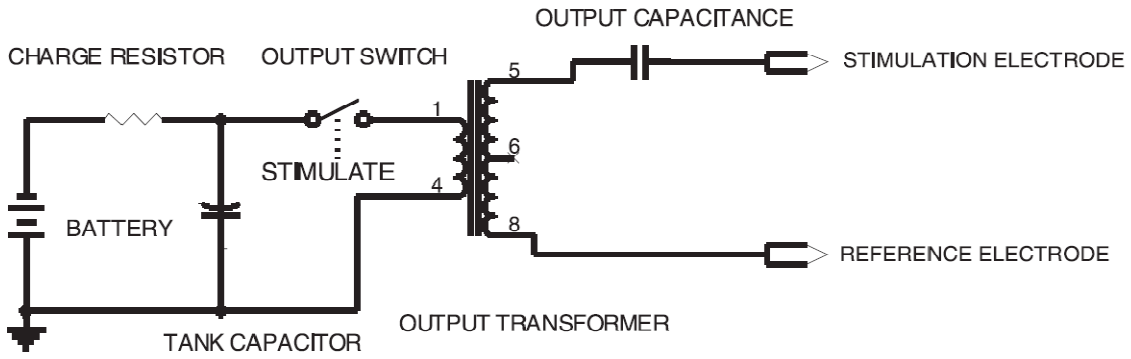

Figure 3-1 – Typical transformer output stimulation circuit (Prutchi & Norris, 2005)

A battery charges a capacitor to a desired level and when an output switch is pressed, the capacitor discharges through an output transformer. The output transformer must have step up ratios so that the voltage that is delivered to the electrodes is high enough to stimulate the tissue. The problem with this type of stimulator is that a constant voltage output will not always produce a constant response in the patient. Variables such as skin impedance, electrode size, and electrode positioning may alter the response over time. To rectify one of these problems, self adhesive electrodes can be used. This would ensure that electrode positioning is maintained over time. However, skin impedance will still

change over time. To counter this problem, the output of the stimulator must be changed to a constant current type.

Constant current stimulators, as the name suggests, provide a constant current regardless of the load impedance. There is one limitation however, and it is the maximum voltage the constant current source can supply. This is known as the compliance voltage (Horowitz & Hill, 1989). From Ohms law, the compliance voltage would set the impedance range that the stimulator can function over. The maximum current that the stimulator can output would be 100 mA (FDA regulation). A compliance voltage of 200 V would then allow us to maintain maximum stimulation levels at impedances below 2 KΩ.

Many constant current designs exist but not all are designed to deliver current at levels up to 100 mA. The major design for constant current sources comes from a voltage to current converter. The simplest design comes from an op-amp based voltage to current converter as shown in Figure 3-2.

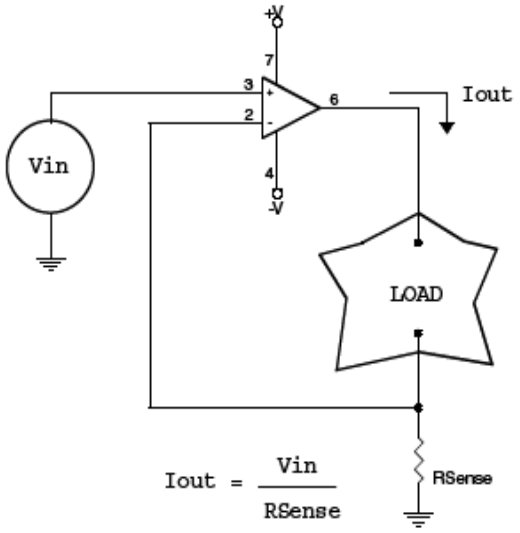

Figure 3-2 – Simple op-amp based voltage to current converter (Prutchi & Norris, 2005)

The output waveform is a current representation of the input voltage waveform. In this simple design the load is floated – not connected to ground – as this offers the optimal performance for constant current sources (Prutchi & Norris, 2005). Another design topology is the Howland current pump, as shown in Figure 3-3.

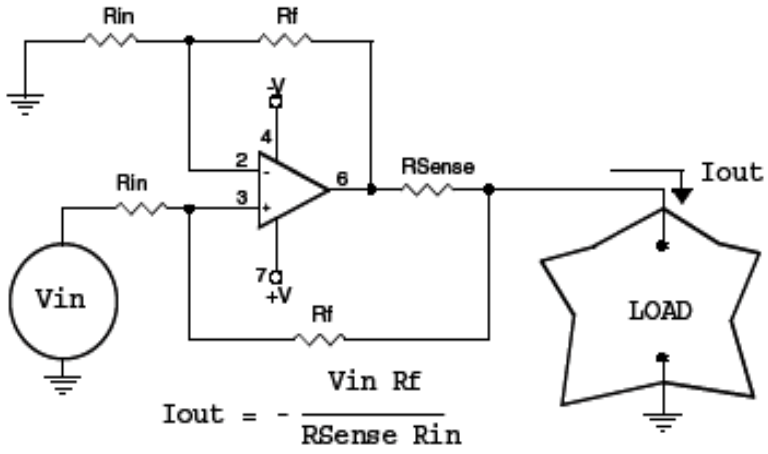

Figure 3-3 – Howland current pump implementation (Prutchi & Norris, 2005)

The problem with both of these implementations is that the voltage compliance is limited by power supply voltages for the op amps. For high stimulation currents in resistive loads of 1 KΩ, these power supply voltages must be at least 100V. This would dictate the op-amps be of high voltage variety.

Another output stage is the op-amp bridge as shown in Figure 3-4. By connecting the op-amps in a bridge configuration, the output voltage swings are twice that of one op-amp. This makes it possible to increase the compliance voltage of stimulation especially if previous designs had their op-amps operating near their maximum levels. However, the use of high stimulation currents once again limits the usage of normal op-amps and calls for the high voltage variety. It is actually this type of design that Poletto and van Doren used in their studies on increasing pain thresholds in humans (Poletto & Van Doren, 1999). Although this design works well, high voltage operational amplifiers are very costly and hence we did not pursue this type of design.

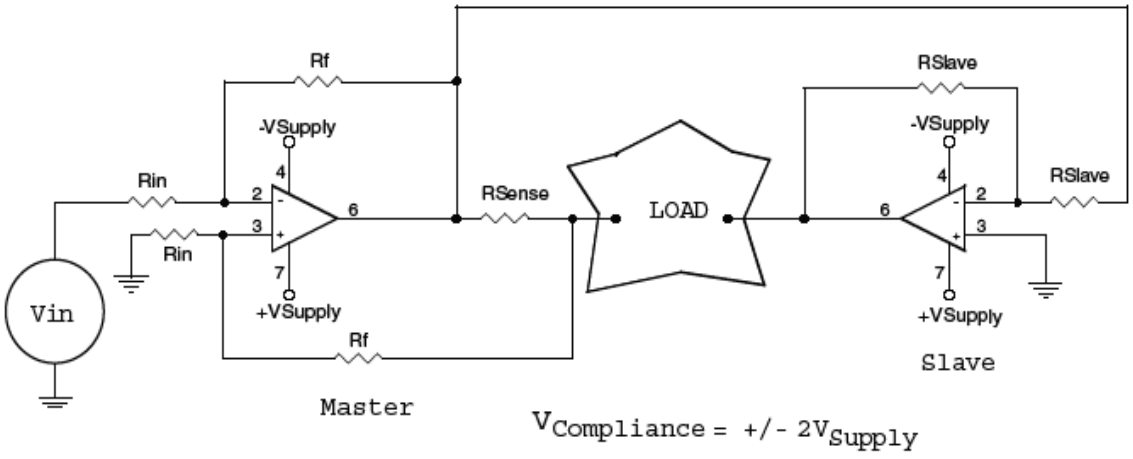

Figure 3-4 – Op-amp bridge design based on modified Howland current pump (Prutchi & Norris, 2005)

Transistor based current sources have also been used quite frequently, especially at the microelectronic level where very small currents, on the order of microamperes, are needed. Figure 3-5 shows a typical transistor current source.

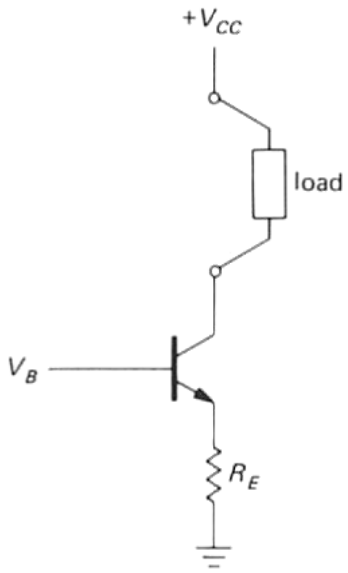

Figure 3-5 – Transistor based current source (Horowitz & Hill, 1989)

When a voltage greater than 0.6 is applied to V_B it causes a current to flow from V_{CC} down through the load, the transistor, R_E and out to ground. The current that flows through the load is known as the collector current of the transistor, or I_C, and its magnitude is approximately equal to $(V_B - 0.6) / R_E$. Since there is no feedback circuitry to monitor the output current a few problems arise and need to be discussed. First, the output current varies with temperature. The current gain, or β value of the transistor, along with the base-emitter voltage (V_{BE}) vary with temperature. Typically V_{BE} varies approximately 2 mV/°C (Horowitz & Hill, 1989). To address this issue, a simple modification of the above circuit is needed. By placing an op-amp before the base of the

transistor, as shown in Figure 3-6, and connecting a feedback line, detrimental effects due to varying base-emitter voltages can be eliminated. The output current is then equal to the input voltage, V_{IN}, divided by the sense resistor. A minor error is present due to the small base current but in our case is negligible with the high currents we will be using. It is this simple design that we utilized for our constant current output stage.

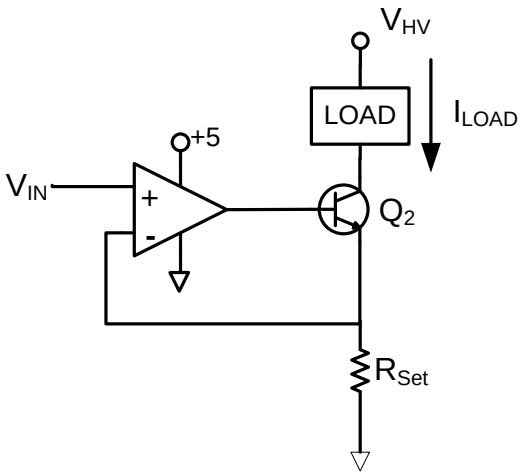

Figure 3-6 – Constant current source used in stimulator design

3.2.1 Overall System Design

With the stimulator output type chosen, an overall system design could be put together. The system is split up into a number of modules in case future upgrades need to be made. Figure 3-7 depicts a block diagram view of our system design. The goal of our design is to implement a single channel and have the stimulator ready for future modification when more channels can be added with ease. The next few sections will detail the design of each module.

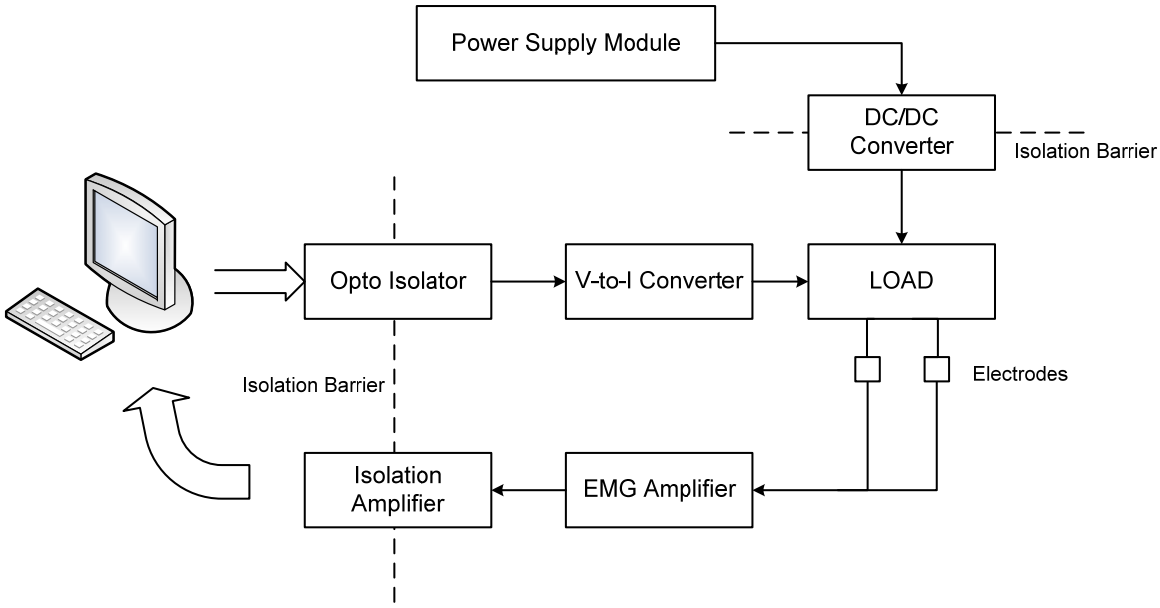

Figure 3-7 - Overall system design block diagram

3.2.2 Power Supply Module and DC/DC Converter

The power supply module provides power to each separate module in the system and hence had to be selected according to the total power that the rest of the system demands. The module that requires the most power is the DC/DC converter. The DC/DC converter takes in a DC voltage and steps it up to a desired high voltage level. Details on how DC/DC converters work can be found in various electronic design textbooks. Our required output voltage was 200 V. To calculate the maximum power that the DC/DC converter would require we needed to set some constraints on our stimulus output parameters. The highest amplitude stimulus we would output would be 100 mA at a maximum duration of 200 microseconds. Maximum power would be drawn during pulse train stimulation where a maximum of 30 pulses per second can be delivered. The

formula for calculating power output is given by $P = VI\left(\frac{PW}{\tau}\right)$, where V is the voltage, I is the current, PW is the pulse width , and τ is the period of stimulation. Putting in the values for our stimulus pulse we obtain a power output of 0.12 W. With such short duration pulses it is not surprising that the power output is minimal. On the other hand, the prepulse with its long duration will consume considerably more power. A 500 ms prepulse delivered 2 times a second with a maximum amplitude of 25 mA (more than enough to elicit a strong contraction) will consume 5 watts of power. However, typical prepulse durations if used to elicit muscle contractions in the 20-30 Hz range would be from 5-20 ms. At 20 ms, 30 Hz, and 25 mA of stimulus current, the power consumption would be 3 W. Adding the stimulus pulse power we have a combined power output of 3.12 W. Adding a small safety margin, we can safely assume that a 4 W DC/DC converter will meet our requirements. If we assume that the remainder of the circuitry (consisting of op-amps and transistors) consumes no more than a few watts, we can approximate our total power consumption per channel at 6 W. Rounding each channel to 10 W allows us to add any extra circuitry without worrying about excessive power being drawn. Therefore, our power supply module must supply at least 10 W of power per channel. To allow for extra channels in the future, we chose to use a 60 W medical grade power supply. Medical grade power supplies are tested and certified to meet medical standards for leakage currents.

3.2.3 Voltage to Current Converter

The heart of the stimulator is the voltage to current converter. This module provides the constant current that is used to stimulate the tissue. As mentioned previously, the constant current source we chose is based on an op-amp transistor design. However, we modified the design slightly to provide an added safety measure as shown in Figure 3-8. On the high end we added a gating transistor controlled by an optocoupler. This transistor would prevent any stray currents from passing through the patient when the stimulator output is set to zero.

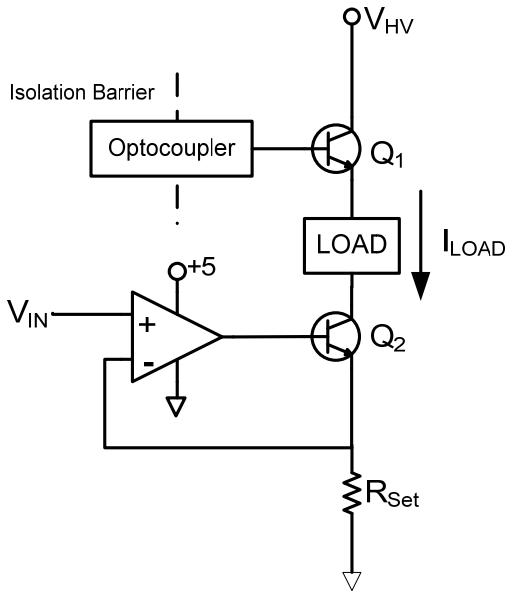

Figure 3-8 – Voltage to current converter with high end gating

3.2.4 Electromyography Amplifier

To record the M-wave responses a custom designed EMG amplifier was developed. Figure 3-9 shows a block diagram outline of this module. An input signal is first provided

to the instrumentation amplifier (INA 126) with a gain of 10. Keeping this first stage at low gain helps eliminate unwanted noise levels. Subsequent gain stages are used to further amplify the signal for processing in an analog to digital converter. The second stage is a passive high pass filter with a cutoff of 1.6 Hz. This is used to eliminate any DC offsets that might be present in the signal. EMG signals do not have valuable information at DC levels and hence these are removed with passive filtering (Prutchi & Norris, 2005). The third stage is an active low pass filter (LM358). This filter sets our desired bandwidth with a cutoff frequency of 500 Hz. This stage also gains our signal by 10 providing a total gain of 100 before being passed into our final gain stage. The last stage is a simple non-inverting op-amp configured to provide variable gains. Overall output gains of 250, 500, 1000, 1500, and 2000 were chosen.

The power for the EMG module is supplied by a mini Texas Instruments DC/DC converter (DCH010505DP) which is powered by the power supply module. This DC/DC converter receives a 5 V input and converts it to a ± 5 V signal. Since EMG signals are bipolar, a negative voltage was needed for the op-amps. The DC/DC converter also provides inherent isolation from other circuitry in the system. However, when the output of the EMG module is connected to a computer based data acquisition device, the ground plane in the EMG circuit would be referenced to the ground plane in the computer and hence isolation would be broken. To truly make this EMG module a standalone completely isolated device, one more form of isolation was needed on the output. This is provided by a mini isolation amplifier (AD202) that isolates the output EMG signal from the data acquisition device. The AD202 requires +15V to operate and this higher voltage

is derived from another mini DC/DC converter (DCH010515). However, the input and output ground pins are connected on this DC/DC converter, thus removing the inherent isolation. The AD202 provides its own isolated power supply; hence the DC/DC converter is not used to provide isolation, but is only used to boost the voltage from +5V to +15V. A complete circuit schematic can be found in Figure A- 3.

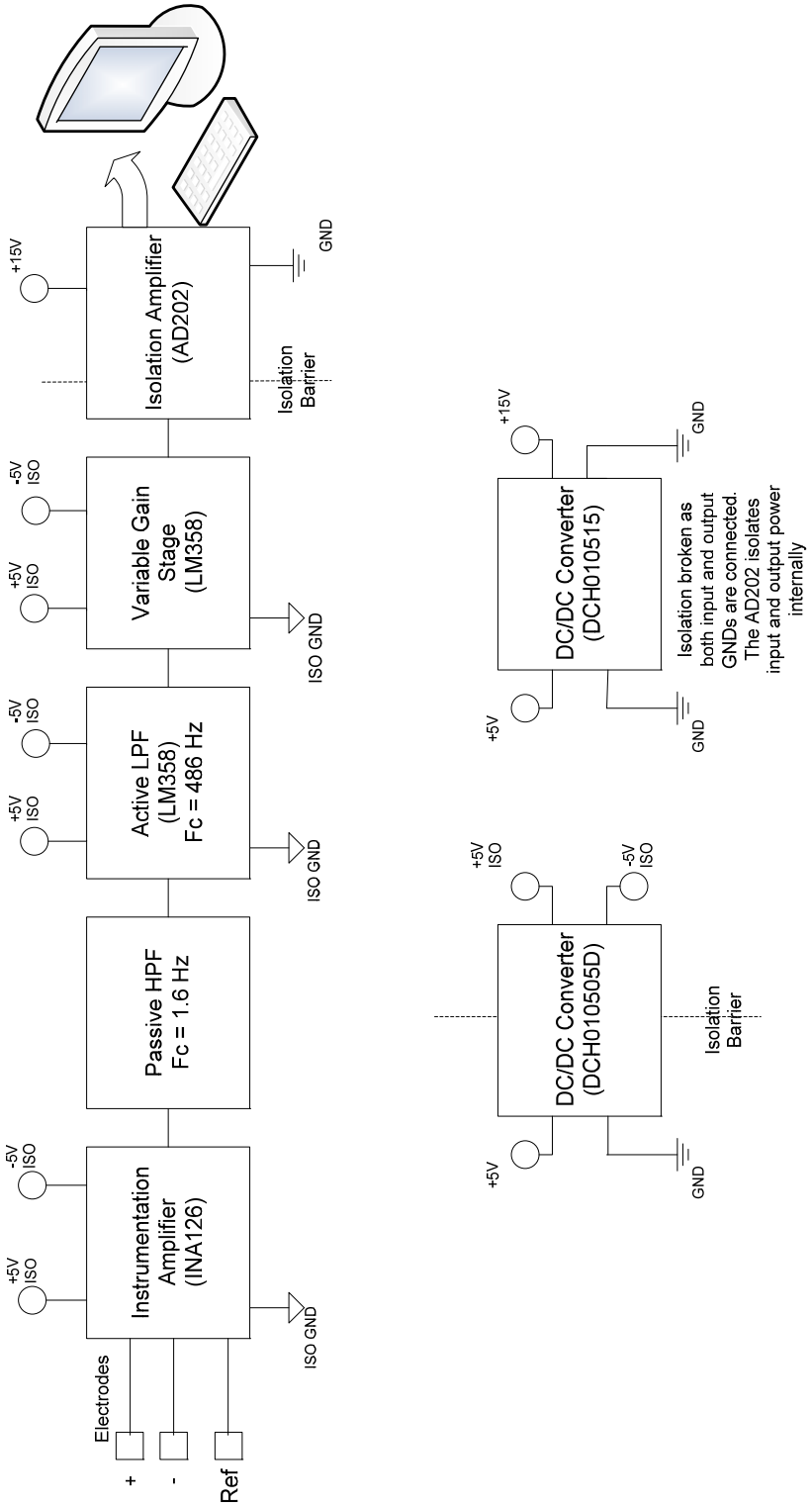

Figure 3-9 – Low level block diagram of EMG module

3.2.5 Opto Isolator

The opto isolator is used to isolate the voltage to current converter control signal. The signal is provided via LabVIEW's data acquisition board. Since this signal is derived from the computer, it is referenced to ground. To remedy that we pass the signal through an analog opto isolator that isolates the computer ground plane from the stimulator ground plane. Most optical isolators are used for digital signals where the input is either high (5V) or low (0V). However our system required an analog isolator. An interesting circuit was found which uses a high linearity optocoupler (HCNR201) to achieve this (Prutchi & Norris, 2005). This circuit takes the input voltage and converts it to a current which lights an LED in the optocoupler. The optocoupler has a photodiode which receives the input from the LED and this signal is then fed to a current to voltage converter to reconstruct the original input signal. A block diagram of this module is shown in Figure 3-10. The circuit schematic for this module is found in Figure A- 2.

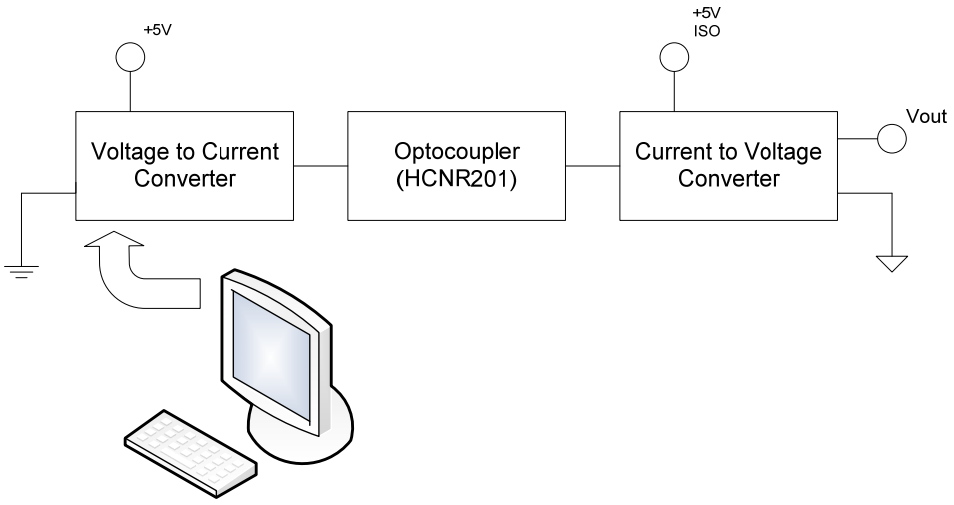

Figure 3-10 – Block diagram of opto isolator

3.3 Software Design Implementation

To control the stimulator output and visualize the EMG data, a National Instruments data acquisition board (PCI-6024E) was used in conjunction with custom written software. Two versions of the software were designed: a single stimulus version and a pulse train version.

3.3.1 Single Stimulus Program

The single stimulus version, shown in Figure 3-11, provides user controllable prepulse amplitude, prepulse duration, stimulus amplitude, and stimulus width.

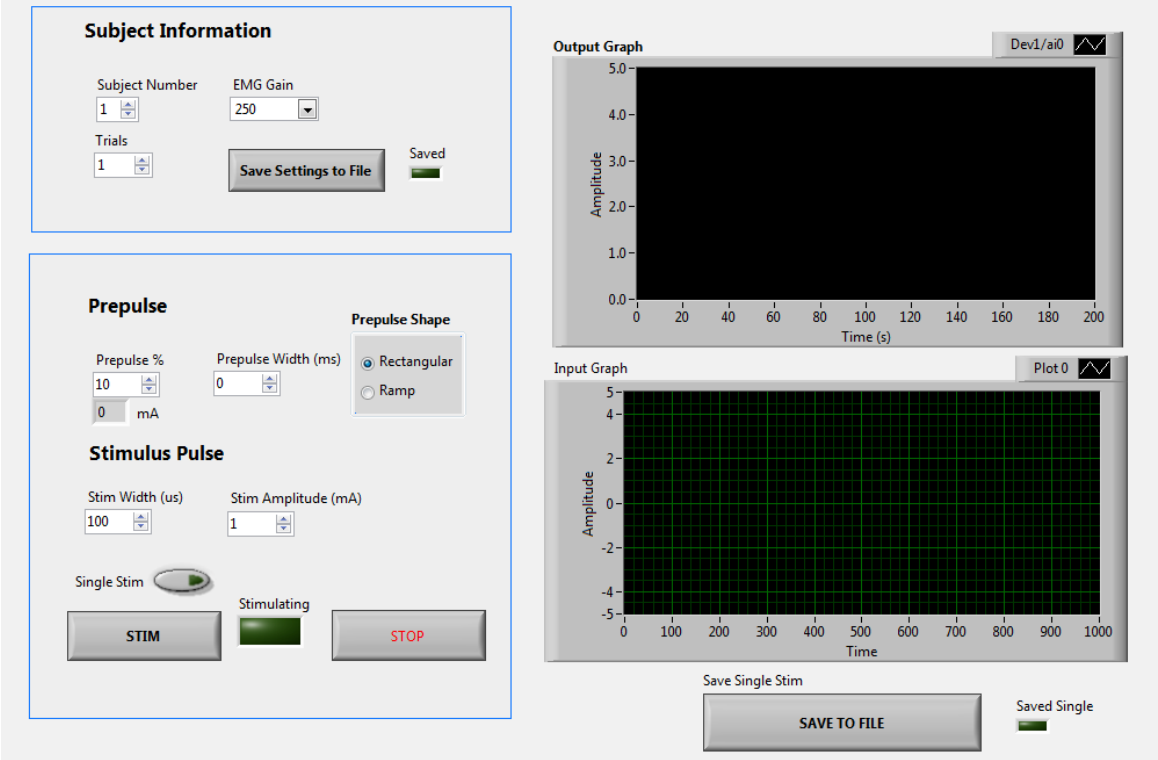

Figure 3-11 – Front panel of single stimulus program

An extra feature in this program is the ability to run a number of trials for each data set. If for example we wanted to average 5 responses at each stimulation level we can adjust the number of trials to 5 and have the program automatically send 5 stimuli with an inter-stimulus interval of 1 second. This allows for more accurate results without the extra time added if stimulating manually. A flow diagram of how this particular program works is shown in Figure 3-12. Once the user has started the program the software waits for an event to occur. Two events have been defined, saving the displayed EMG data or proceeding with the stimulation. If the user chooses to begin the stimulation, the program checks to see if multi-trial stimulation single stimulus output should occur. Both multi-trial and single stimulus function the same manner. The output function receives the relevant stimulation parameters from the front panel and generates 1 second worth of output data. The data input is triggered with the data output so that EMG data can be recorded while stimulation is taking place. The input is completely handled by LabVIEW and receives 500 ms worth of data. Details of output generation are shown in Figure 3-13. The output is generated by a separate function (a subVI) to minimize programming clutter. The VI works by taking in the various stimulation parameters and then the computer generates a prepulse with the desired shape and a stimulus pulse. The two waveforms are then added and returned as a single waveform to the main program to output. Full LabVIEW block diagrams are found in the appendix.

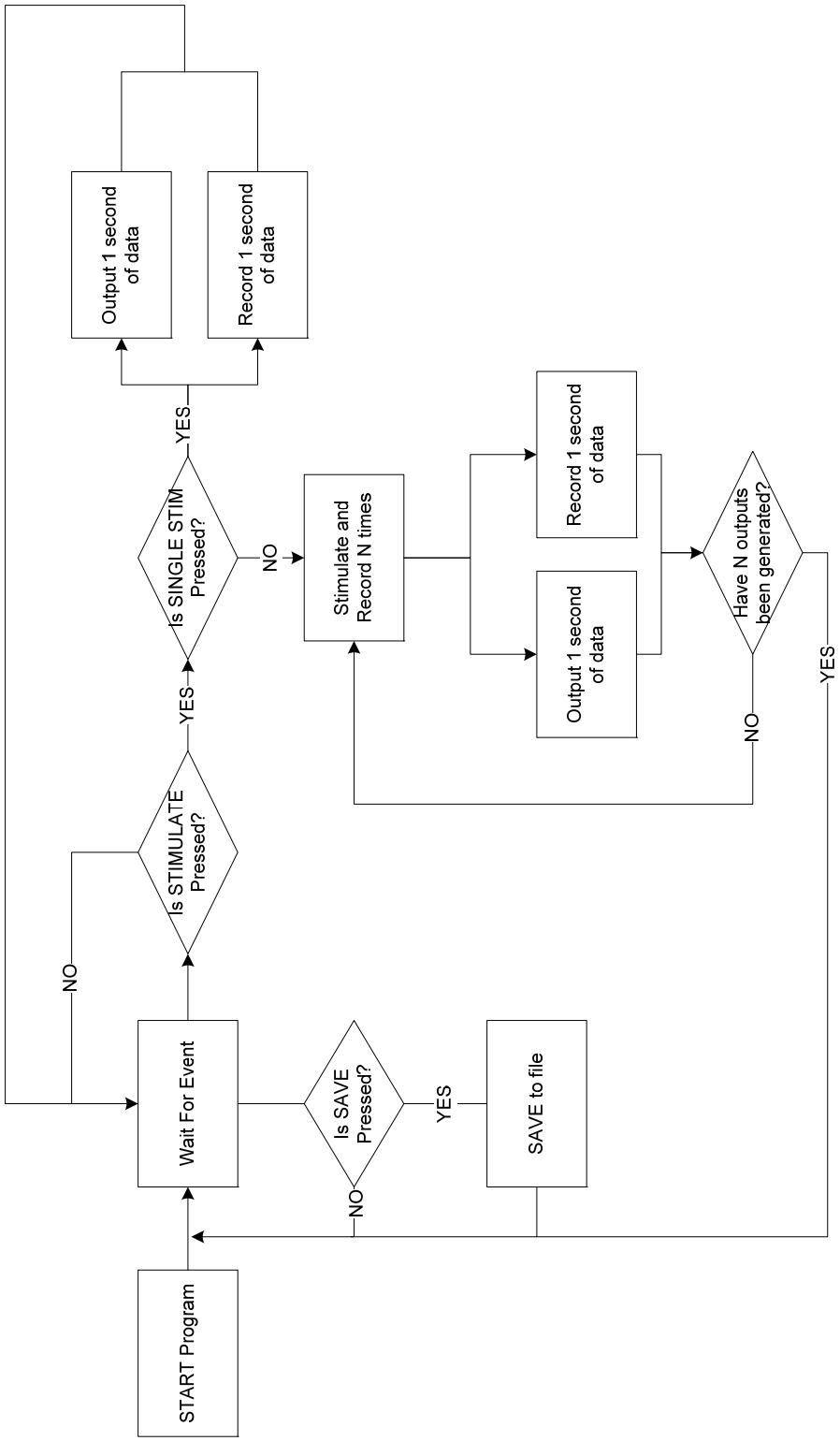

Figure 3-12 – Block diagram of single stimulus software program

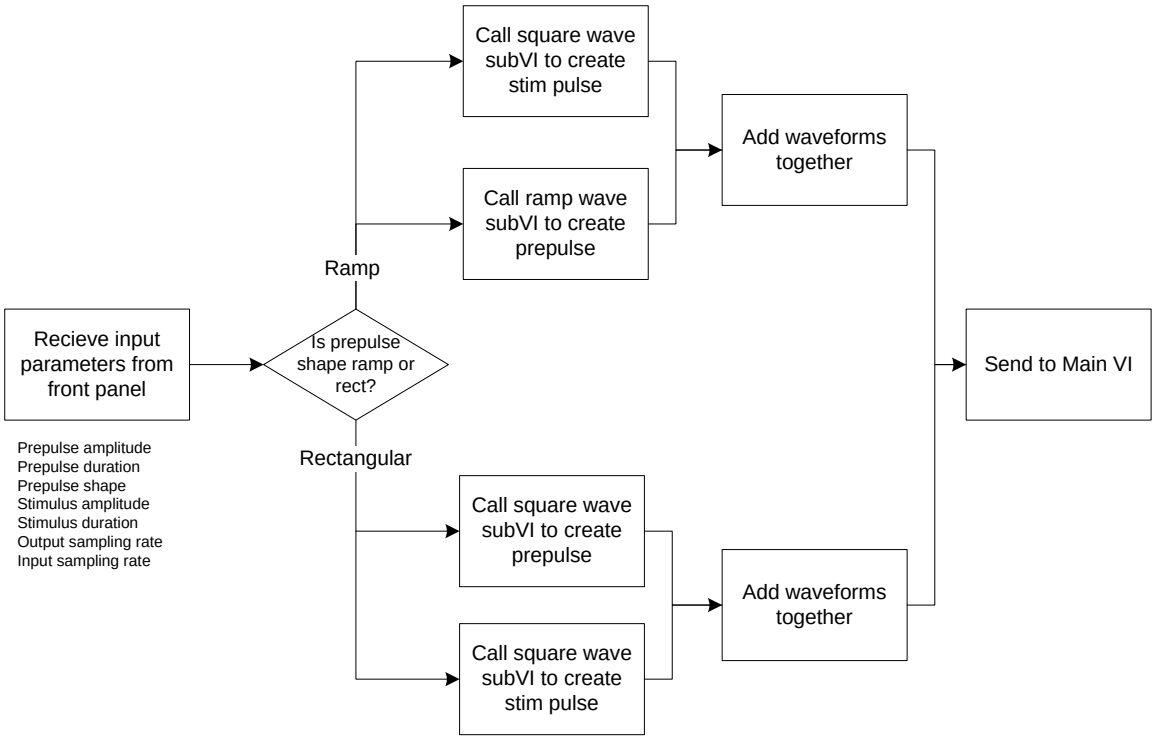

Figure 3-13 – Block diagram of pulse output VI

3.3.2 Pulse Train Program

The pulse train program has a very similar front panel to the single stimulus version with the addition of pulse train settings (ramp up time, ramp down time, plateau time, off time, and stimulation frequency). The front panel is shown in Figure 3-14. The pulse train settings add major differences in terms of program flow when compared to the single stimulus version. In order to accommodate for the different pulse train settings, the program was designed in a state machine manner. The state machine diagram is shown in Figure 3-15.

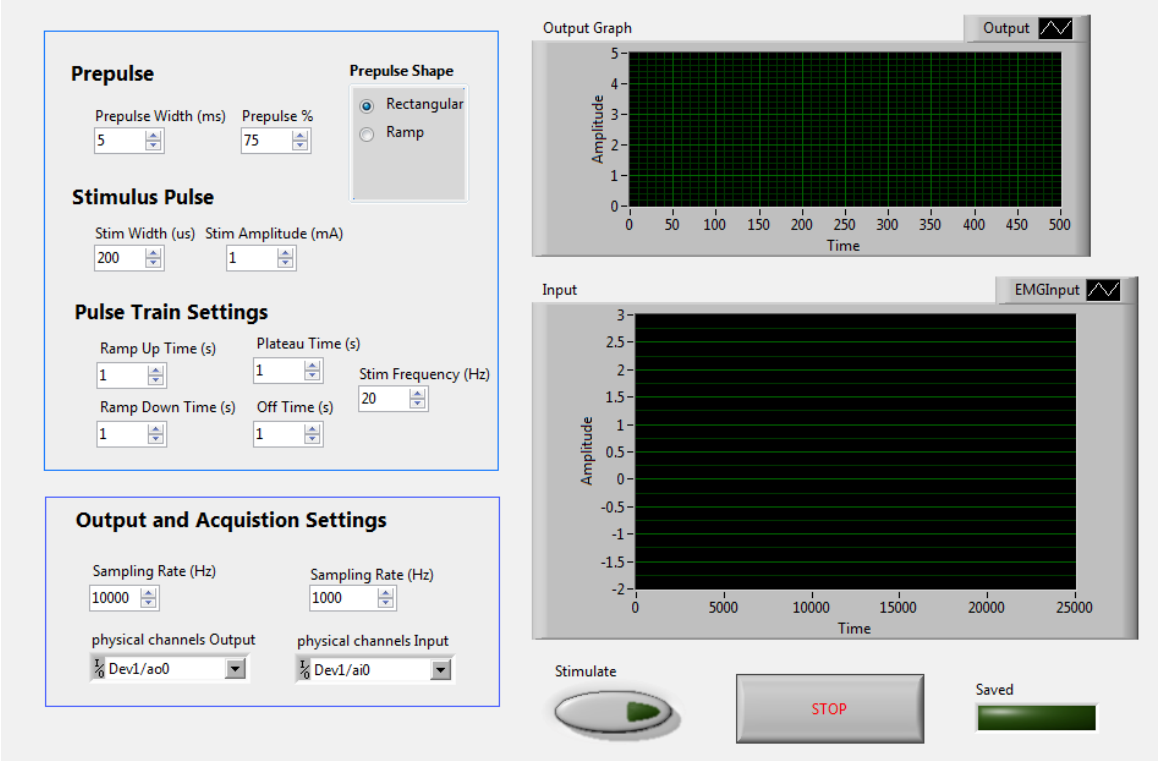

Figure 3-14 – LabVIEW Front panel for pulse train program

Once the program is started the first state it enters is the data acquisition setup state. This sets up the timing of both the input and output channels and also synchronizes the two. The next state is the initialize state. This state initializes all variables and graphs visible in the front panel. It also waits for an event, the stimulate button being pressed, to take place. Once this has occurred, the program jumps into the ramp up state where the stimulus is ramped up from zero amplitude to specified level. The next few states (plateau, ramp down, and off) are essentially the same as the ramp up stage in terms of function. One important feature to have is a stop button. If this button is pressed at any time the stop state is elicited. This state ensures that the stimulator is set to zero output

before stopping the program, otherwise a stimulus amplitude could be present indefinitely.

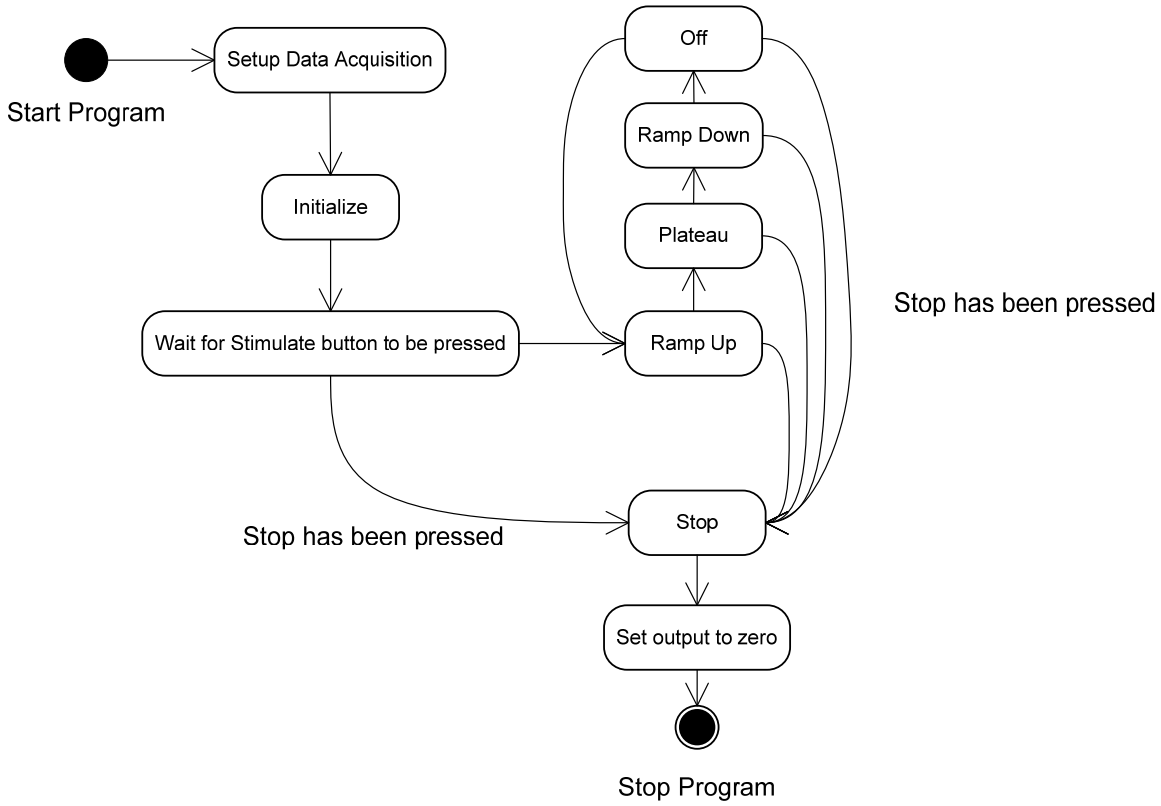

Figure 3-15 – State machine diagram for pulse train program

To generate the waveforms a separate VI was made. This VI takes in the relevant parameters from the front panel and creates the ramped or plateau waveforms. A block diagram of the ramp up VI is shown in Figure 3-16. When this VI is first executed it receives the value of the prepulse amplitude from the front panel and then proceeds to calculate the incremental step value over the ramp time duration using the equation step value = ramp up time ÷ stimulation frequency. This value is then added to a prepulse feedback value which is initially – on the first run of the program – set to zero. This total

value is compared to the maximum prepulse amplitude. If the total value is greater than or equal to the maximum value then the prepulse has been fully ramped up to the desired level and the next state can begin. If not, the prepulse is incremented by the step value and the prepulse feedback value is adjusted accordingly. The next state will still be the ramp up state as the prepulse has not yet reached the desired maximum level.

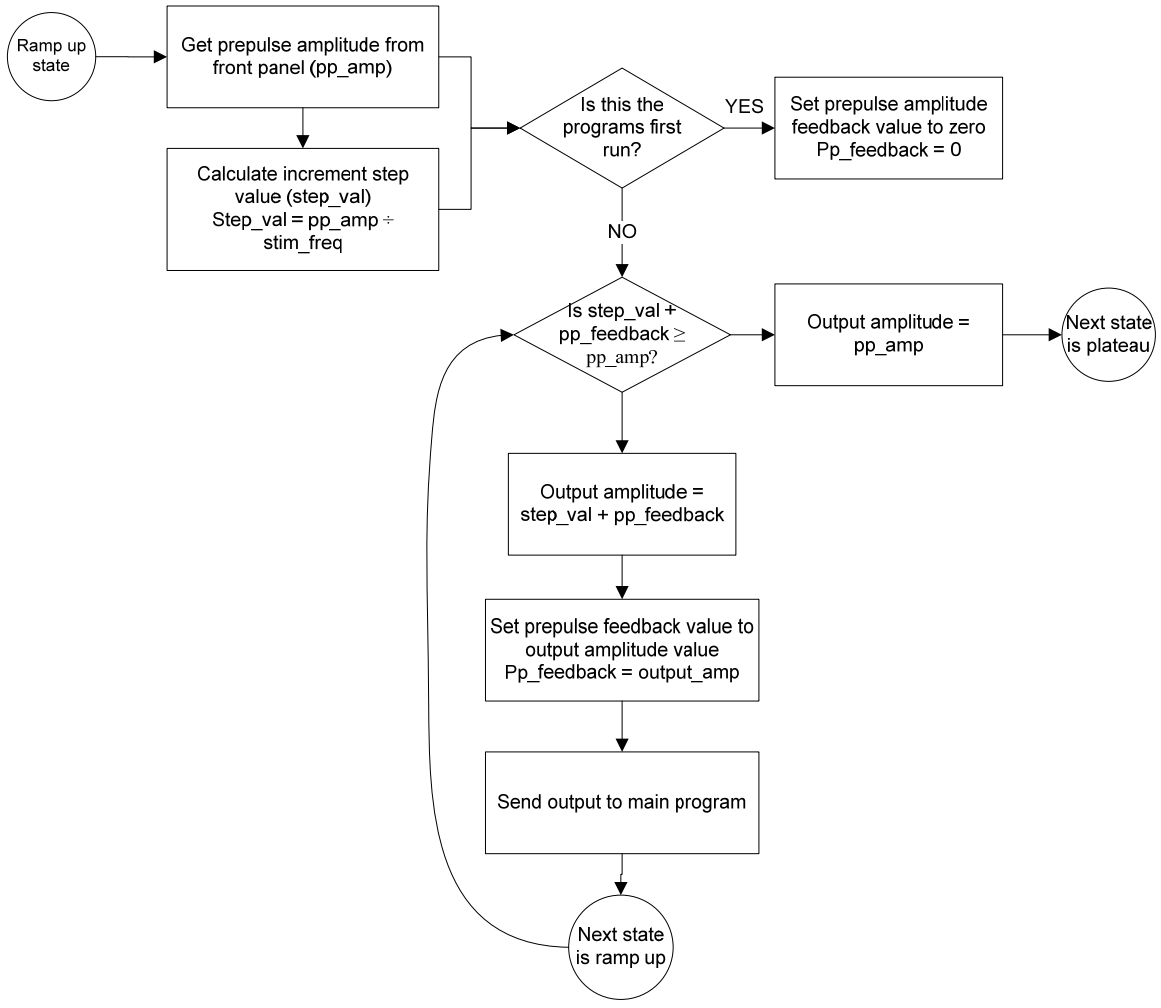

Figure 3-16 – Block diagram for ramp up VI

The other VIs that control the ramp down and plateau portions of the stimulation function in a similar manner to the ramp up VI. Full LabVIEW wiring diagrams are found in the appendix.

3.4 Design Prototype and Testing

With the design requirements and implementation finalized, a prototype of the stimulator was built. The stimulator was placed in a plastic enclosure as shown in Figure 3-17.

Figure 3-17 – Stimulator prototype in plastic enclosure casing

The front panel of the stimulator utilized standard BNC connectors and had a variable switch to control the gain settings. Switches are used to control the high voltage source and the main 5V power supply to the system. The front panel is shown in Figure 3-18.

Figure 3-18 – Front panel of stimulator prototype

A photo of the opened enclosure is shown in Figure 3-19. All cables are twisted pairs to reduce noise and connect between modules with the use of 2 pin molex headers. Each module, with the exception of the isolation amplifier, was implemented on a printed circuit board. Standard creepage spacing was used between the system ground plane and the isolated ground plane. Figure 3-20 shows the printed circuit board for the main stimulator circuit. All inputs and outputs are connected through the use of 2 pin molex headers. The 5V regulator (LM7508) was heatsinked since the input power supply was a 12V 60W source. This created a large amount of heat and in future designs the power supply may need to be dropped down in terms of power output. The control transistor on the high end is also heatsinked since this transistor holds off the stimulating voltage pulse until a positive signal is received at its base through the optocoupler. The isolated power supply used by the control circuitry is provided by a mini DC/DC converter

(DCH010505) located at the top of the circuit board. The other isolation barriers are provided by the optocoupler and the large 12V to 200V DC/DC converter.

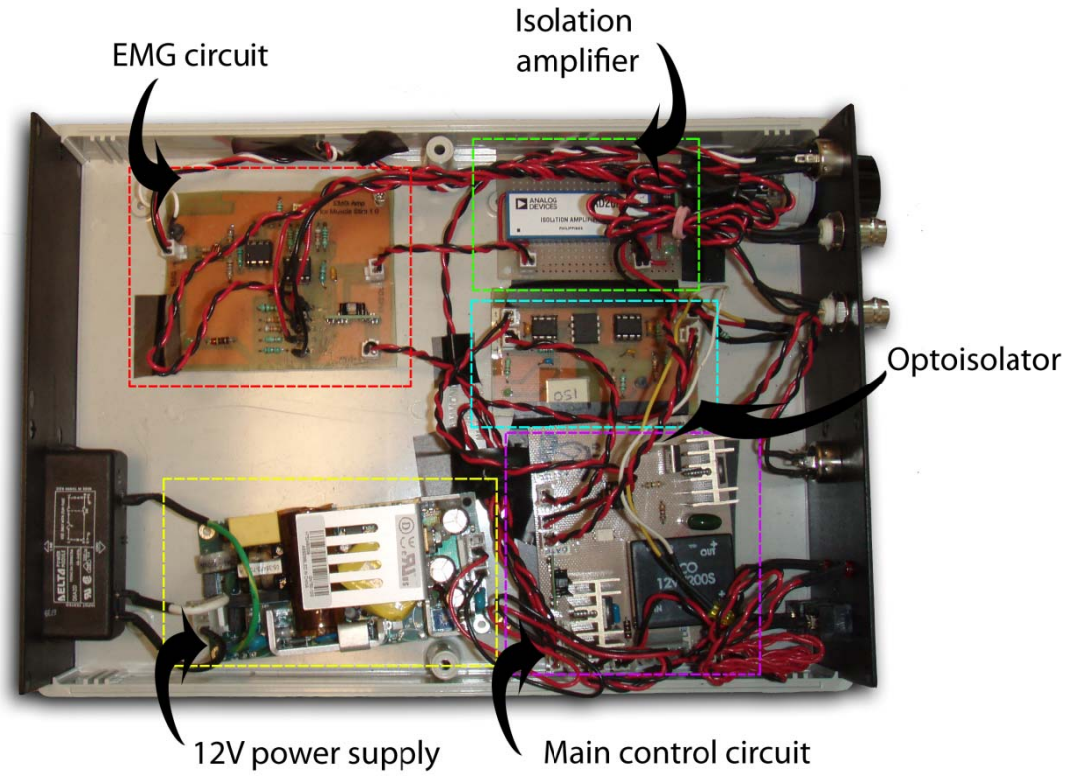

Figure 3-19 – Inside view of the stimulator enclosure. All modules are shown here.

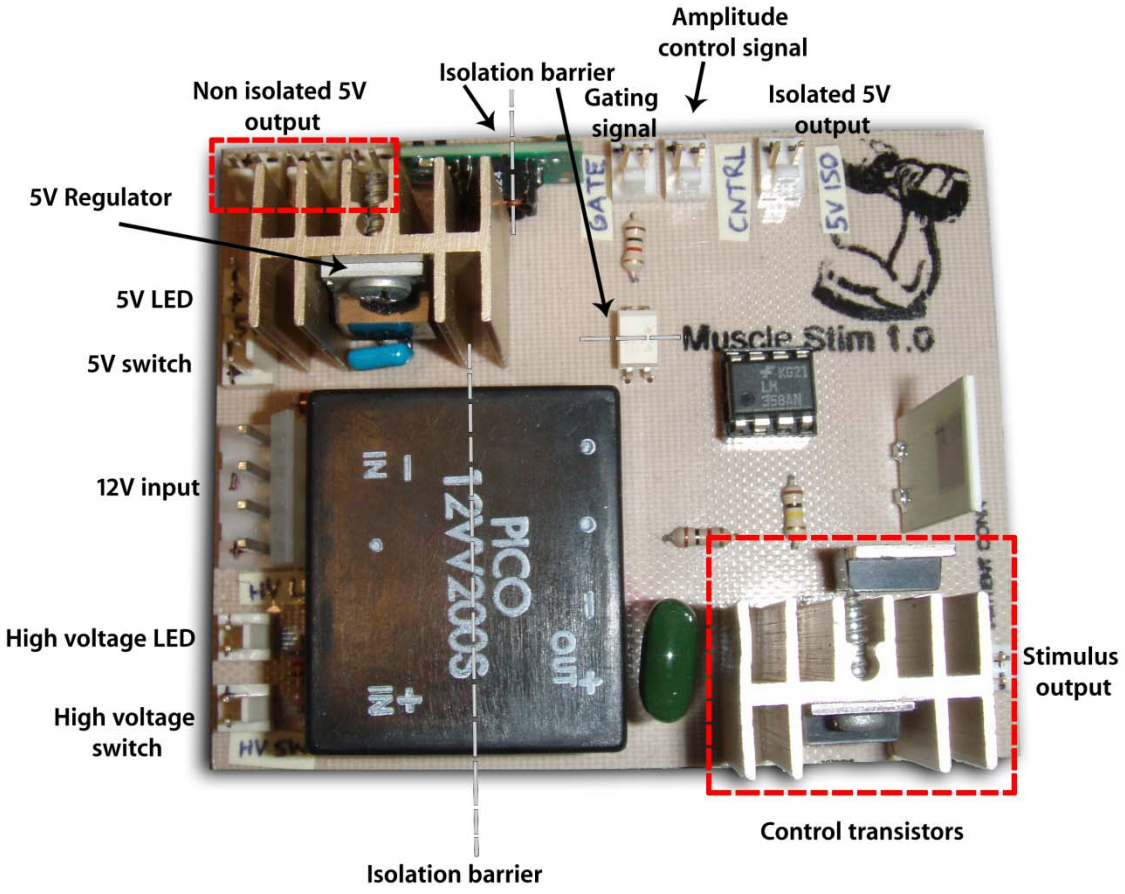

Figure 3-20 – Main circuit board prototype

The optoisolator circuit prototype is shown in Figure 3-21. As mentioned in the previous section, this design is a standard application from the HCNR201 datasheet and was also featured in *Design and Development of Medical Electronic Instrumentation* (Prutchi & Norris, 2005). The physical separation of the ground planes is evident beneath the main optocoupling chip (HCNR201). All connections were again provided via 2 pin molex headers. LEDs on the board provide visual notification that the isolated or non-isolated side of the board is receiving power.

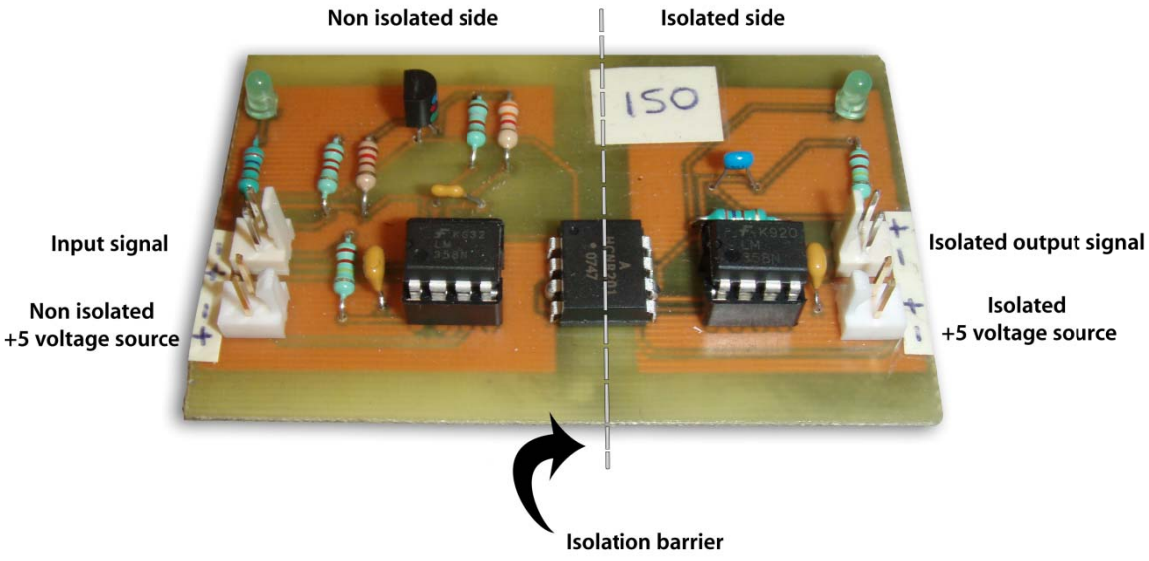

Figure 3-21 – Optocoupler prototype.

The last module is the electromyography amplifier. This is shown in Figure 3-22. The isolation amplifier on the output stage of the EMG amplifier was created on a regular perforated prototyping board and not on a printed circuit board. The output of the EMG amplifier is connected to the isolation amplifier through the use of a twisted cable pair. The different gain stages are highlighted in the figure. Isolated power is again provided through the use of mini DC/DC converters (DCH010505). However, the mini DC/DC converter used to power the isolation amplifier (DCH010515) is not used in an isolated fashion since the input power of the isolation amplifier must be referenced to system ground, as per the AD202 datasheet ("Data sheet for AD202: Low Cost, Miniature Isolation Amplifier Powered Directly From a +15 V DC Supply ").

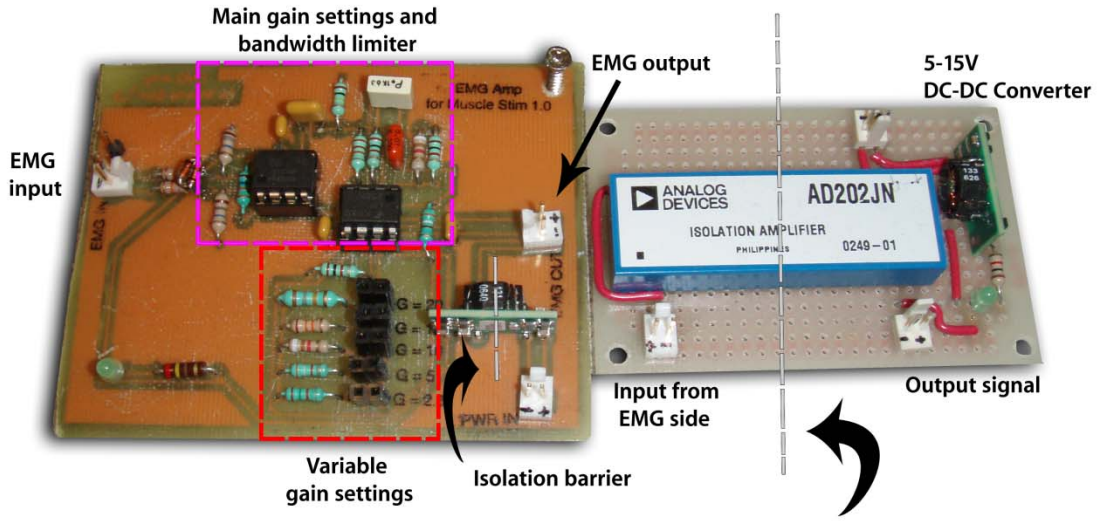

Figure 3-22 Electromyography amplifier and isolation amplifier prototype

To test the stimulating hardware, a resistive load, comprising several resistors, for a total of 2480 ohms was used. We tested both high and low amplitude long duration prepulses. High level prepulses would not be used in physiological testing as passing large DC currents to the body can induce electrochemical effects at the skin electrode interface. Using large currents can also increase the probability of burning sensations underneath the stimulating electrode (Nelson et al., 1999). Therefore, high prepulse currents were only used to test the stimulator output.

Figure 3-23 to 3-26 show the typical outputs that the stimulator produces. Each measurement was taken across a 560 ohm resistor in series with the remaining resistors. The waveforms were recorded using an Agilent 54621A oscilloscope and formatted using Matlab. The measurements showed that our stimulator functioned as desired and, that if

needed, the stimulator could output high current levels to large loads. Typical electrode skin impedances vary with the size of the electrode (Geddes, 1972). When stimulating large muscle groups, such as the quadriceps, patients who are less mobile than the average person tend to have much more subcutaneous fat. This fat presents a much higher resistance to the stimulator and hence a higher voltage is necessary to elicit the same level of stimulation.

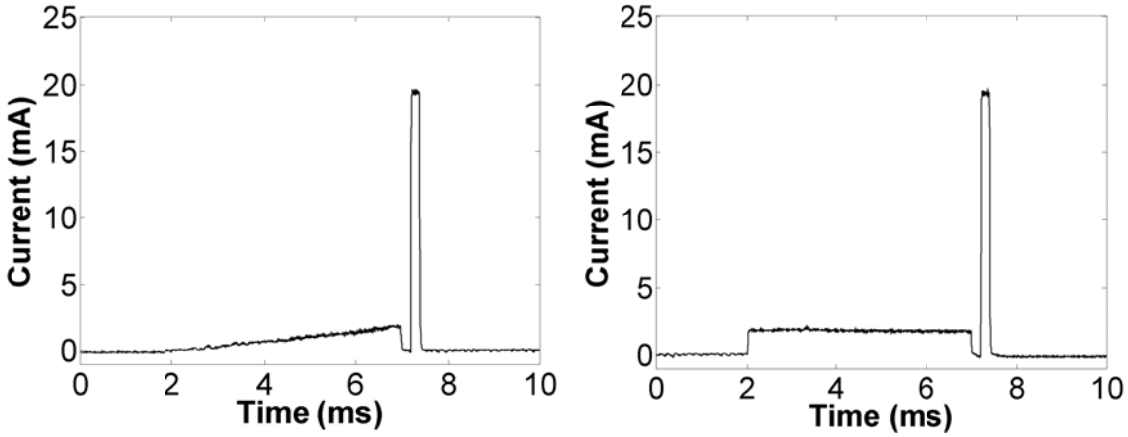

Figure 3-23 - Low amplitude 5 ms prepulse at 2 mA, stimulus pulse at 20 mA

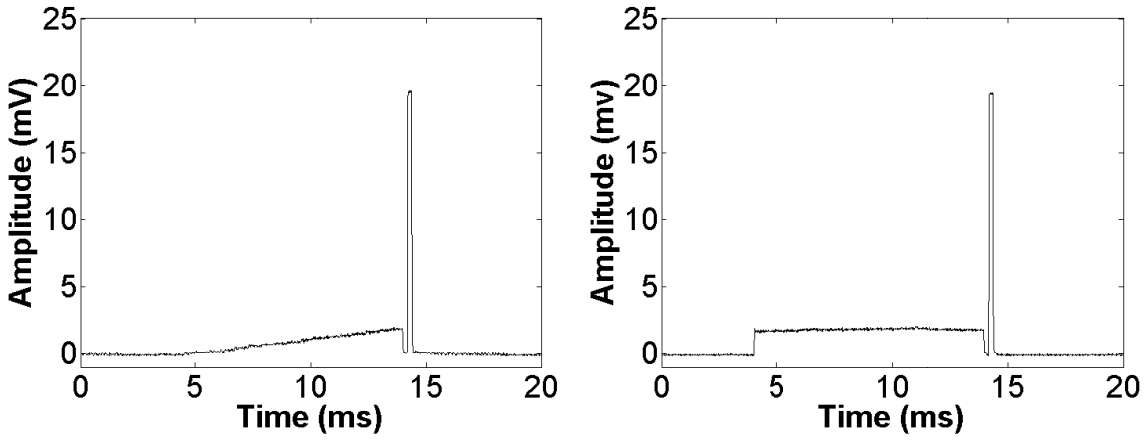

Figure 3-24 - Low amplitude 10 ms prepulse at 2 mA, stimulus pulse at 20 mA

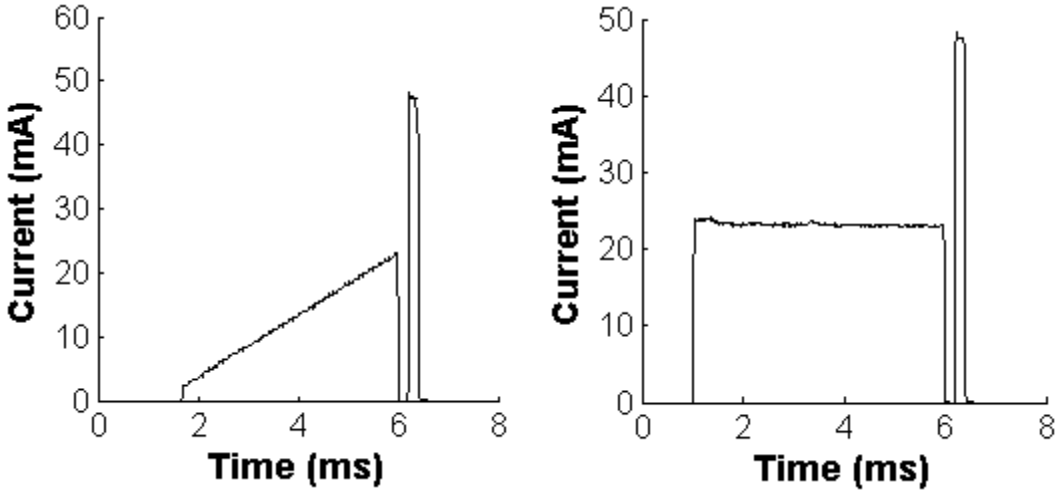

Figure 3-25 - High amplitude 5 ms prepulse at 25 mA, stimulus pulse at 50 mA

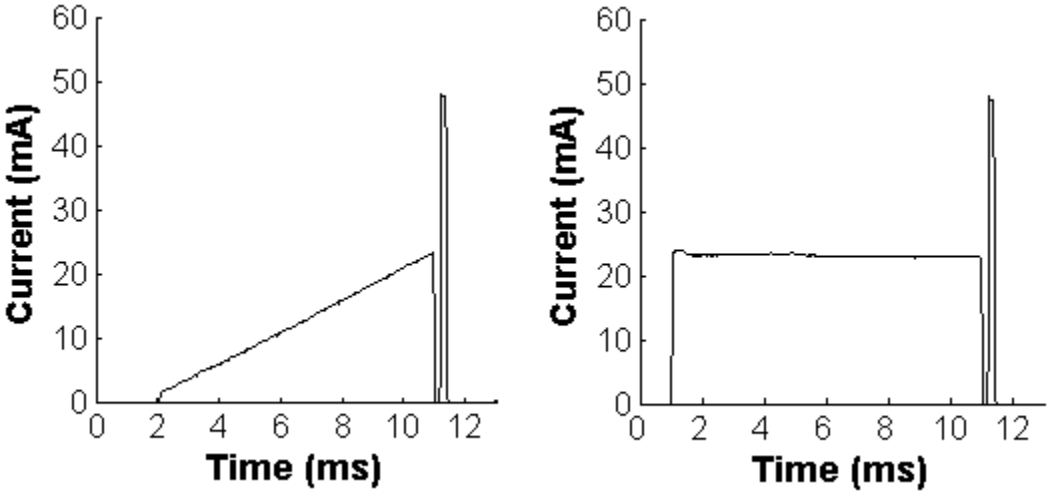

Figure 3-26 - High amplitude 10 ms prepulse at 25 mA, stimulus pulse at 50 mA

Chapter 4: Physiological Testing and Results

Ultimately the main purpose of designing the stimulator was to use it on humans to test whether or not prepulses can reduce the painful sensations elicited by high stimulation levels. This chapter presents the physiological responses elicited by the stimulator, methods employed to reduce 60 Hz noise in the recordings, and results from our pilot study on the effects of prepulse stimulation.

4.1 Physiological Testing

To test our EMG amplifier, a simple low amplitude sinusoidal wave could be used but we instead opted to use a physiological response elicited by a stimulus pulse that was delivered by our stimulator. All of our physiological testing, including the pilot studies conducted to observe prepulse effects on the M-wave, were conducted on the median nerve of a 63 year old male subject with recording electrodes placed on the thenar muscle. We chose to do our studies on the median nerve since stimulation setup is fairly simple with the median nerve being easy to locate on almost any individual. It is also prudent to note that the median nerve in the area we are stimulating includes both small diameter sensory nerve fibers and large diameter motor nerve fibers. Figure 4-1 shows the typical setup employed. The stimulating bar electrode was first placed over the medial portion of the forearm. An initial stimulus is given to determine if the placement of the bar is adequate. If a response, a muscle twitch, is not present, the bar is moved around until a response is elicited. Once the bar placement is set, a wrist strap is used to secure the bar in place. This ensures that subsequent stimuli are depolarizing the nerve in the same place.

Recording electrodes are placed on the thenar muscle as shown in Figure 4-1. The ground or reference electrode is placed on the posterior side of the hand. All the electrodes were

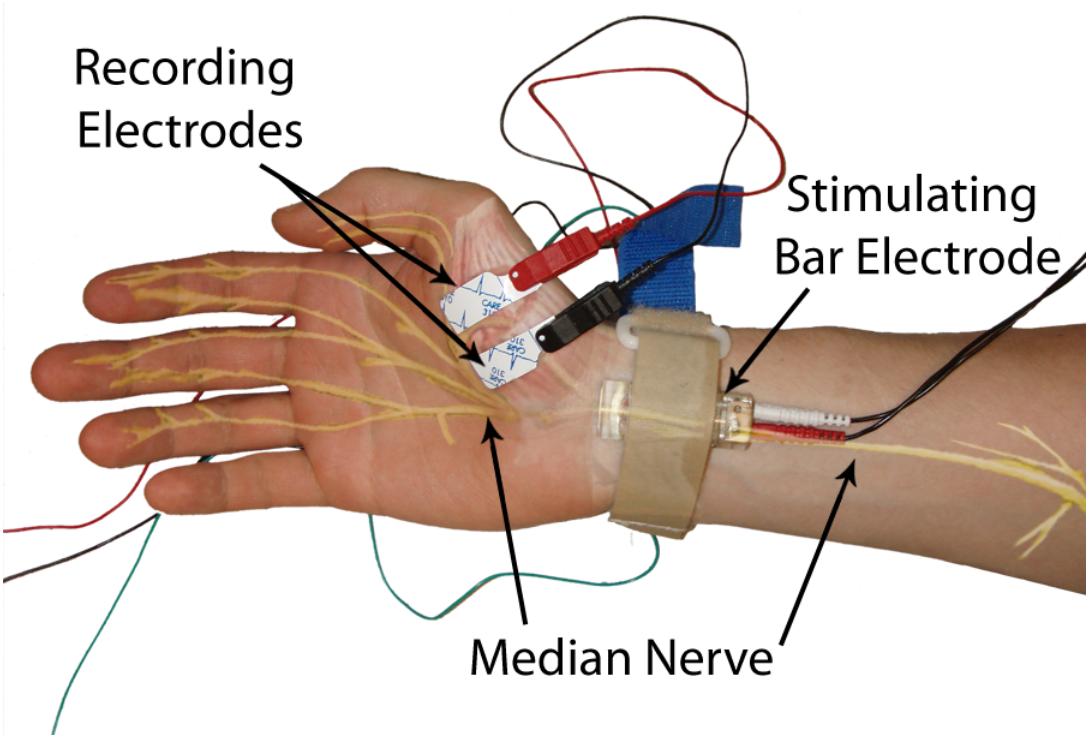

Figure 4-1 – Stimulation and recording electrode placement setup. Illustration modified from (Netter, Craig, & Perkins, 2002).

made from disposable self adhesive ECG electrodes (Product No: 30807732, Tyco Healthcare Group, Mansfield, MA). The recording electrodes were constructed by cutting the original ECG electrode in half. The smaller electrode size is much more conducive to thenar muscle recording where two electrodes are placed within a very small distance to one another and have to span a small muscle.

A single stimulus with a 28 mA amplitude was delivered as a test stimulus. This amplitude produced a maximum M-wave response and the response is shown in Figure 4-2. The recording shows a stimulus artifact and an M-wave response, however, large 60

Hz noise is seen to contaminate the signal and hence signal processing measures had to be employed.

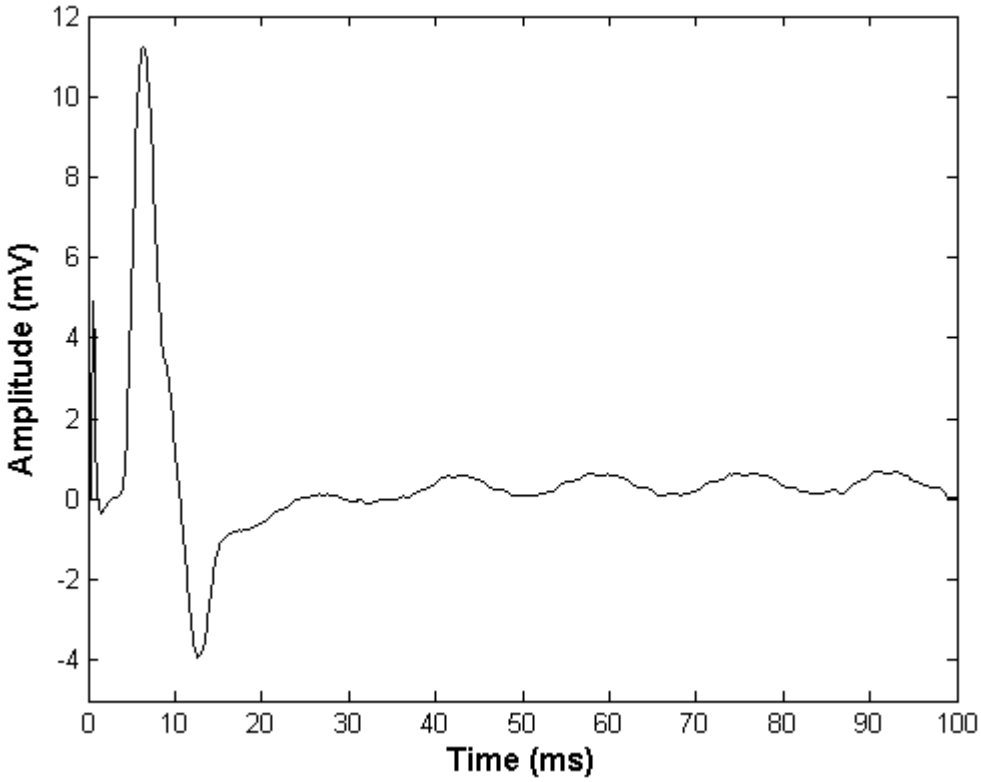

Figure 4-2 – Raw EMG recording showing signal contaminated with 60 Hz noise.

4.2 60 Hz Noise Removal

60 Hz noise is present in almost every room in today's modern society. All electronic items are powered from a 60 Hz, 120 V, alternating current supply. When measuring any sort of biopotential signal, our bodies act like an antenna via capacitive coupling, gathering 60 Hz noise emitted from computers, light sources, and various electronic devices. The raw EMG recording shown in Figure 4-2 is an example of how the 60 Hz

noise signal contaminates our signal of interest. The noise is especially large in this case because the electrode cables were unshielded and the subject was close to all the electronic equipment. A simple solution to this problem may is the use of a notch filter, however, EMG signals contain valuable information in this frequency range and the use of a notch filter would distort our EMG signal.

One of the easiest methods to remove 60 Hz noise is through the use of a coherent detection and elimination filter. This type of filtering is done after the raw signal has been recorded. Since the noise in our case has a fundamental frequency of 60 Hz without any complex variations, simply generating an equal amplitude 60 Hz wave with a phase shift 180° from the original signal and adding this to our raw recording would remove the 60 Hz contamination. Figure 4-3 shows the effect of this type of filter on our raw EMG recording. The filter was developed in Matlab and a description of the functionality follows.

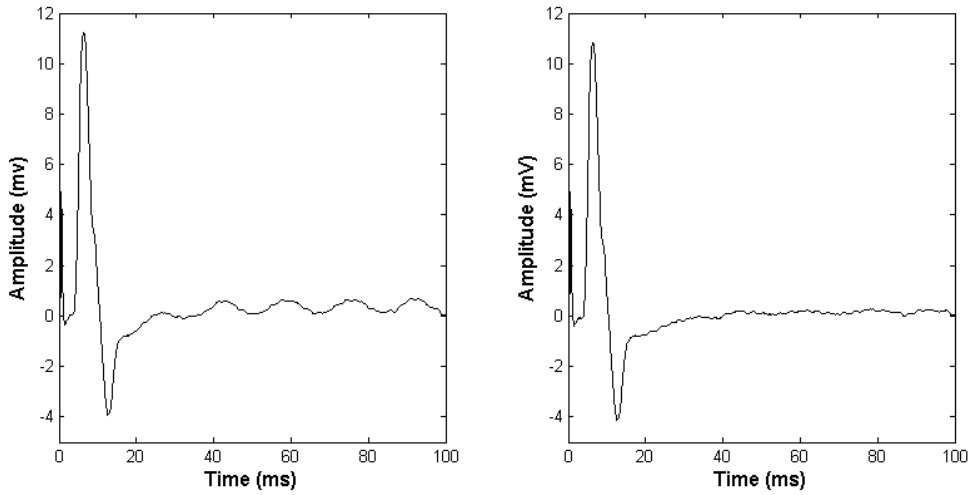

Figure 4-3 – Raw EMG recording (left), filtered version using coherent detection and elimination filter (right).

The first step in the coherence and elimination filter is to find a consistent stationary 60 Hz signal. The LabVIEW software used to control and record signals acquires 1 second worth of EMG data. The signal of interest is actually very short, approximately 25 ms in duration. The rest of the signal, from 25 ms onwards, is a clean 60 Hz noise source. The filter first takes the raw signal as an input and time inverts it so that the last sample in the raw signal is now the first sample in the processed signal. 100 ms of data is then stored in a vector; this vector contains our raw 60 Hz noise. The raw noise is, however, not perfectly smooth and in order to accurately detect the phase, some smoothing is necessary. The data is smoothed using an averaging window of 2.5 ms. Once the data is smoothed, a peak detection algorithm is used to determine the location and values of the peaks and troughs of the signal. The average peak to peak amplitude of the smoothed signal is calculated and this is used as the amplitude of the new generated reverse phase 60 Hz wave. The final step is to calculate the phase of the smoothed data. This is carried out by first creating a new 60 Hz wave with zero phase and comparing the time difference between the first peak in the new 60 Hz wave with that of the smoothed 60 Hz wave. This time difference is the phase between the generated signal and the raw smoothed data. The phase is then added to the generated signal and this signal is subtracted from the original unprocessed EMG signal. Figure 4-4 shows the results of the phase shift portion of the filter. The zero phase generated signal is shown in red and the green signal is the smoothed version of the raw EMG 60 Hz noise. Once the phase is detected both waveforms would be superimposed on one another.

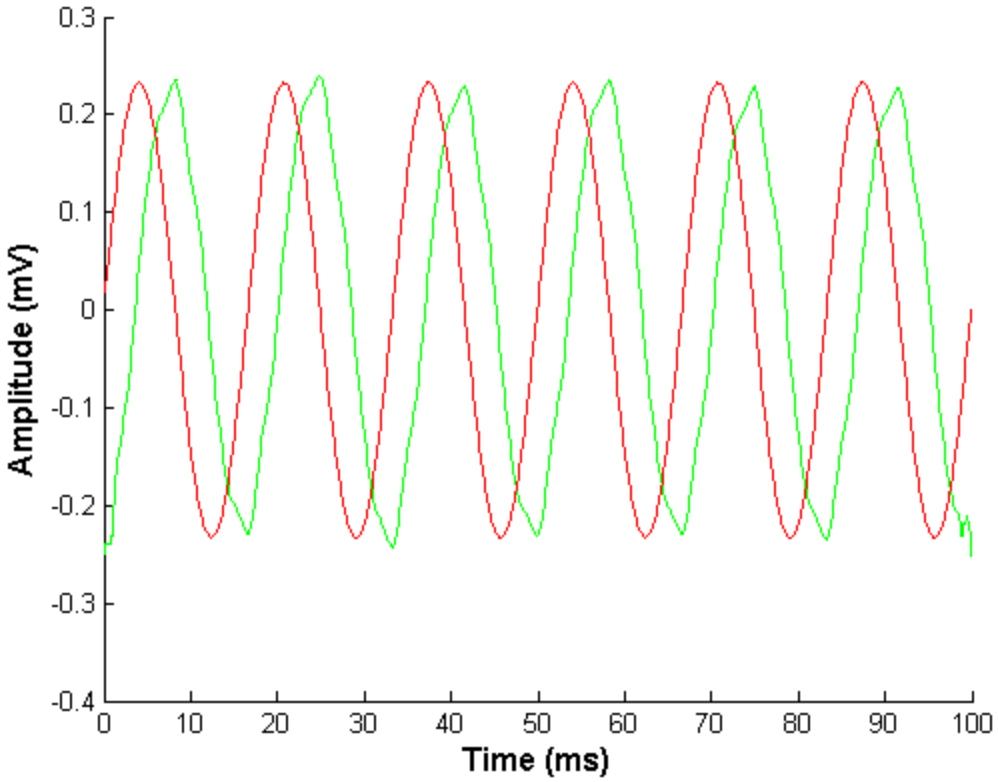

Figure 4-4 – Result before phase detection portion of filtering code. In red is the generated signal. In green is the smoothed 60 Hz input data.

4.3 Pilot Study

A number of different single subject pilot studies were carried out to determine the effectiveness of prepulses. The experiments included: looking at the effects of 5 and 10 ms prepulses while increasing stimulus amplitude, observing the effects of increased prepulse duration while keeping the stimulus amplitude constant, and observing the effects of prepulses during pulse train stimulation.

4.3.1 5 ms Prepulse Experiment

For our first experiment, we followed a similar protocol to the one used in the Poletto study (Poletto & Van Doren, 2002). The prepulse amplitude was kept at 10% of the stimulating pulse amplitude. The protocol consisted of first obtaining the stimulus amplitude where a maximum M-wave is elicited with no prepulse. Once the maximum amplitude was found, the study began at a low amplitude where three successive stimuli were delivered (no prepulse, ramped prepulse, and rectangular prepulse). The stimulus amplitude would then be increased in 1 mA increments until the amplitude that elicited the maximum M-wave response is reached. In our experiment the subject obtained a maximum M-wave response at 28 mA of stimulus amplitude. With the prepulse set to 10 % of the stimulus amplitude, the maximum prepulse amplitude was then 2.8 mA. Figure 4-5 and 4-6 show the results from the experiment. The control signal in each case is the stimulus with no prepulse (shown in blue). The ramped stimulus is shown with a dotted black line and the rectangular prepulse stimulus is shown with a red line. The first stimulus was delivered at 11 mA and no response was elicited. At approximately 50-60%

of the maximal M-wave response, the prepulses have a very large effect. The rectangular prepulse had the largest effect creating a maximum 42 % increase in peak to peak amplitude. The ramped prepulse also had augmenting effect on the M-wave response. At best, the ramped prepulse provided a 33 % increase in peak to peak M-wave response over the control (no prepulse stimulus). Although we had first determined that the maximum M-wave had occurred for a 28 mA single stimulus, Figures 4-5 and 4-6 show that the maximum M-wave was already reached at 18 mA. The current pathways could have changed during the course of the experiment because of increased ion concentration or the electrode could have moved slightly. At any rate, the prepulse had no effect on the signal from 18 mA to 25 mA of stimulus amplitude because all motor units had already been recruited. At 26 mA the rectangular prepulse started to recruit the muscle and this is evident by the early M-wave activity when compared to the control response. Also, with the early activation comes a decrease in peak to peak amplitude since those motor units have already fired and are in a refractory state when the stimulus pulse arrives.

A stimulus duration curve, shown in Figure 4-7, provides an easy visualization of the differences between the ramped, rectangular and control stimuli. This graph was smoothed using a 3 span moving average window.

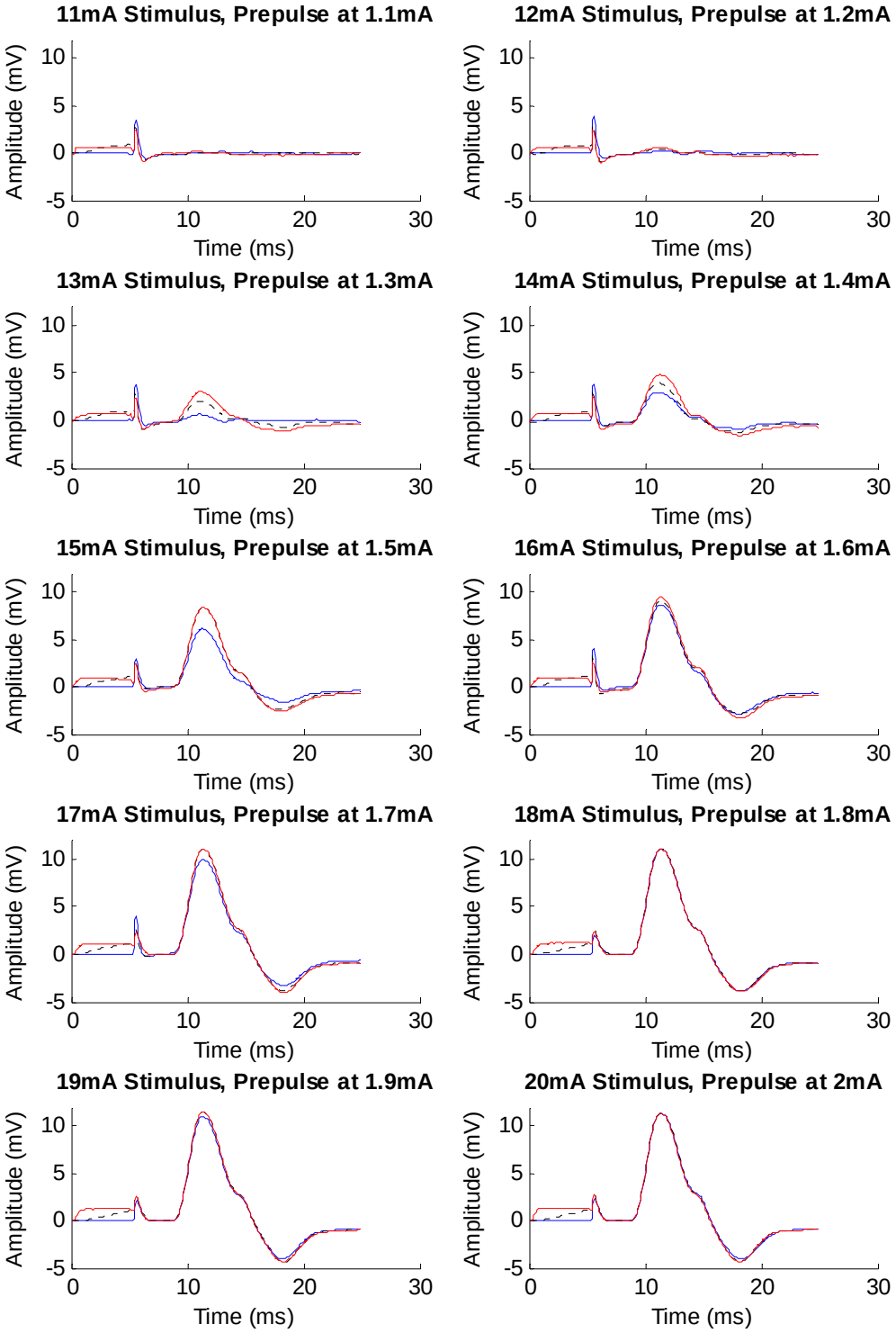

Figure 4-5 – Results from the 5 ms prepulse experiment. The blue line represents the control signal (no prepulse). Dotted line is the ramped prepulse and red line is the rectangular prepulse.

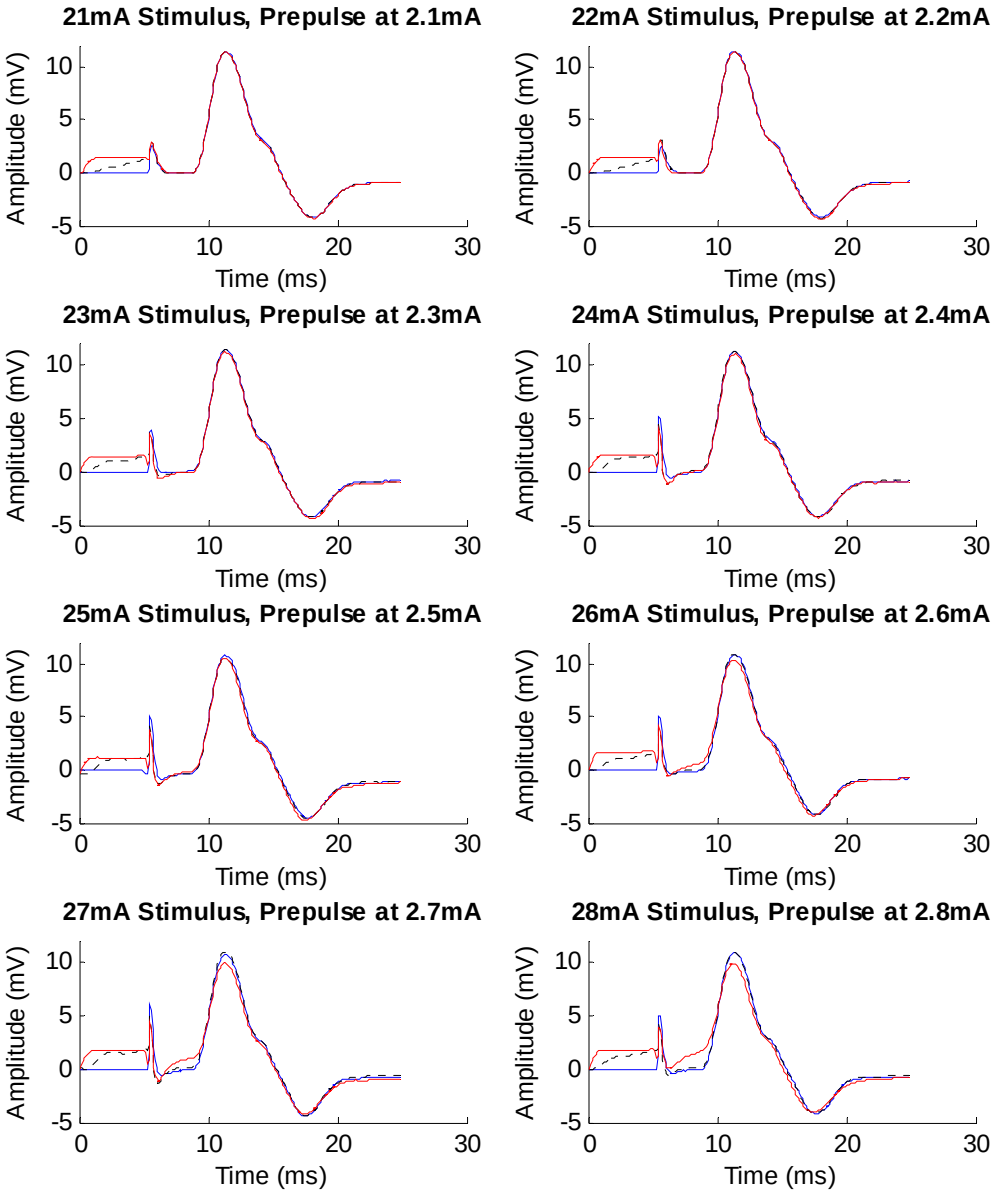

Figure 4-6 – Continuation of the 5 ms prepulse experiment.

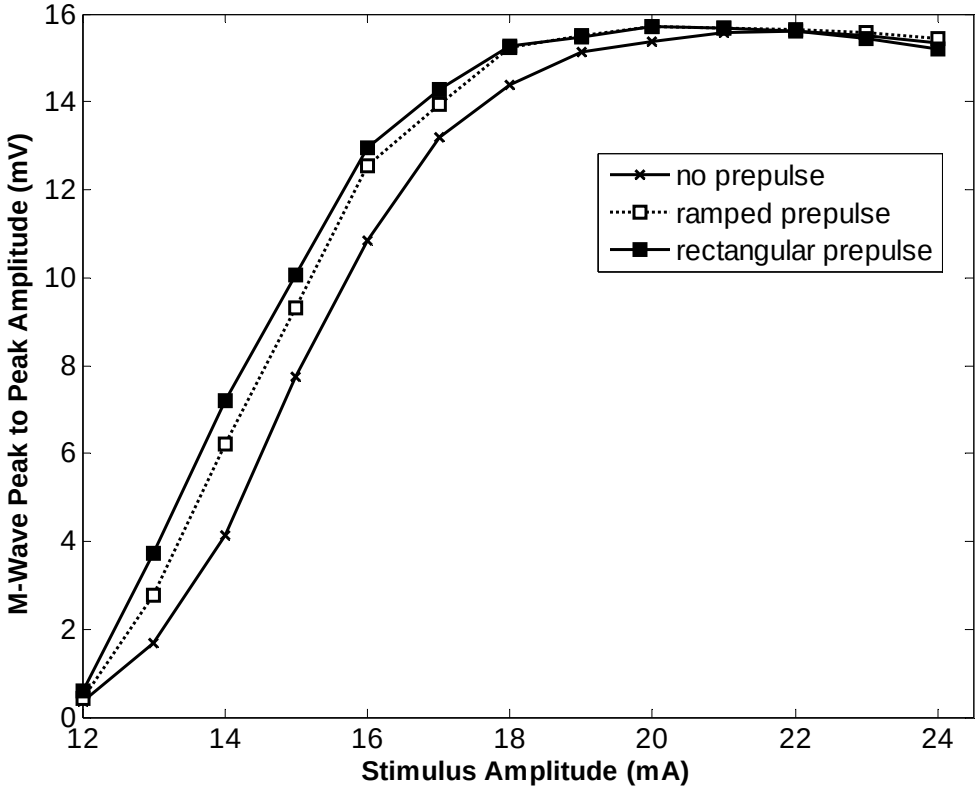

Figure 4-7 – Stimulus response curve for the 5 ms prepulse experiment.

We also experimented with a 5 ms prepulse at an amplitude of 20 % of the stimulus amplitude. The problem with this was that at 20 % of the amplitude, high prepulse levels would recruit the motor units before the stimulus pulse could. This would then cause a lower peak to peak M-wave response along with a bimodal waveform. It is obvious that these levels are much too high for any useful purpose. Figure 4-8 shows the results at approximately 60 % of maximal M-wave response. It shows that at this level, the ramped prepulse is still not recruiting motor units and augments the response nicely. However, the rectangular prepulse is already recruiting motor units as seen by its early response and lower peak to peak amplitude. At even higher levels both the rectangular and ramped

prepulses recruit motor units themselves. This is shown in Figure 4-9. A stimulus response curve was plotted for this experiment and is shown in Figure 4-10. The graph shows that at approximately 60 % of maximal M-wave response the rectangular prepulse start to recruit motor units itself. The ramped prepulse starts to recruit motor units at amplitudes near the maximal M-wave response.

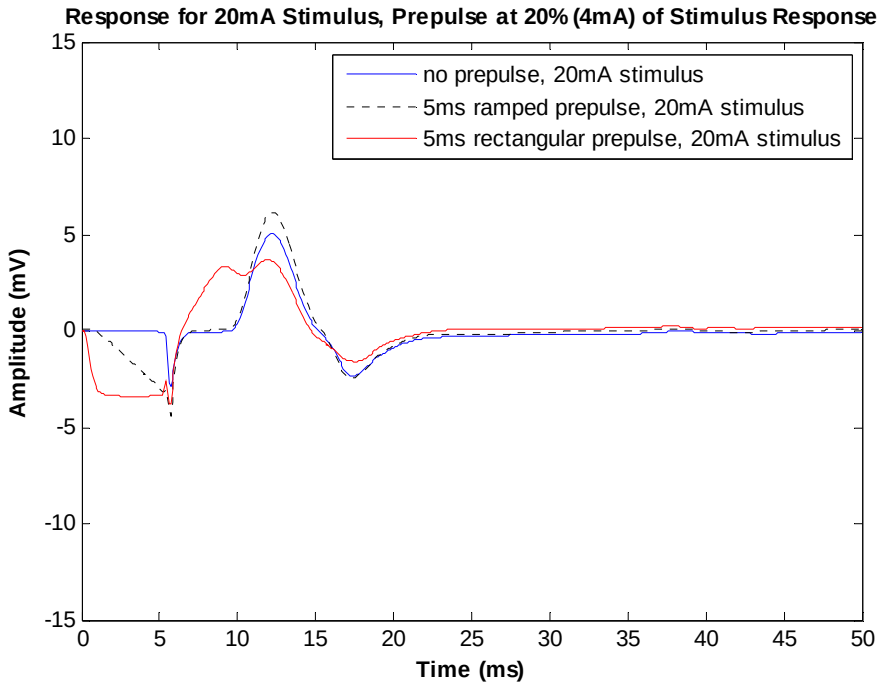

Figure 4-8 – Response for 60 % of maximal M-wave response using a 5 ms prepulse at 20% of the stimulus amplitude.

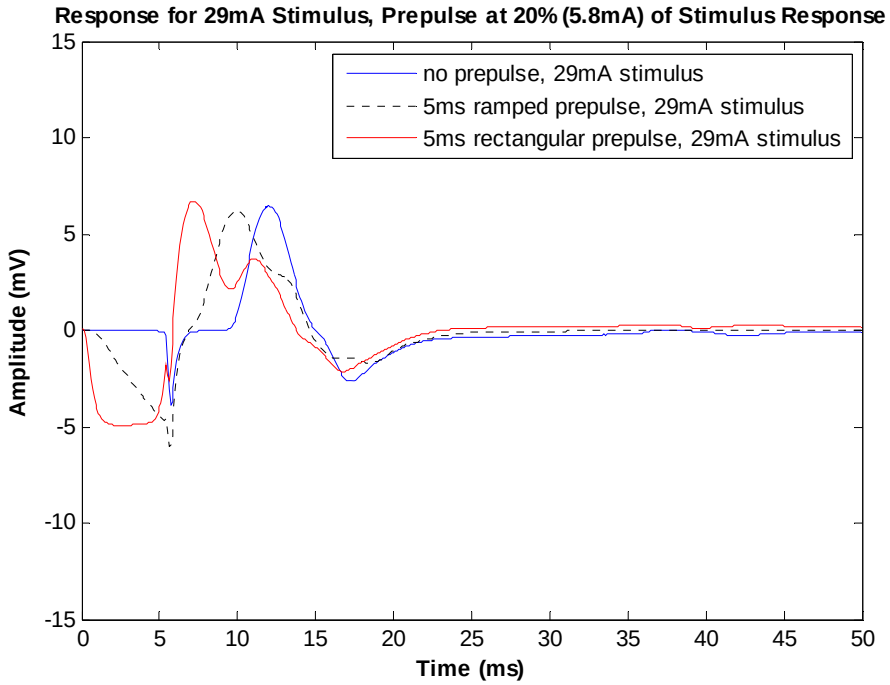

Figure 4-9 – Reponse for near maximum M-wave using a 5 ms prepulse at 20% of the stimulus amplitude

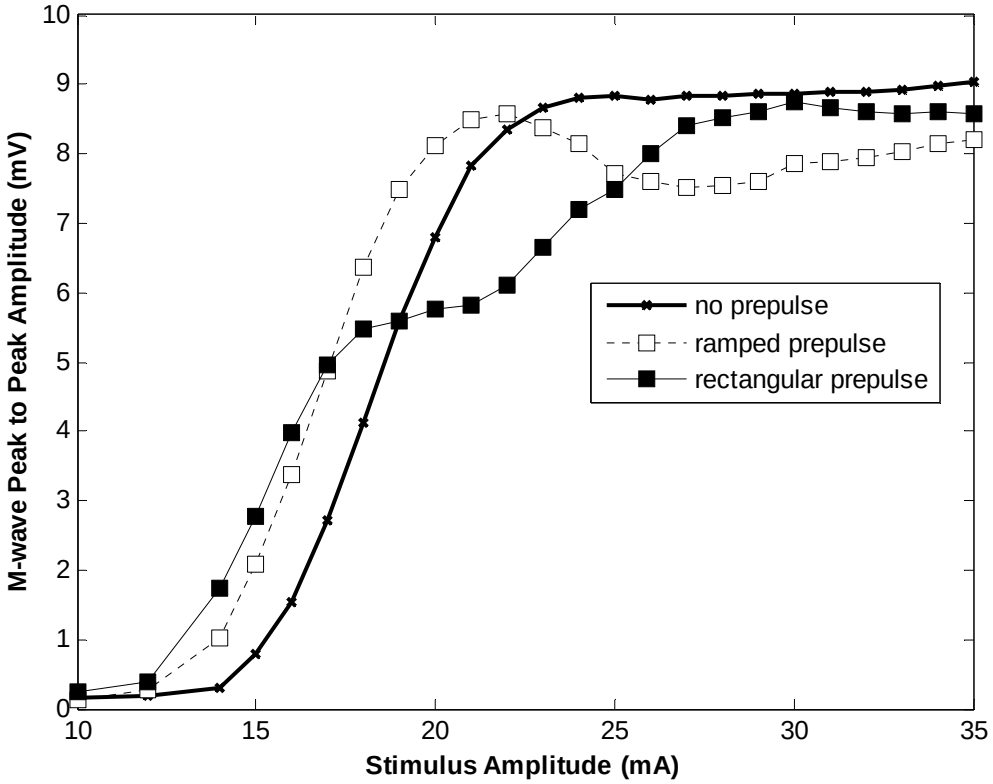

Figure 4-10 – Stimulus duration curve for 5 ms prepulses at 20 % of the stimulus amplitude.

4.3.2 10 ms Prepulse Experiment

We conducted a study similar to the 5 ms prepulse experiment but instead utilized 10 ms prepulses at 10% of the stimulus amplitude. A stimulus duration curve is shown in Figure 4-12. When using 10 ms prepulses we ran into the same problem that occurred when using 5 ms 20% prepulses in that the motor units would be recruited by the prepulse itself rather than by the stimulus pulse. A burning sensation also occurred with the longer duration prepulses at higher levels. However, the augmenting effect was much larger at

60 % of maximal M-wave response when compared to the 5 ms experiment. The ramped prepulse augmented the M-wave by approximately 51 %. The rectangular prepulse augmented the M-wave by 64 %. Clearly the 10 ms prepulse is much more effective than the 5 ms prepulse. Individual results for the experiment are shown in Figure 4-12.

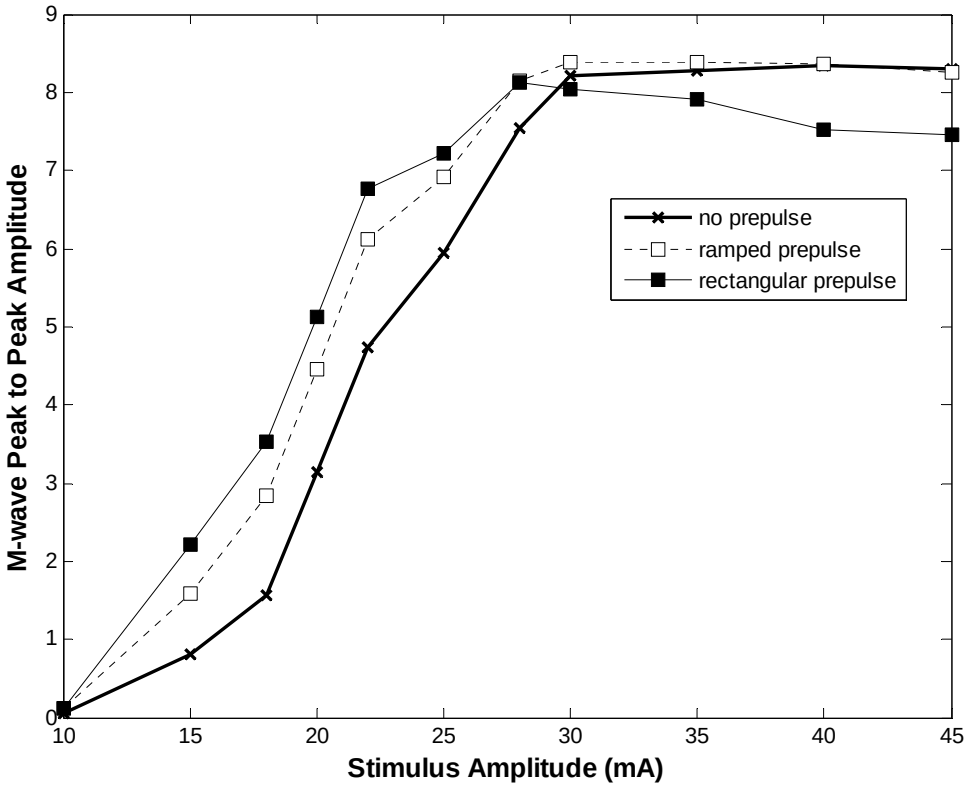

Figure 4-11 - Stimulus duration curve for 10 ms prepulse experiment

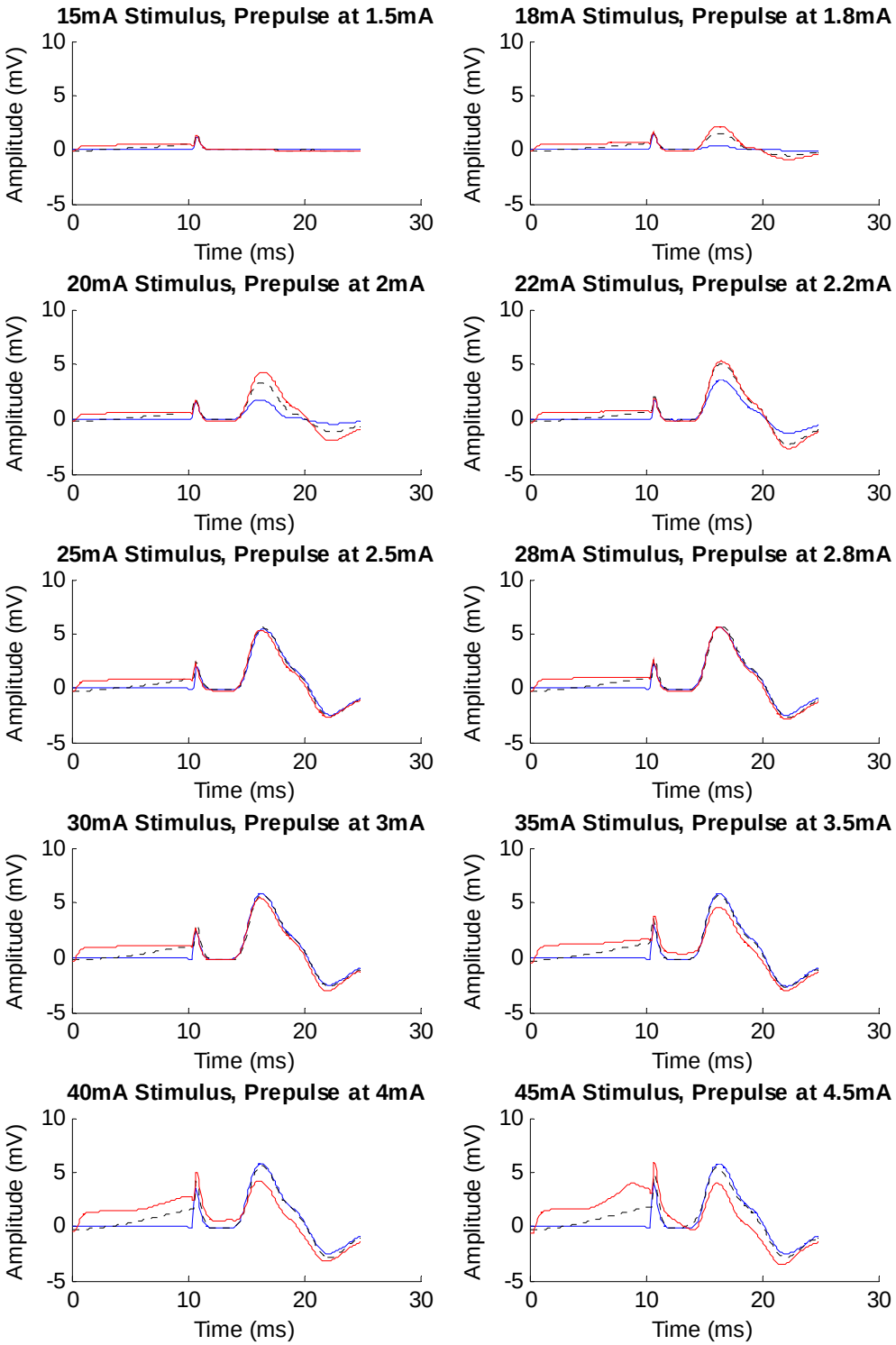

Figure 4-12 - Results from the 10 ms prepulse experiment. Prepulse amplitude set at 10 % of the stimulus amplitude.

As with the 5 ms experiment, we also carried out a 10 ms 20 %, prepulse experiment. The results were not favorable as very low levels of stimulation caused the prepulse to directly recruit motor units. Although there is an augmenting effect at these low levels, the prepulse itself causes some of the recruitment. Figure 4-13 shows one such event at low stimulus amplitudes. As the amplitudes increased, the M-wave became distorted as the motor units were almost entirely being recruited by the prepulse. Figure 4-14 shows a result at higher amplitude levels.

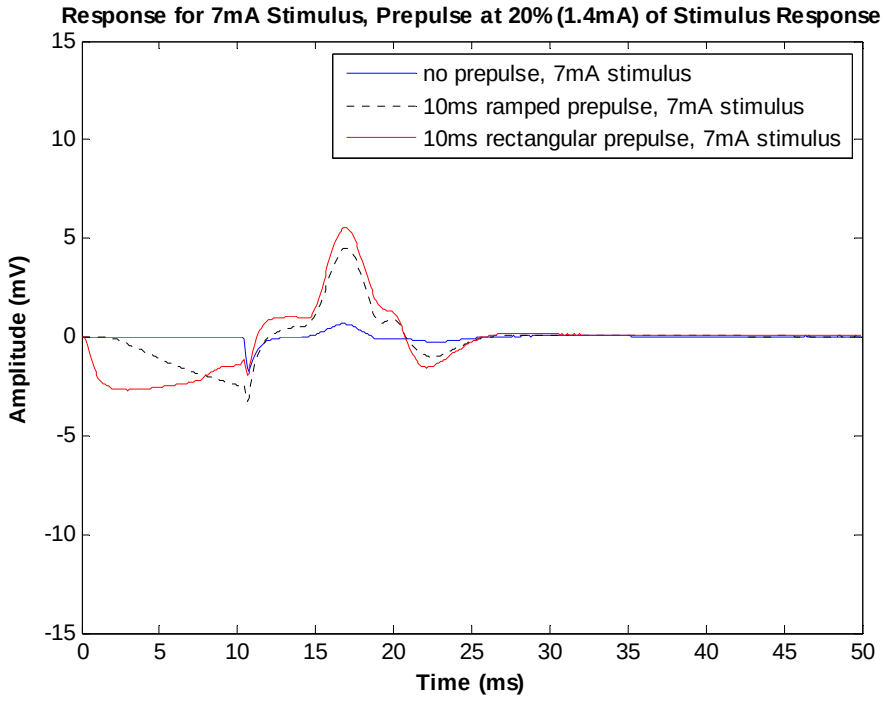

Figure 4-13 – Response for 7 mA stimulus, less than 40% of maximal M-wave response. Prepulse at 10ms duration and 20% of stimulus amplitude

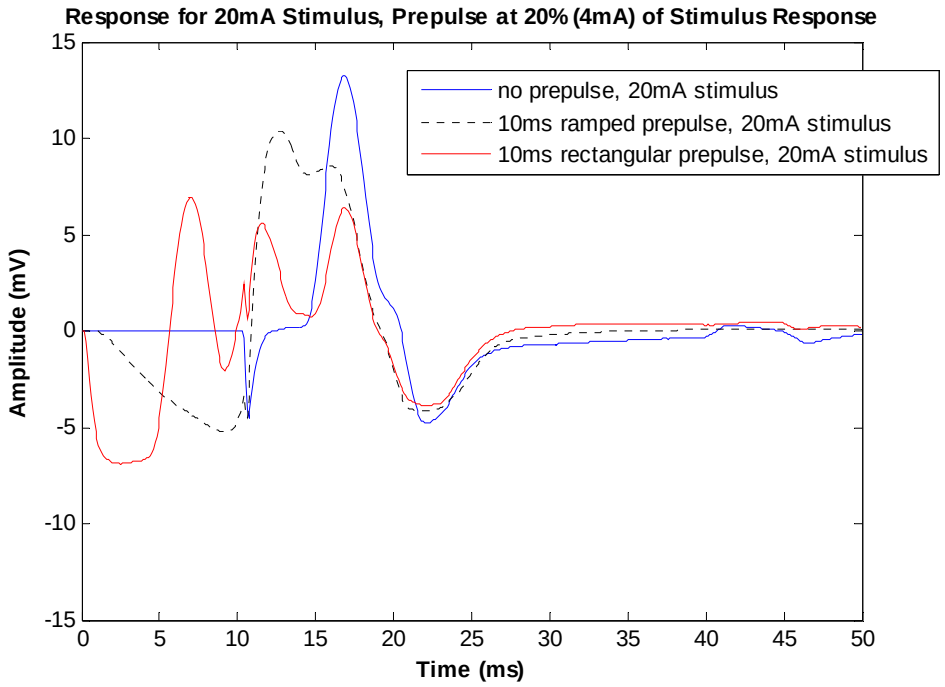

Figure 4-14 – Response for 20 mA stimulus at near maximal M-wave response. Prepulse at 10 ms duration and 20% of stimulus amplitude.

4.3.3 Prepulse Duration Study

Our next experiment focused on finding what prepulse duration produces the most augmenting effect on the M-wave. From the first two experiments we realized that the prepulses have the most pronounced effect at levels about 50 – 60 % of the maximum M-wave response. We also noted that longer duration prepulses have a much more augmenting effect but also tend to recruit motor units themselves. This was also true when the prepulse was set to 20% of the stimulus amplitude. This experiment then focused on the prepulse duration only. We kept the stimulus amplitude fixed at 15 mA which produced an M-wave at 60 % of its maximal level when stimulated with no

prepulse. The prepulse duration was then varied from 0 ms to 20 ms while keeping the prepulse amplitude fixed at 10% of the stimulus amplitude which in this case was 1.5 mA. The protocol consisted of once again delivering three stimuli at each level. First the control stimulus was given which consisted of no prepulse. Then a ramped prepulse at the the set duration and finally a rectangular prepulse was delivered. The results are shown in Figure 4-15. The maximum prepulse effect occurs at around 12 ms of duration. The rectangular prepulse provided a peak to peak amplitude over 2 times more than the control, whereas the ramped prepulse provided a peak to peak amplitude of under 2 times that of the control stimulus. At longer durations, past 12 ms, the rectangular prepulse normalized amplitude started to diminish. However, this was not due to early motor unit recruitment by the prepulse. By looking at the individual responses, it was evident that no early recruitment was taking place at prepulse durations past 12 ms. It may be that the prepulse is inhibiting larger motor units and the order of nerve recruitment could be changing. Hennings et al. reported that very long duration ramped prepulses (500 ms) could change the order of recruitment (Hennings, Arendt-Nielsen, & Andersen, 2005). We noted that rectangular prepulses can accomplish what a ramped prepulse can in terms of augmentation but at lower amplitude levels. This makes sense since a rectangular pulse contains twice as much energy as a ramped pulse. By looking at Figure 4-15, the ramped prepulse normalized amplitude does not decrease at these durations. It seems to be stabilizing at a level about 1.8 times larger than the control stimulus. At durations under 5 ms the ramped prepulse performed much better producing peak to peak amplitudes about

1.2 – 1.4 times larger than the control stimulus. Full results for each prepulse duration are shown in Figure 4-16 and 4-17.

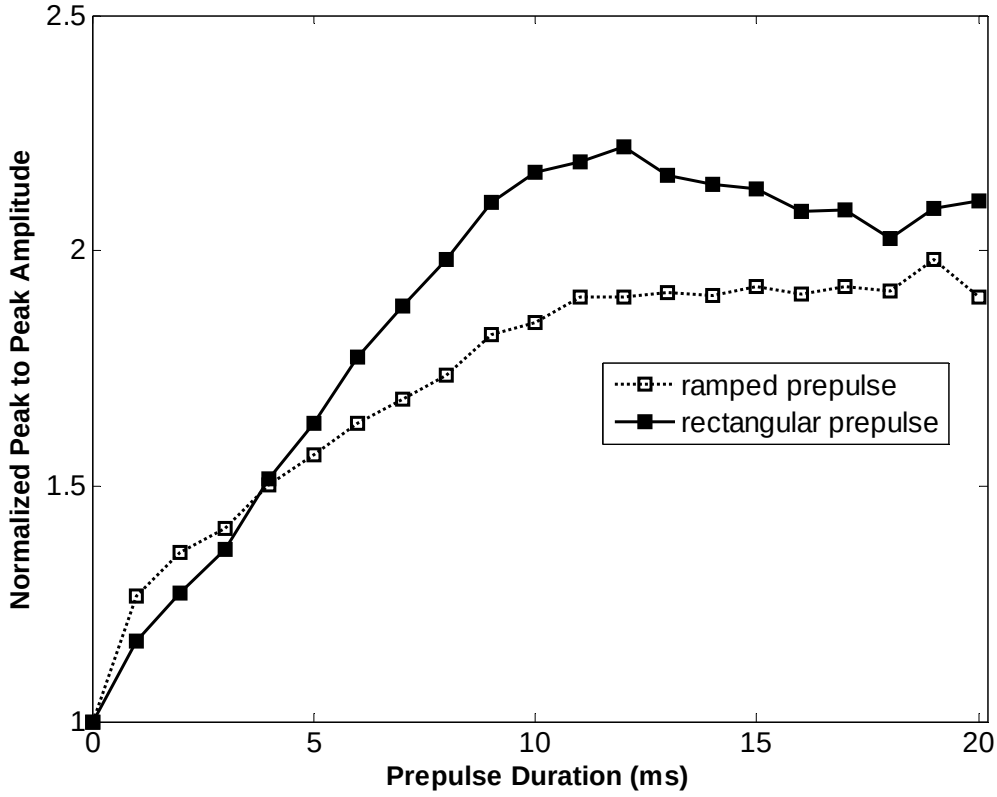

Figure 4-15 – Stimulus response curve for increasing prepulse duration. Peak to peak amplitude was normalized by the control at each prepulse duration.

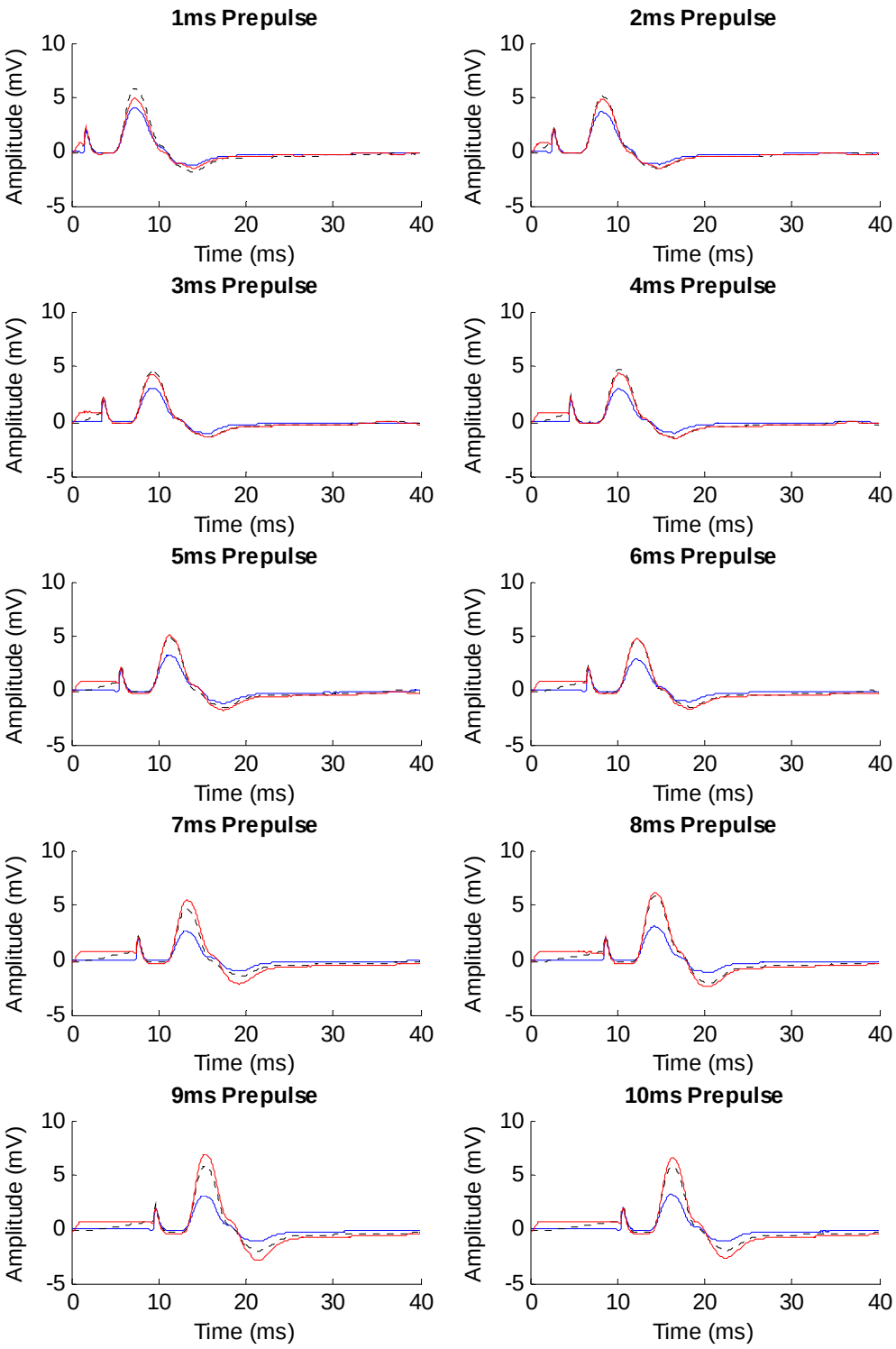

Figure 4-16 – Results from prepulse duration experiment. Durations range from 1 to 10ms.

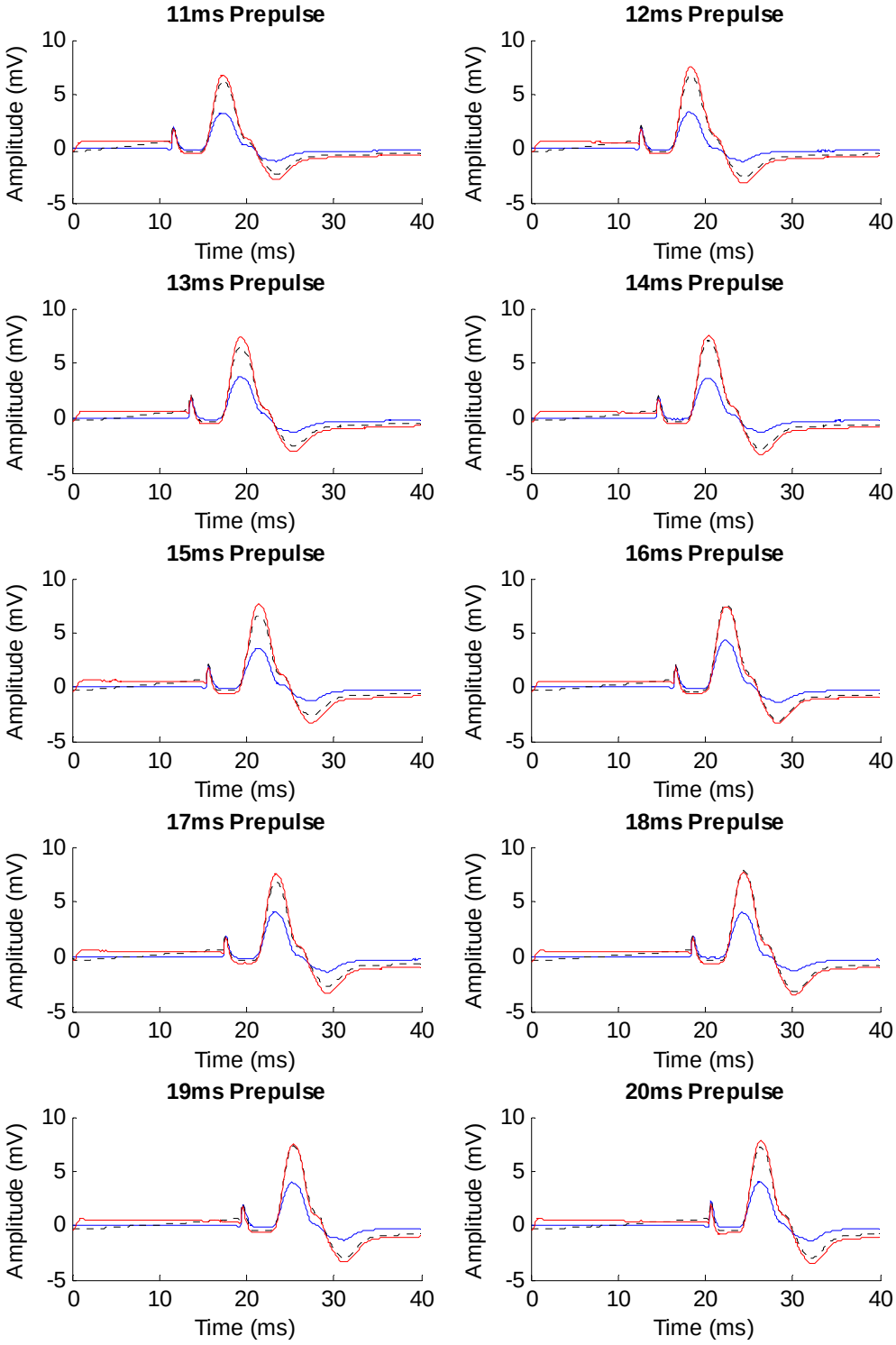

Figure 4-17 – Prepulse duration experiment results continued.

4.3.4 Pulse Train Study

The last study that was carried out was an experiment to look at the effect of prepulses on pulse train stimulation. The previous studies we carried out all utilized a single stimulus followed by a recording and a second stimulus a few seconds later. In pulse train stimulation each subsequent pulse must be delivered at a rate fast enough to elicit a smooth contraction rather than just a twitch. The reason to use pulse trains is that it resembles a natural physiological contraction and can be used to build muscle in patients with atrophy (Banerjee et al., 2005). The use of a single stimulus is more for physiological research rather than rehabilitory purposes. The purpose of conducting this experiment was not only to see the effect of prepulses in train stimulation, but also to see if it was possible to stimulate in a pulse train fashion and record M-waves between stimuli. Normal electrophysiological instrumentation used in the clinic does not provide train stimulation and is used for nerve conduction velocity tests where a single stimulus is delivered. Typical uses of pulse train stimulation arise in a physiotherapy clinic, but again no M-wave recordings are made. Ideally, the minimization of pain during train stimulation would provide the most clinical benefit and restore muscular strength to patients much more comfortably than traditional stimulation.

The protocol we used was to stimulate the motor nerve using 100 μsec pulses 20 times per second. This would provide a constant contraction at the muscle. The 5 ms prepulse was kept at 10 % of the stimulus amplitude since this is deemed the most comfortable. The stimulus amplitude was varied from 5 to 14 mA with the maximum eliciting an M-wave that was 60 % of the maximal response. The stimulus was first ramped up for 1

second to the desired amplitude and then held for 2 seconds and finally ramped down for 1 second to zero amplitude. A recording of the control stimulus at 14 mA is shown in Figure 4-18. This shows that our ramp up and down functions work very well.

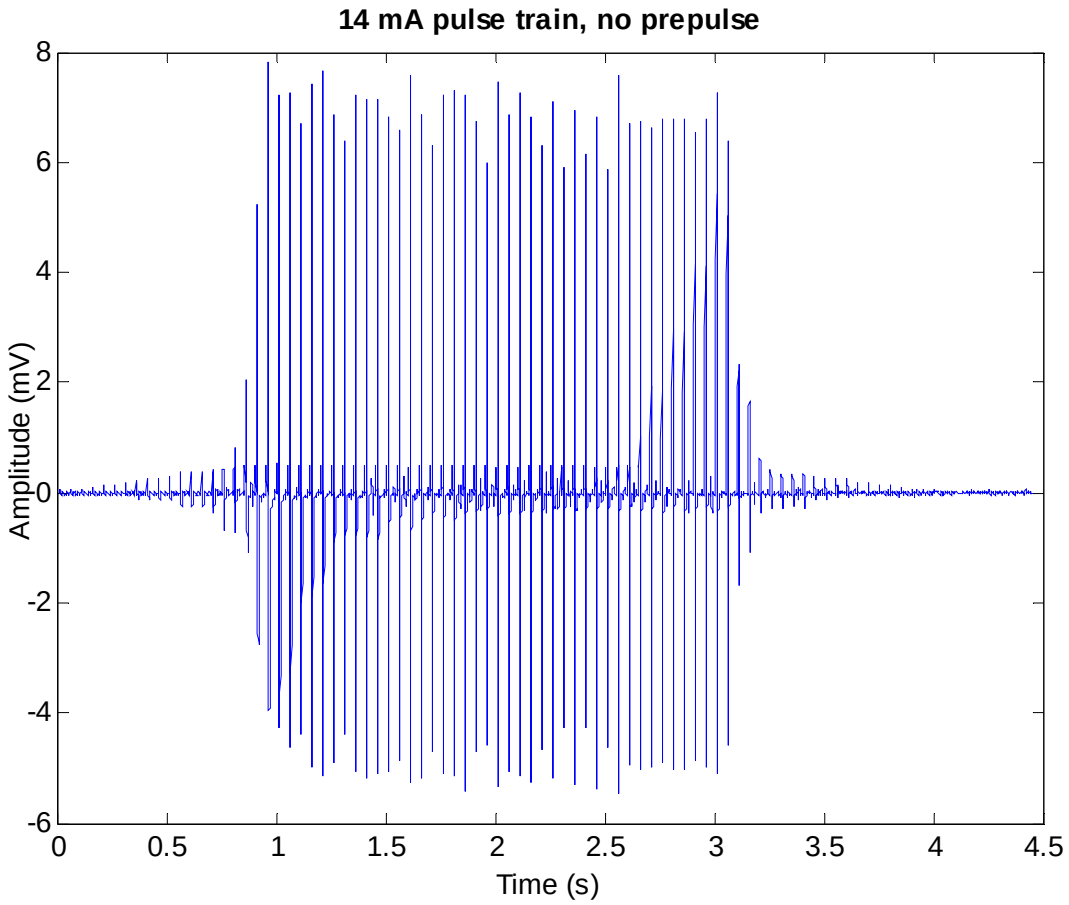

Figure 4-18 – Result from 14 mA pulse train stimulation with no prepulse. The modulated waveform in bold blue is an image artifact and is not present when the data is viewed with a smaller time base

Observing M-waves during train stimulation at lower levels was problematic. Significant noise of the 60 Hz variety was present during the recording but had a varying baseline. Removal of this baseline was difficult since simple filtering techniques would also

corrupt the EMG signal of interest. The baseline was contributed by motion artifact arising from the contractile movement of the thenar muscle. A 20 Hz high pass filter may be used to remove the varying baseline followed by 60 Hz removal technique. Better skin preparation under the recording electrodes and longer shielded cables should attenuate most of the 60 Hz. It was decided to use results where a high signal to noise ratio was present. This occurred at higher amplitudes where the M-wave was much larger than the stimulus artifact. An example of the corrupted data is shown in Figure 4-19. This recording was taken at 9 mA of stimulus amplitude. The stimulus artifact is much larger than the M-wave and overshadows it. The M-wave itself is corrupted by the 60 Hz noise. A closer look at the corrupted M-wave is shown in Figure 4-20.

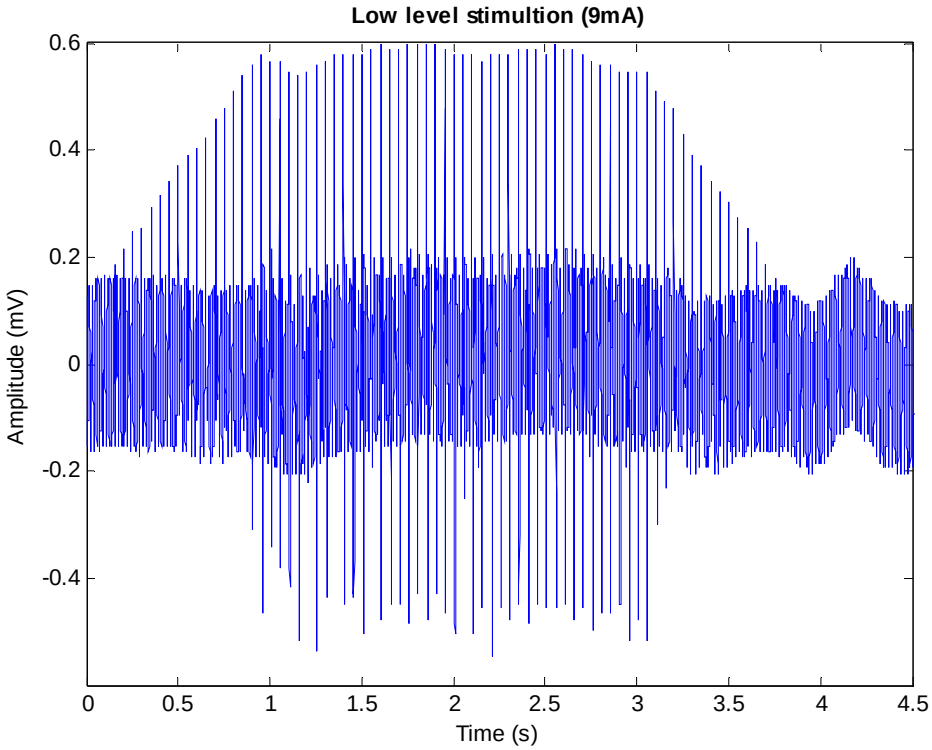

Figure 4-19 – Pulse train recording at 9 mA of stimulus intensity with no prepulse. Large 60 Hz noise corrupts the EMG signal. Note the varying baseline of the noise.

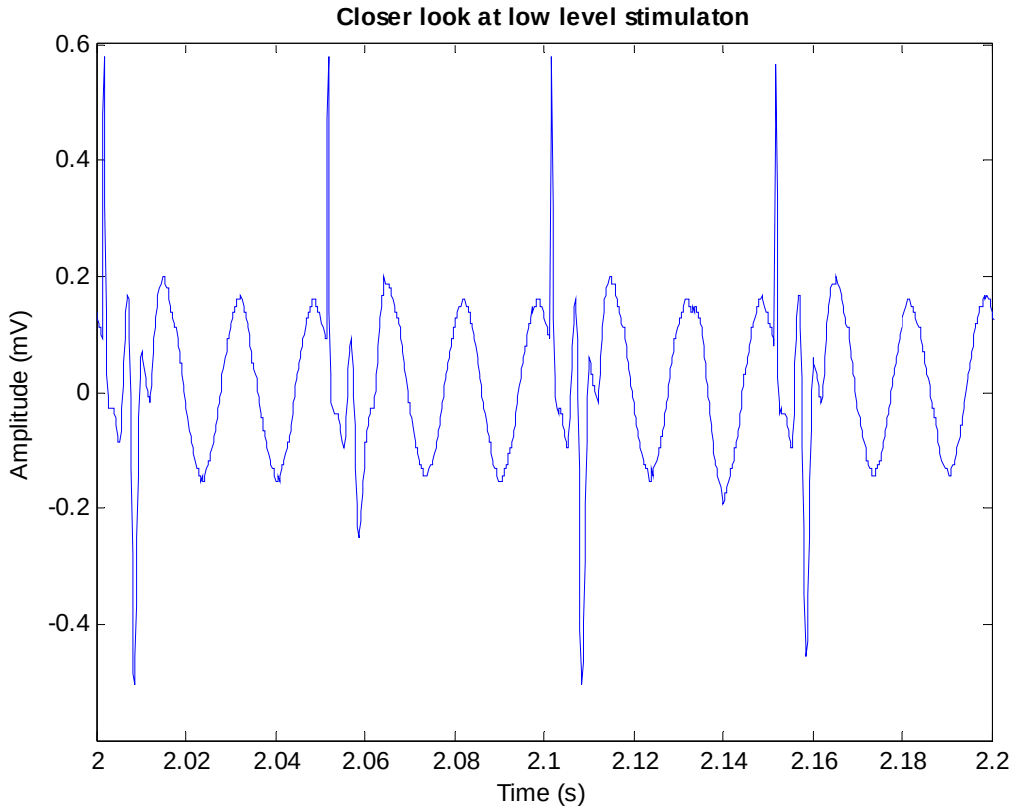

Figure 4-20 – Closer look at low level stimulation recording. The stimulus artifact is quite large compared to the M-wave which is drowned out by 60 Hz.

With low amplitude results being corrupted by noise, our viable data came from higher amplitudes used. The results, shown in Figure 4-21, come from our maximum stimulus amplitude used, which was 14 mA. The entire recording is not shown since the M-wave would be difficult to distinguish with the large time base. Instead, a small portion of the recording, approximately 200 ms, is shown. These results show that using prepulses during train stimulation can affect the M-wave response. The ramped prepulse, shown by the dotted line, produced an average M-wave response approximately 20 % greater than the control stimulus, shown in blue. The rectangular prepulse, shown in red, had an even

greater effect. The average M-wave peak to peak response was approximately 38 % greater than the control stimulus. When compared to the prepulse augmentation levels in our single stimulus experiments, the pulse train study showed decreased levels of augmentation. This is due to the fact that we were stimulating at greater amplitudes with most of the motor units already being activated by the stimulation pulse only case. Only a much smaller number were available for augmentation by the prepulse.

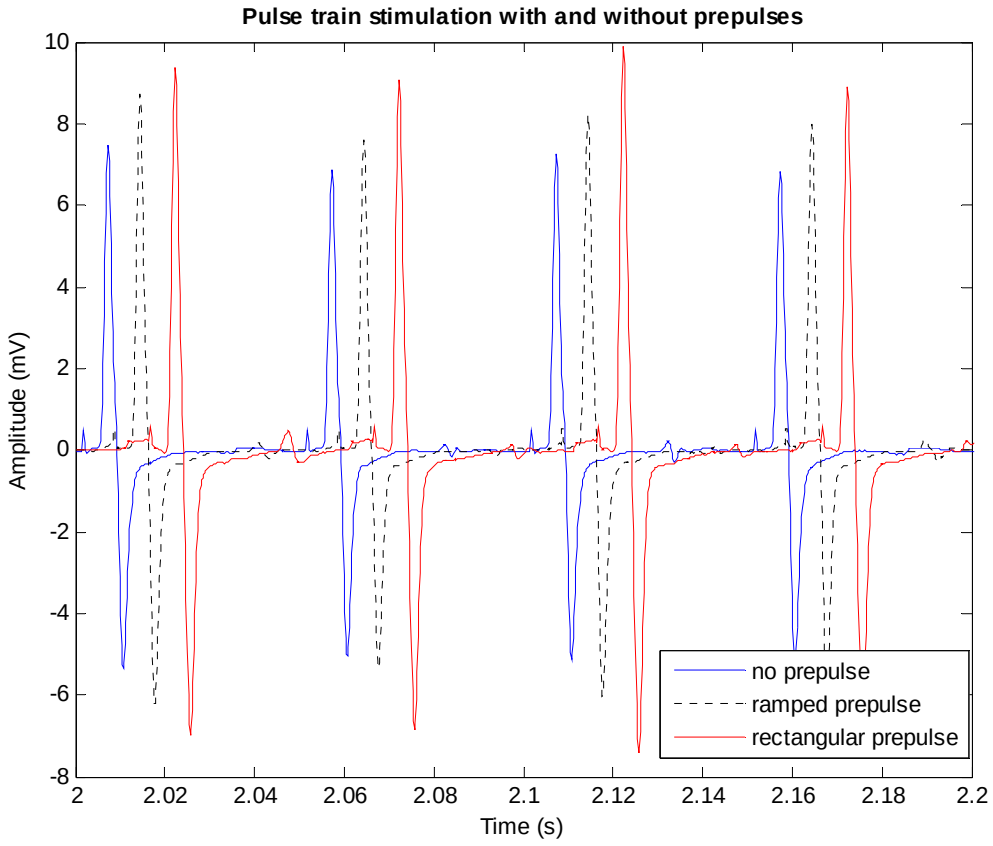

Figure 4-21 – Results from 14 mA pulse train stimulation with and without prepulses.

Another important fact is the minimal stimulus artifact present. Depending on the placement of the stimulating and recording electrodes, small stimulus artifact can be obtained. This also proves that our isolation circuitry is working properly, isolating the EMG amplifier from the stimulation circuit.

Chapter 5: Conclusions

The goal of this thesis project was to design and develop a novel muscle stimulator that can deliver prepulses. We also set out to perform some physiological tests with the stimulator to determine the merits of prepulse stimulation. In terms of hardware design, the stimulator that was prototyped met all our design requirements. It could deliver prepulses of various durations and two shapes: rectangular and ramped. With the stimulator being controlled by a computer, any waveform could be programmed in and delivered to the patient. A fully working LabVIEW interface was developed that was user friendly and customizable. It controlled the various parameters associated with stimulation and recording: amplitude, duration, frequency, and sampling rates. The stimulator delivered constant current pulses and was verified using resistive loads and a small pilot study.

The pilot study that was carried out was used to both test the stimulator and look at the merits of prepulse stimulation. Some interesting data were collected and analyzed. It showed that the maximum benefit when using prepulses occurs at durations around 12 ms. However, at these durations, an increased sensation was felt underneath the stimulating electrode. This could be due to the amplitudes we were using and not due to the duration. We found that prepulses could lower the firing threshold of motor units and hence, for the same stimulus amplitude, a much larger M-wave can be elicited. Our results showed that during single stimulus events, an increase of 42 % can be achieved using 5 ms rectangular prepulses, and an increase of 33 % can be achieved using 5 ms ramped prepulses. With the duration increased to 10 ms, a 64 % increase could be seen in

the M-wave when using rectangular prepulses. Ramped prepulses produced a 51 % increase at 10 ms durations. For our subject, the most comforting stimuli occurred with 5 ms prepulses. In terms of energy delivered for each stimulus, the ramped prepulse has half the energy of the rectangular prepulse. However, the M-wave responses elicited by ramped prepulses augment the peak to peak response by more than 50 % of the augmentation of the rectangular pulse. This makes the ramped prepulse much more efficient in terms of augmenting the M-wave.

The most clinically relevant result came from pulse train stimulation. If amplitude requirements could be lowered during pulse train stimulation then perhaps perceived pain could also be lowered. Our results showed that using 5 ms rectangular prepulses the peak to peak M-wave response could be increased almost 40 %. When ramped prepulses were used an increase of almost 20 % was achieved.

Using prepulses to lower amplitude requirements during muscle stimulation could be a method to lower the pain perceived by patients. This thesis outlined the design of a stimulator to deliver the prepulses, and with our preliminary data we showed significant peak to peak M-wave increases with the use of both ramped and rectangular prepulses.

5.1 Future Work

With the stimulator designed and , many physiological tests can now be undertaken. First, a much larger sample size is needed to verify the preliminary results we obtained. A detailed study should be conducted to look at the effects of prepulse amplitude without any stimulus pulse present. We only carried out studies that varied the prepulse duration and kept the prepulse amplitude fixed to 10 or 20 % of the stimulus amplitude. In order to

observe the amplitude effects of the prepulse, a study should be carried out that varies the amplitude of the prepulse while keeping the duration fixed and observing for any M-waves. Once this study is carried out, a pulse train study can be undertaken. However, on the signal processing front, a more elaborate method to remove 60 Hz noise during train stimulation would be necessary. This study would have the most interesting results in terms of clinical benefit. The pulse train study should be tied together with a pain perception study. A look at whether or not prepulses can increase the pain threshold is very important. If in fact, as we hypothesize, that pain arises from high stimulus amplitudes, the lowering of amplitude requirements would decrease pain perception. Different prepulse waveforms should also be tested since the stimulator design allows for any waveform to be programmed in.

Currently the stimulator is controlled by LabVIEW and data input and output is passed through a National Instruments data acquisition board that resides inside a desktop PC. In order to make the system much more portable and remove the bulky desktop PC, a new design for the control system should be looked at. With the advent of USB enabled microcontrollers, perhaps a total data acquisition and output solution can be implemented in a microcontroller. This would allow a laptop to control all the stimulus parameters and make the system much more hospital friendly.

References

Alon, G., Kantor, G., & Ho, H. S. (1994). Effects of electrode size on basic excitatory responses and on selected stimulus parameters. *J Orthop Sports Phys Ther, 20*(1), 29-35.

Balogun, J. A. (1986). Pain complaint and muscle soreness associated with high-voltage electrical stimulation: effect of ramp time. *Percept Mot Skills, 62*(3), 799-810.

Banerjee, P., Caulfield, B., Crowe, L., & Clark, A. (2005). Prolonged electrical muscle stimulation exercise improves strength and aerobic capacity in healthy sedentary adults. *J Appl Physiol, 99*(6), 2307-2311.

Baratta, R., Ichie, M., Hwang, S. K., & Solomonow, M. (1989). Orderly stimulation of skeletal muscle motor units with tripolar nerve cuff electrode. *IEEE Trans Biomed Eng, 36*(8), 836-843.

Cooper, J. B., Jane, J. A., Alves, W. M., & Cooper, E. B. (1999). Right median nerve electrical stimulation to hasten awakening from coma. *Brain Inj, 13*(4), 261-267.

Currier, D. P., & Mann, R. (1983). Muscular strength development by electrical stimulation in healthy individuals. *Phys Ther, 63*(6), 915-921.

Data sheet for AD202: Low Cost, Miniature Isolation Amplifier Powered Directly From a +15 V DC Supply Retrieved July 17, 2008, from http://www.analog.com/static/imported-files/data_sheets/AD202_204.pdf

Delitto, A., Strube, M. J., Shulman, A. D., & Minor, S. D. (1992). A study of discomfort with electrical stimulation. *Phys Ther, 72*(6), 410-421; discussion on 421-414.

Deurloo, K. E., Holsheimer, J., & Bergveld, P. (2001). The effect of subthreshold prepulses on the recruitment order in a nerve trunk analyzed in a simple and a realistic volume conductor model. *Biol Cybern, 85*(4), 281-291.

Dobsak, P., Novakova, M., Siegelova, J., Fiser, B., Vitovec, J., Nagasaka, M., et al. (2006). Low-frequency electrical stimulation increases muscle strength and improves blood supply in patients with chronic heart failure. *Circ J, 70*(1), 75-82.

Fang, Z. P., & Mortimer, J. T. (1991a). A method to effect physiological recruitment order in electrically activated muscle. *IEEE Trans Biomed Eng, 38*(2), 175-179.

Fang, Z. P., & Mortimer, J. T. (1991b). Selective activation of small motor axons by quasi-trapezoidal current pulses. *IEEE Trans Biomed Eng, 38*(2), 168-174.

Geddes, L. A. (1972). *Electrodes and the Measurements of Bioelectric Events*: John Wiley and Sons, Inc.

Grill, W. M., & Mortimer, J. T. (1997). Inversion of the current-distance relationship by transient depolarization. *IEEE Trans Biomed Eng, 44*(1), 1-9.

Guyton, A. C., & Hall, J. E. (2006). *Textbook of Medical Physiology* (11 ed.). Philadelphia: Elsevier Saunders.

Henneman, E., Somjen, G., & Carpenter, D. O. (1965). Excitability and inhibitability of motoneurons of different sizes. *J Neurophysiol, 28*(3), 599-620.

Hennings, K., Arendt-Nielsen, L., & Andersen, O. K. (2005). Orderly activation of human motor neurons using electrical ramp prepulses. *Clin Neurophysiol, 116*(3), 597-604.

Hennings, K., Arendt-Nielsen, L., Christensen, S. S., & Andersen, O. K. (2005). Selective activation of small-diameter motor fibres using exponentially rising waveforms: a theoretical study. *Med Biol Eng Comput, 43*(4), 493-500.

Horowitz, P., & Hill, W. (1989). *The Art of Electronics* (2 ed.). New York: Cambridge University Press.

Kamen, G., & Caldwell, G. E. (1996). Physiology and interpretation of the electromyogram. *J Clin Neurophysiol, 13*(5), 366-384.

Laufer, Y., Ries, J. D., Leininger, P. M., & Alon, G. (2001). Quadriceps femoris muscle torques and fatigue generated by neuromuscular electrical stimulation with three different waveforms. *Phys Ther, 81*(7), 1307-1316.

Laughman, R. K., Youdas, J. W., Garrett, T. R., & Chao, E. Y. (1983). Strength changes in the normal quadriceps femoris muscle as a result of electrical stimulation. *Phys Ther, 63*(4), 494-499.

Lieber, R. L., Silva, P. D., & Daniel, D. M. (1996). Equal effectiveness of electrical and volitional strength training for quadriceps femoris muscles after anterior cruciate ligament surgery. *J Orthop Res, 14*(1), 131-138.

McMiken, D. F., Todd-Smith, M., & Thompson, C. (1983). Strengthening of human quadriceps muscles by cutaneous electrical stimulation. *Scand J Rehabil Med, 15*(1), 25-28.

McNeal, D. R. (1977). 2000 years of electrical stimulation. In T. F. Hambrecht & J. B. Reswick (Eds.), *Functional electrical stimulation - application in neural prostheses* (pp. 3-33). New York: M. Dekker.

Neder, J. A., Sword, D., Ward, S. A., Mackay, E., Cochrane, L. M., & Clark, C. J. (2002). Home based neuromuscular electrical stimulation as a new rehabilitative strategy for severely disabled patients with chronic obstructive pulmonary disease (COPD). *Thorax, 57*(4), 333-337.

Nelson, R. M., Hayes, K. W., & Currier, D. P. (1999). *Clinical Electrotherapy* (3 ed.). Stamford, Conn.: Appleton & Lange.

Netter, F. H., Craig, J. A., & Perkins, J. (2002). *Atlast of Neuroanatomy and Neurophysiology*. Teterboro, NJ: Icon Custom Communications.

Peckham, P. H., & Knutson, J. S. (2005). Functional electrical stimulation for neuromuscular applications. *Annu Rev Biomed Eng, 7*, 327-360.

Poletto, C. J., & Van Doren, C. L. (1999). A high voltage, constant current stimulator for electrocutaneous stimulation through small electrodes. *IEEE Trans Biomed Eng, 46*(8), 929-936.

Poletto, C. J., & Van Doren, C. L. (2002). Elevating pain thresholds in humans using depolarizing prepulses. *IEEE Trans Biomed Eng, 49*(10), 1221-1224.

Prochazka, A., Gauthier, M., Wieler, M., & Kenwell, Z. (1997). The bionic glove: an electrical stimulator garment that provides controlled grasp and hand opening in quadriplegia. *Arch Phys Med Rehabil, 78*(6), 608-614.

Prutchi, D., & Norris, M. (2005). *Design and Development of Medical Electronic Instrumentation*. New Jersey: John Wiley & Sons.

Quittan, M., Sochor, A., Wiesinger, G. F., Kollmitzer, J., Sturm, B., Pacher, R., et al. (1999). Strength improvement of knee extensor muscles in patients with chronic heart failure by neuromuscular electrical stimulation. *Artif Organs, 23*(5), 432-435.

Sassen, M., & Zimmermann, M. (1973). Differential blocking of myelinated nerve fibres by transient depolarization. *Pflugers Arch, 341*(3), 179-195.

Selkowitz, D. M. (1985). Improvement in isometric strength of the quadriceps femoris muscle after training with electrical stimulation. *Phys Ther, 65*(2), 186-196.

Tanner, J. A. (1962). Reversible blocking of nerve conduction by alternating-current excitation. *Nature, 195*, 712-713.

Tortora, G. J., & Grabowski, S. R. (2003). *Principles of Anatomy and Physiology* (10 ed.). New York: Wiley.

van Bolhuis, A. I., Holsheimer, J., & Savelberg, H. H. (2001). A nerve stimulation method to selectively recruit smaller motor-units in rat skeletal muscle. *J Neurosci Methods, 107*(1-2), 87-92.

Ward, A. R. (1980). In *Electricity Fields and Waves in Therapy* (pp. 17-33). Marickville: Science Press.

Appendix 1 – Circuit Schematics

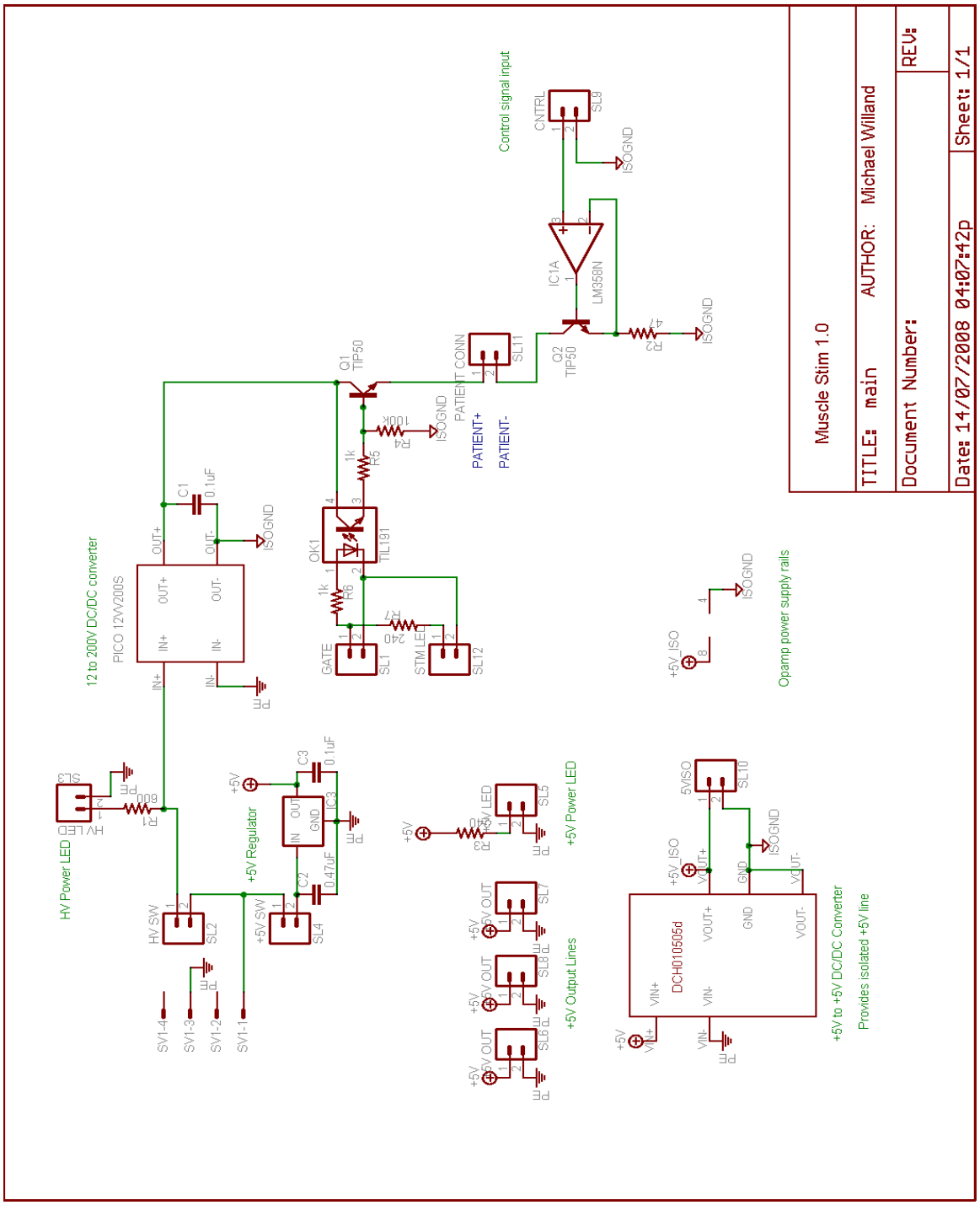

Figure A- 1 – Circuit schematic for main control circuit board

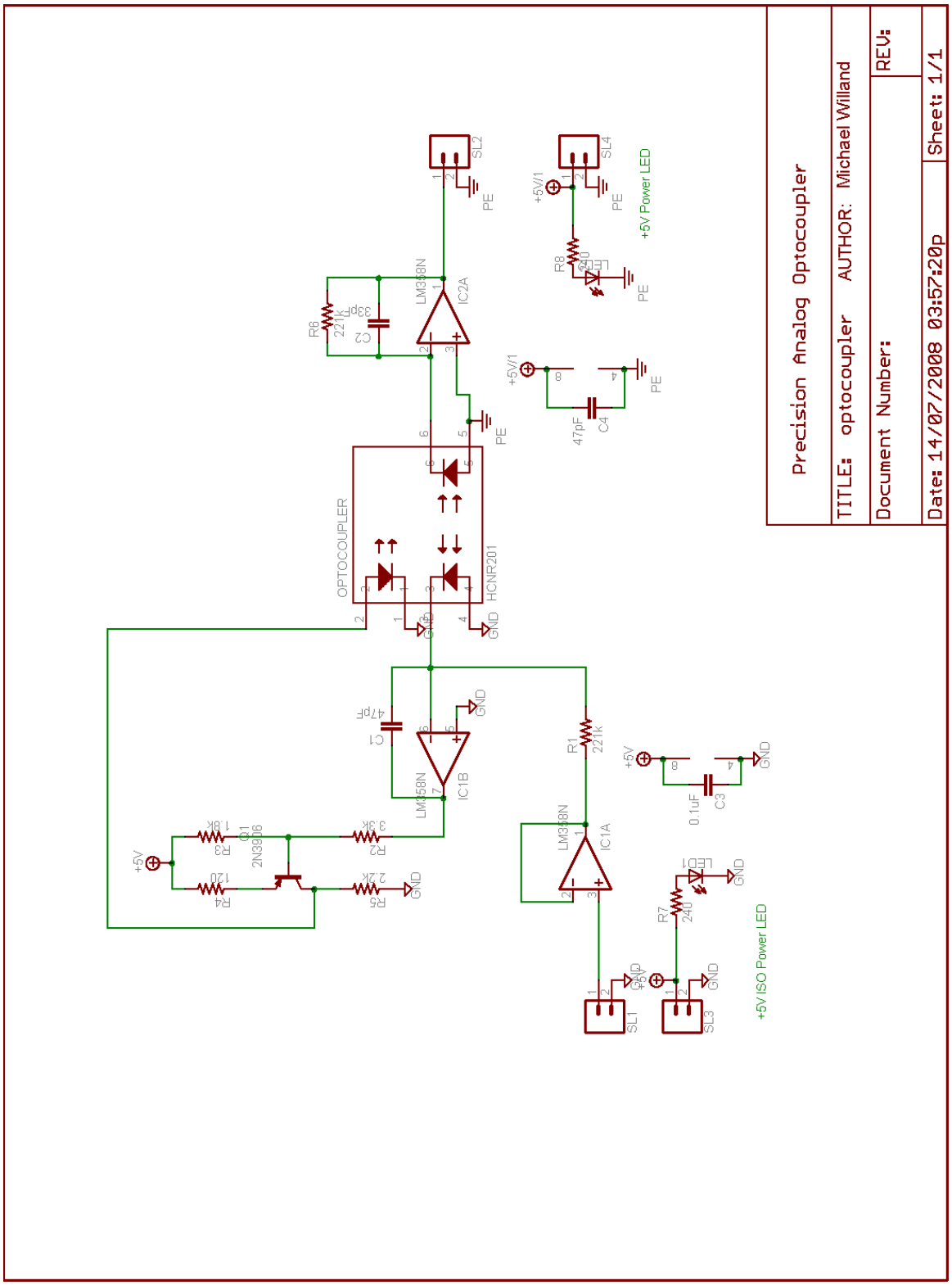

Figure A- 2 – Optocoupler circuit schematic

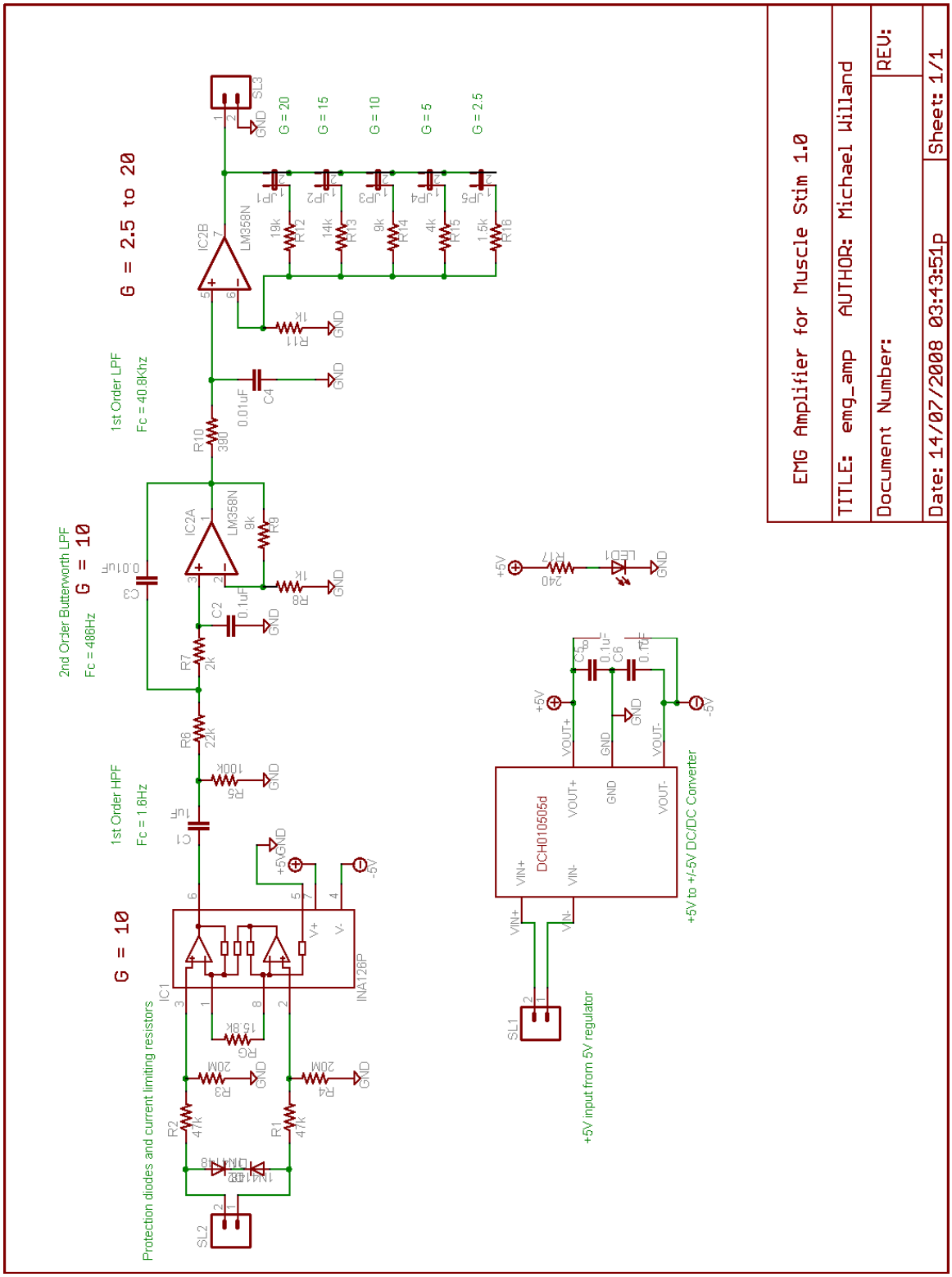

Figure A- 3 – Electromyography amplifier circuit schematics

Appendix 2 – LabVIEW Wiring Diagrams

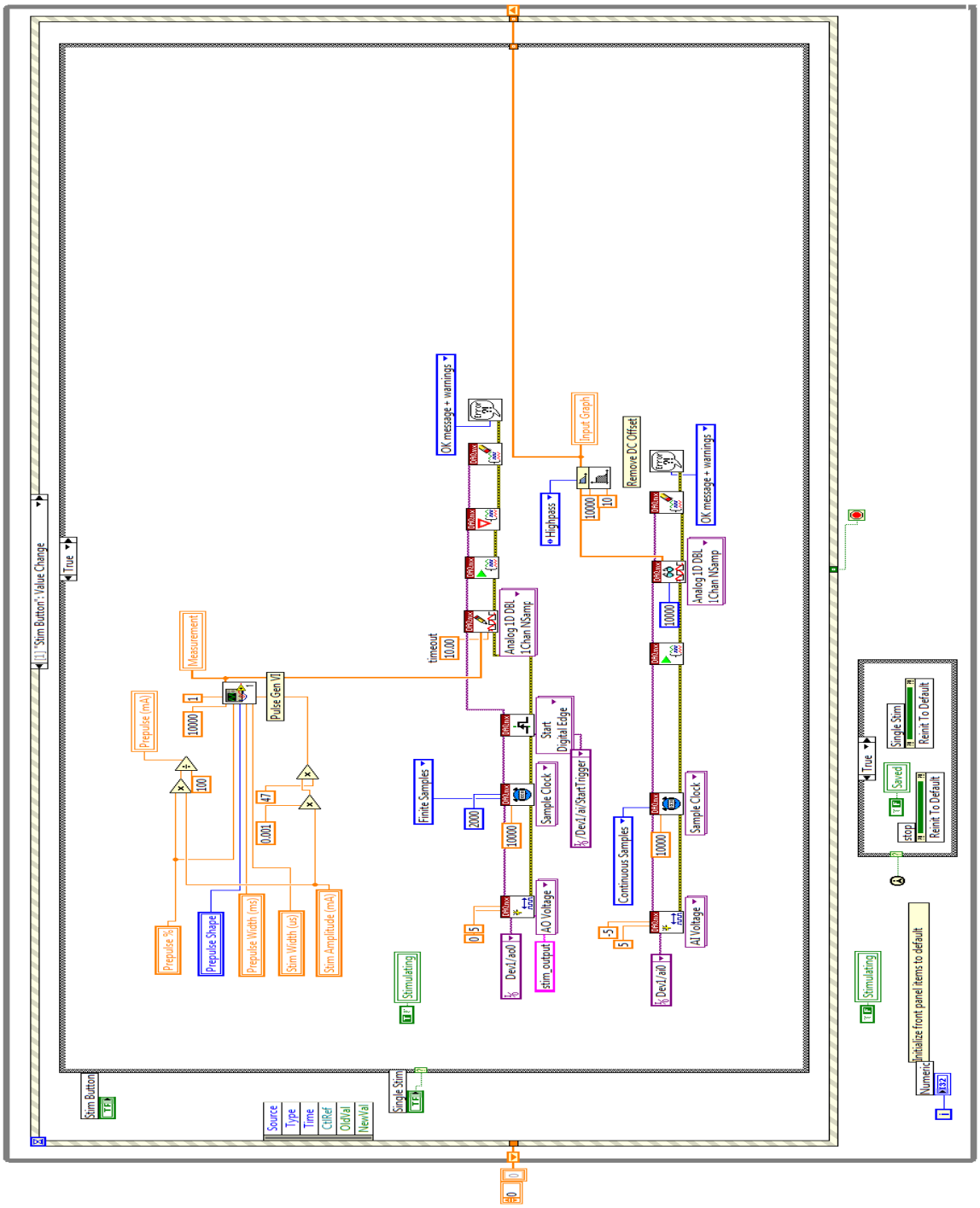

Figure A- 4 – Single Stimulus wiring diagram. Shows the case where only a single stimulus is elicited, no trials.

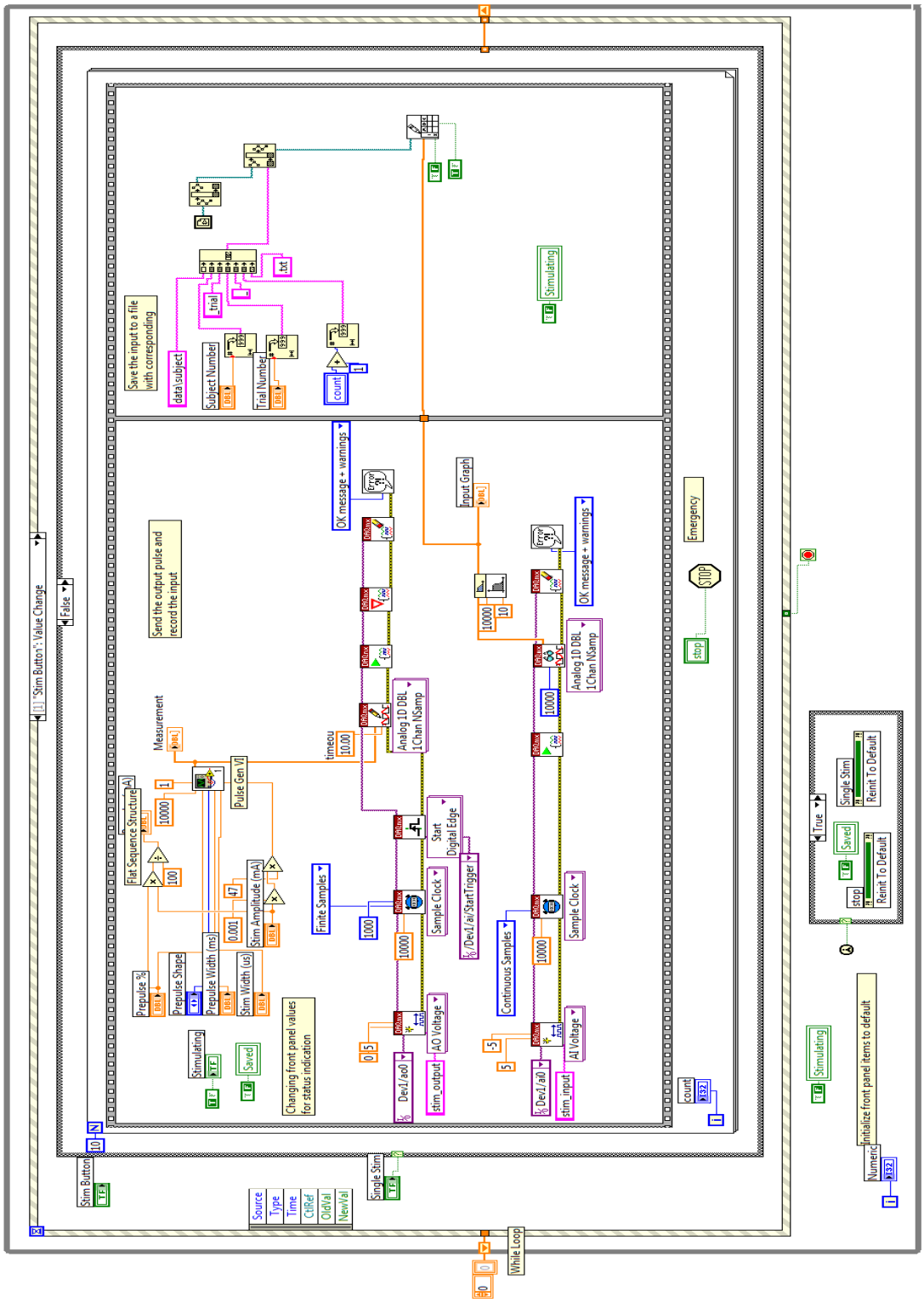

Figure A- 5 – Single Stimulus wiring diagram, multi trial section. After each trial the data is saved to a file.

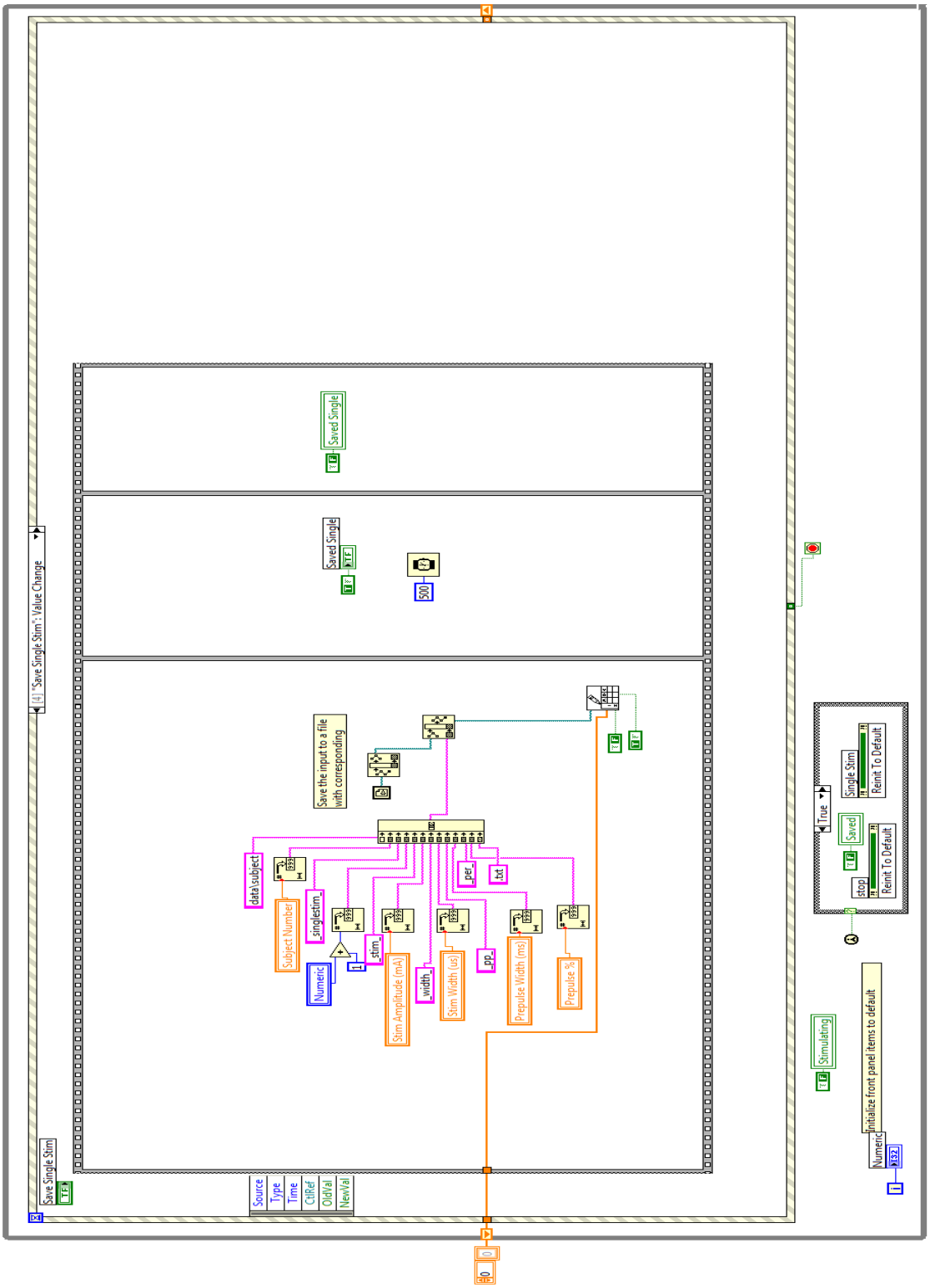

Figure A- 6 – Single stimulus wiring diagram showing file saving section

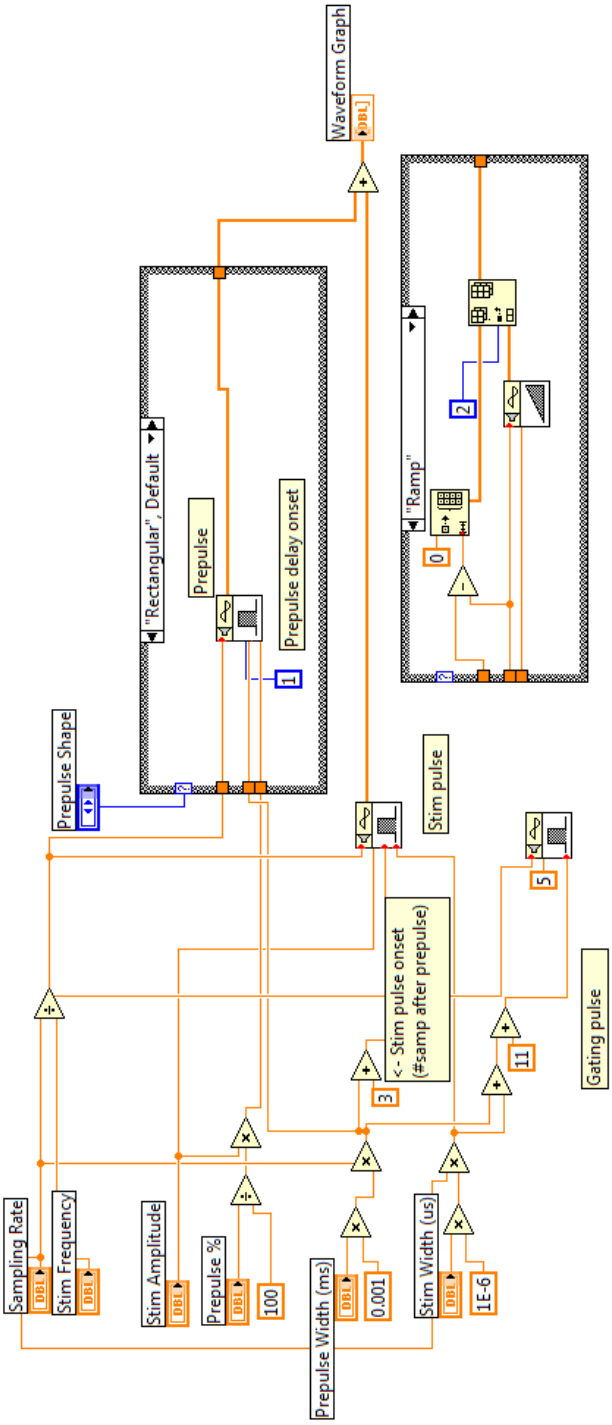

Figure A- 7 – Single stimulus pulse generation VI showing both ramp and rectangular prepulse code

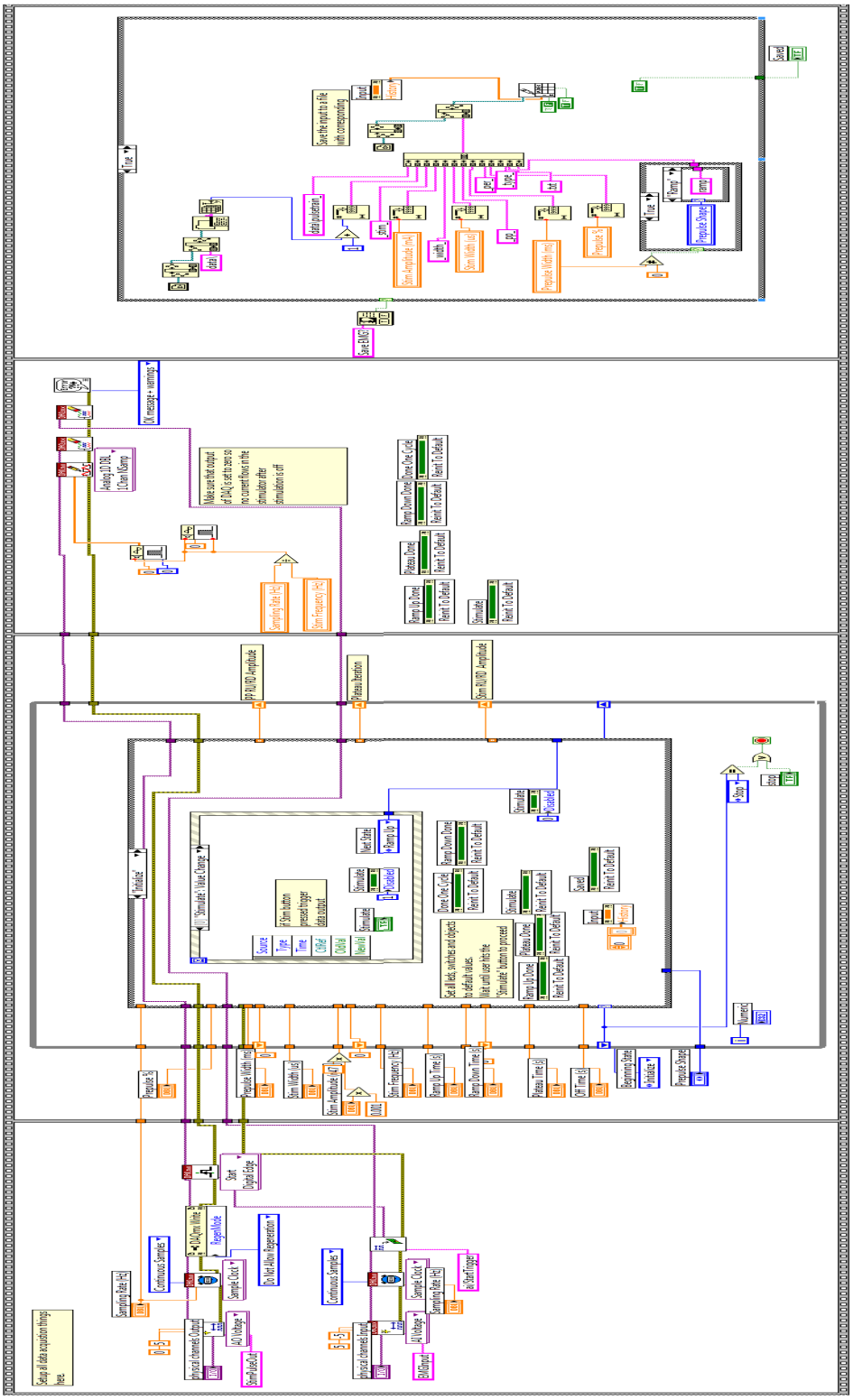

Figure A- 8 – Overview of pulse train generation wiring diagram

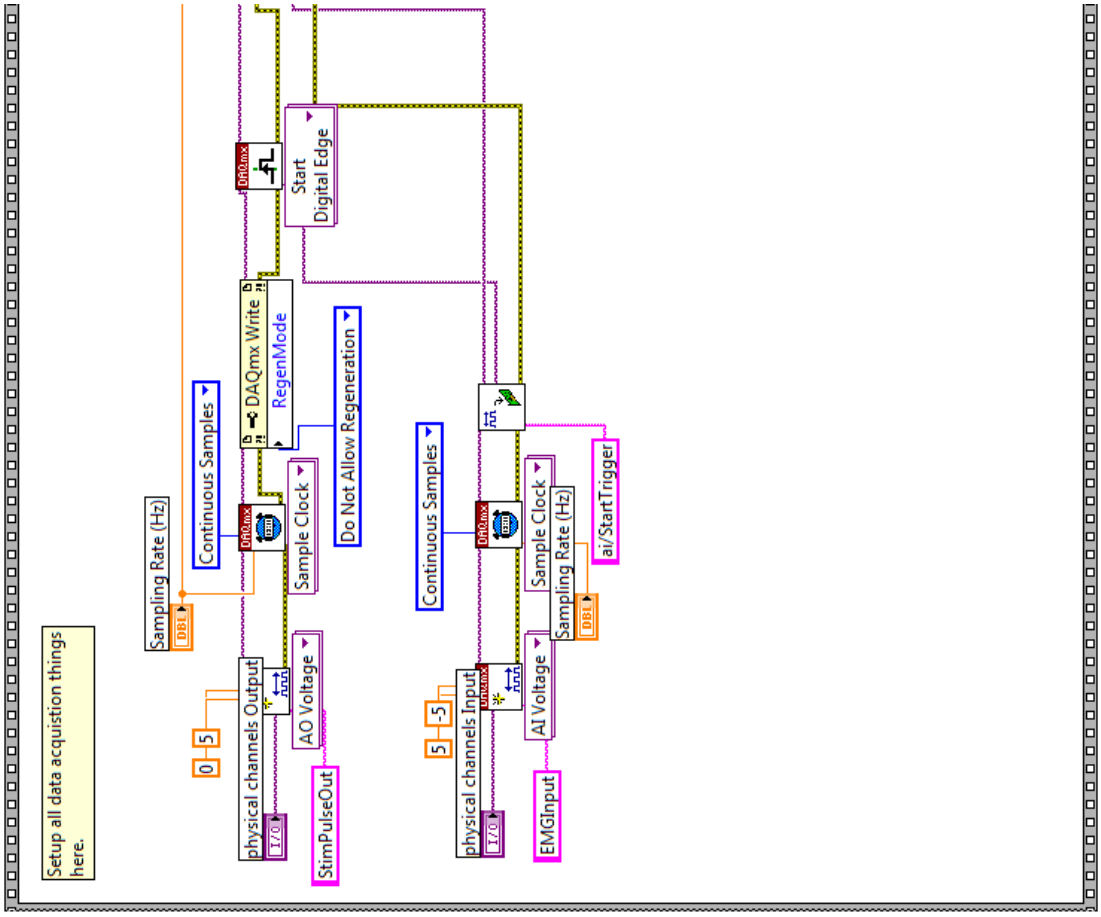

Figure A- 9 – Wiring diagram for acquisition setup in pulse train generation program

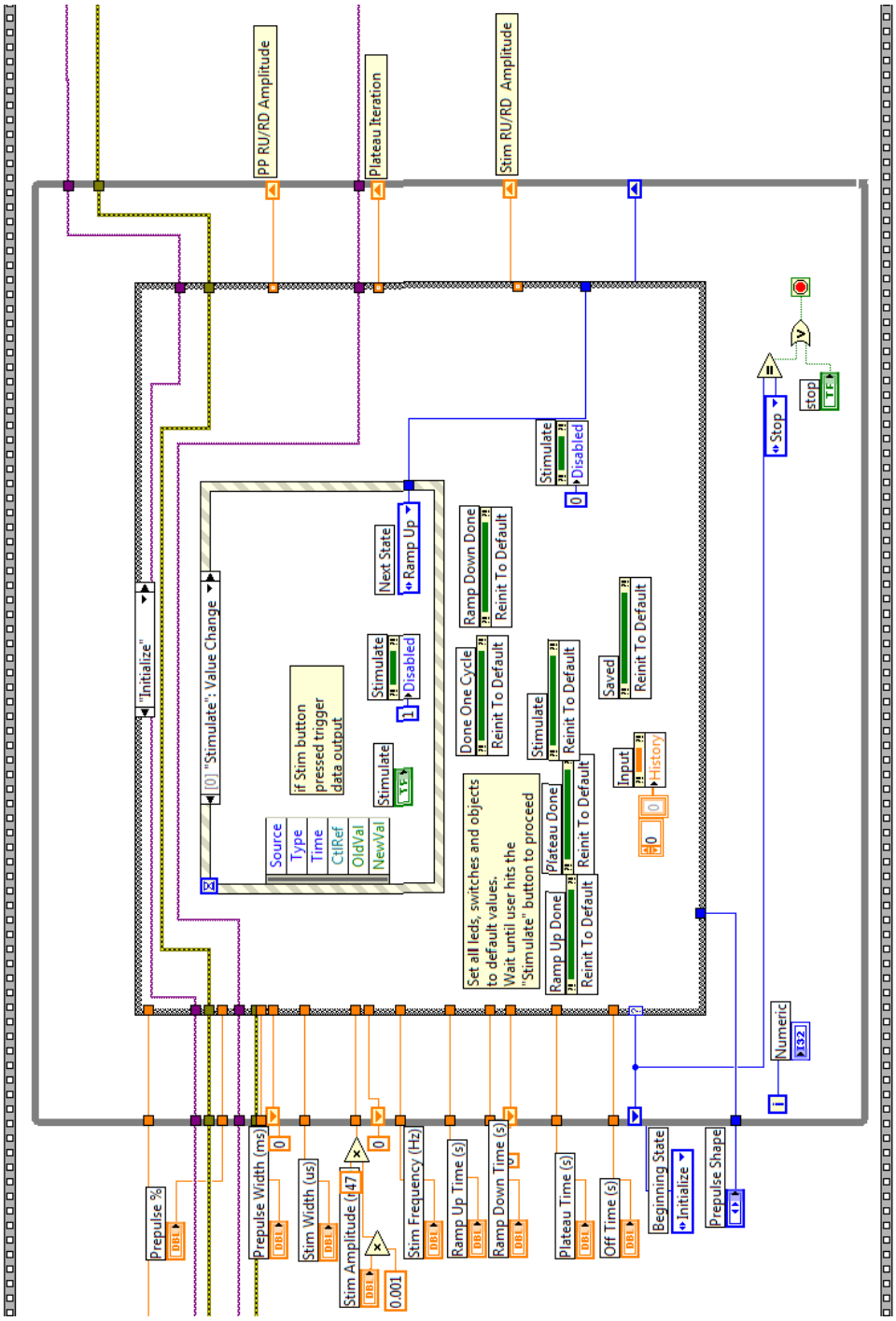

Figure A- 10 – Pulse train wiring diagram showing initialization state

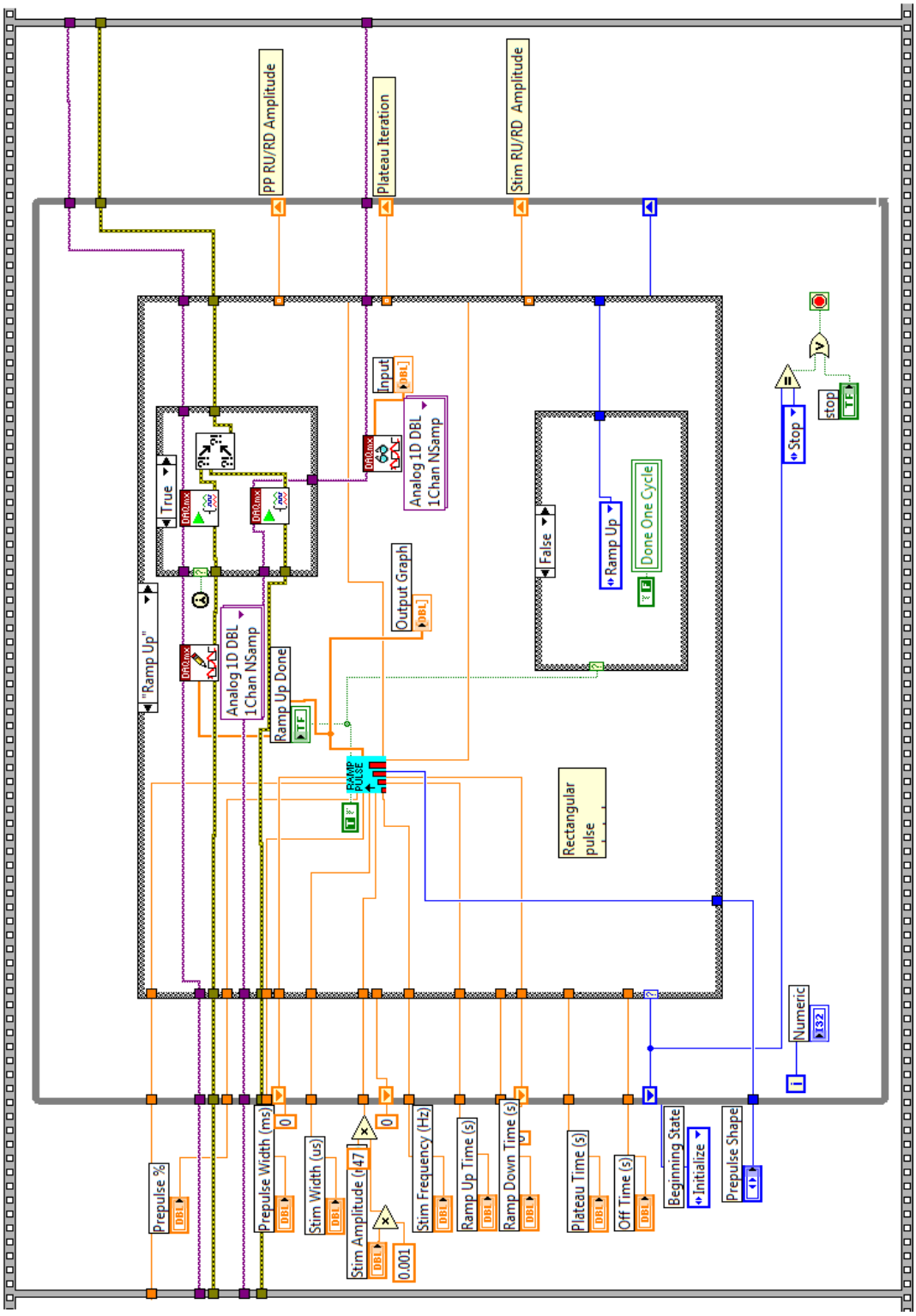

Figure A- 11 – Pulse train wiring diagram showing ramp up state

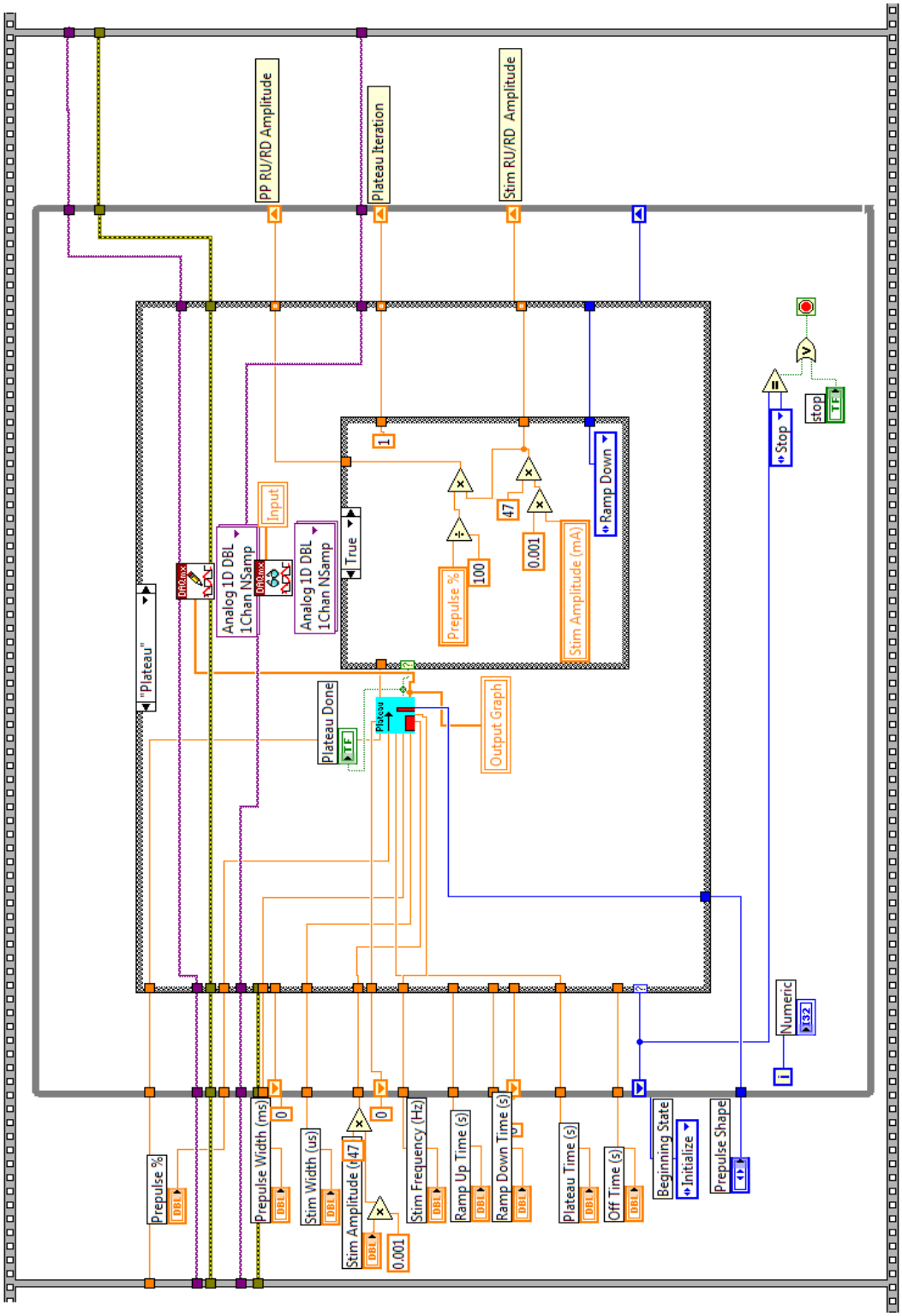

Figure A- 12 – Pulse train wiring diagram showing plateau state

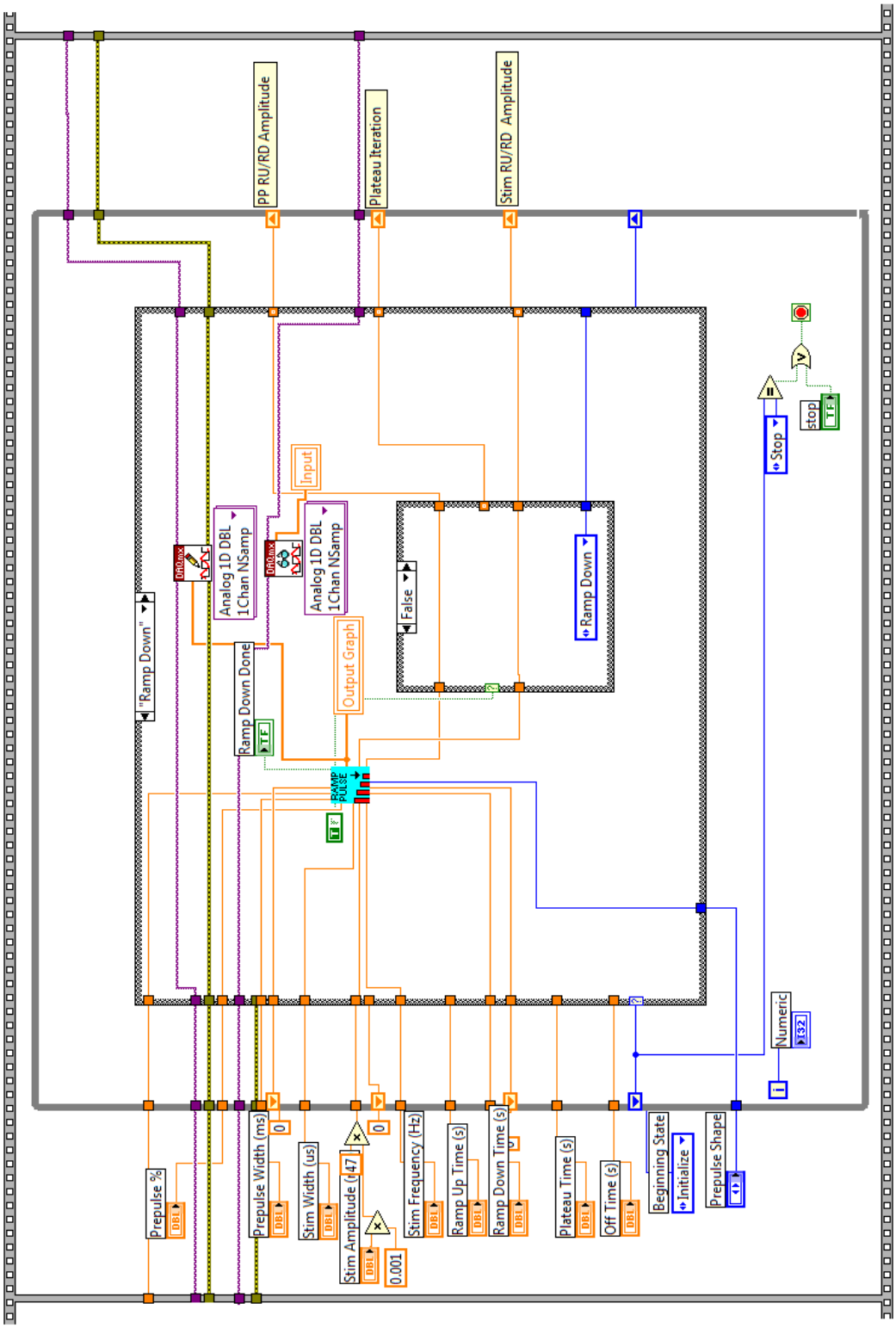

Figure A- 13 – Pulse train wiring diagram showing ramp down state

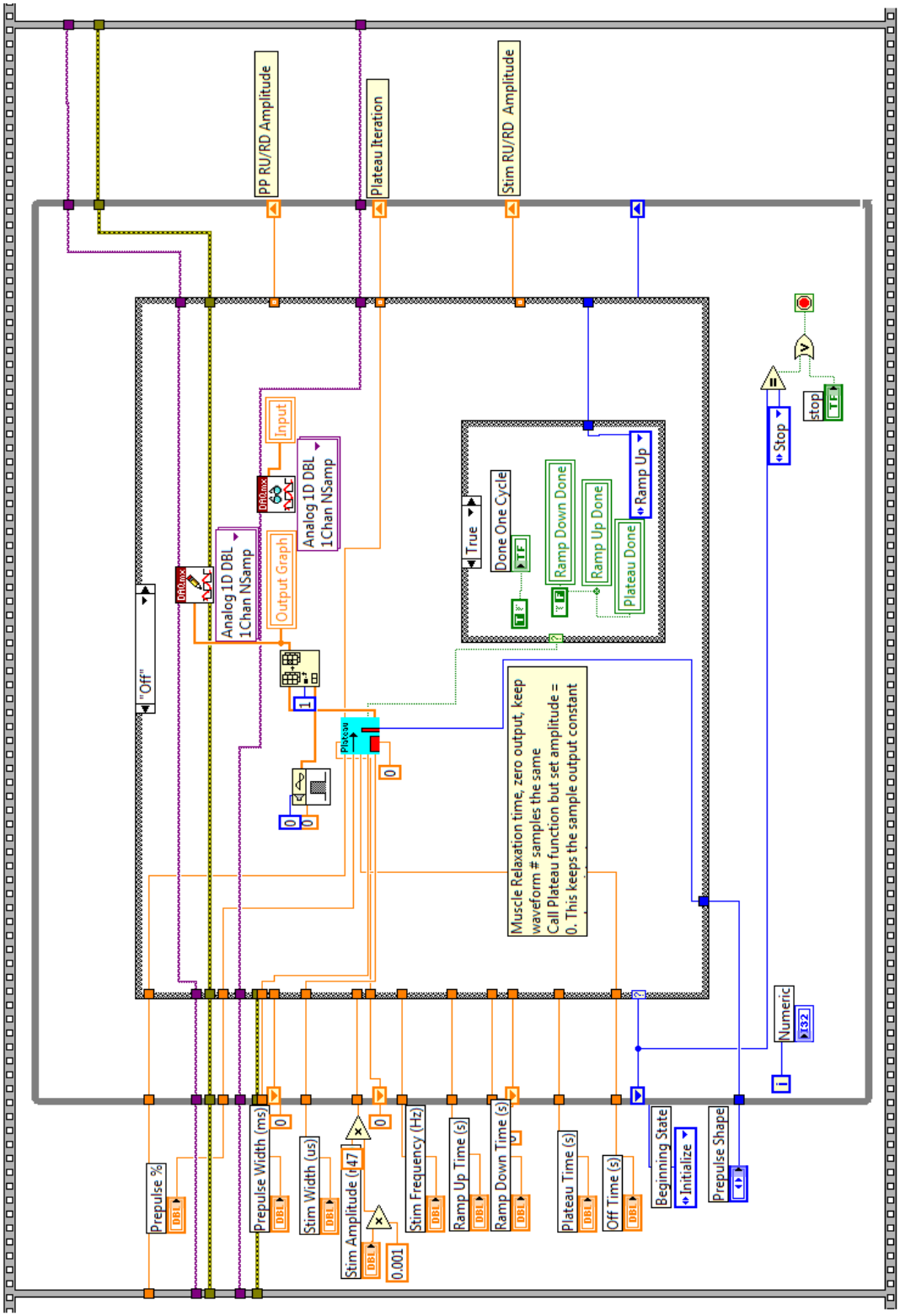

Figure A- 14 – Pulse train wiring diagram showing off state

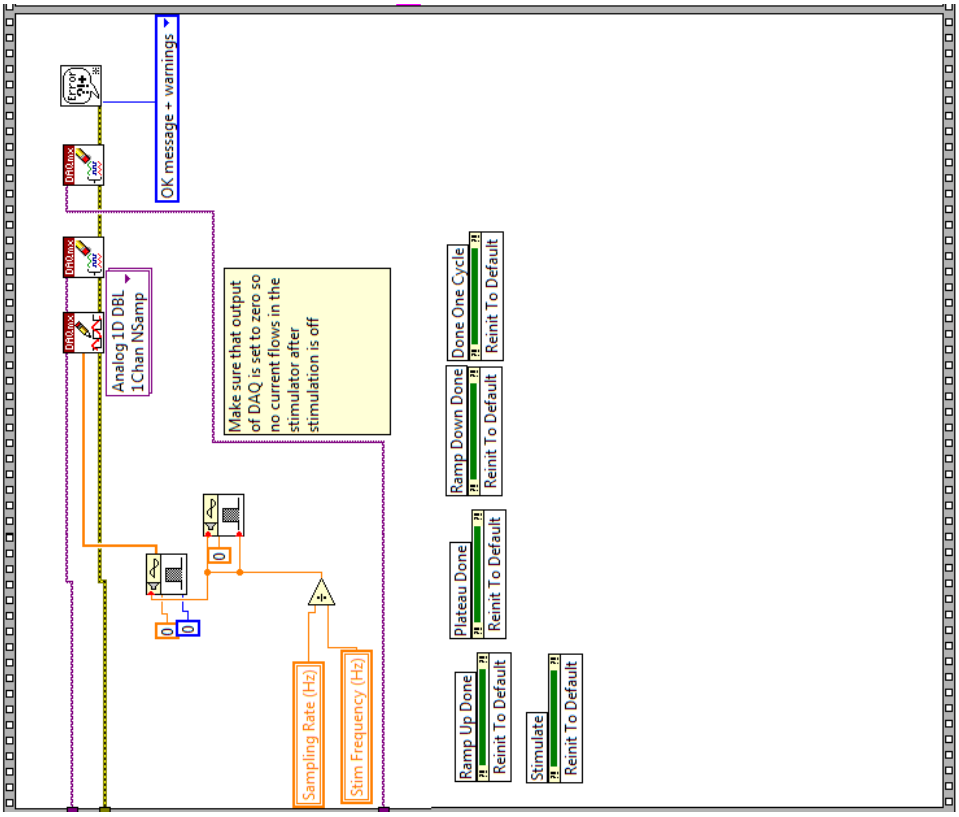

Figure A- 15 – Pulse train wiring diagram showing data acquisition closure stage, notice the zero amplitude square waveforms used to ensure output is set to zero when no stimulation is taking place

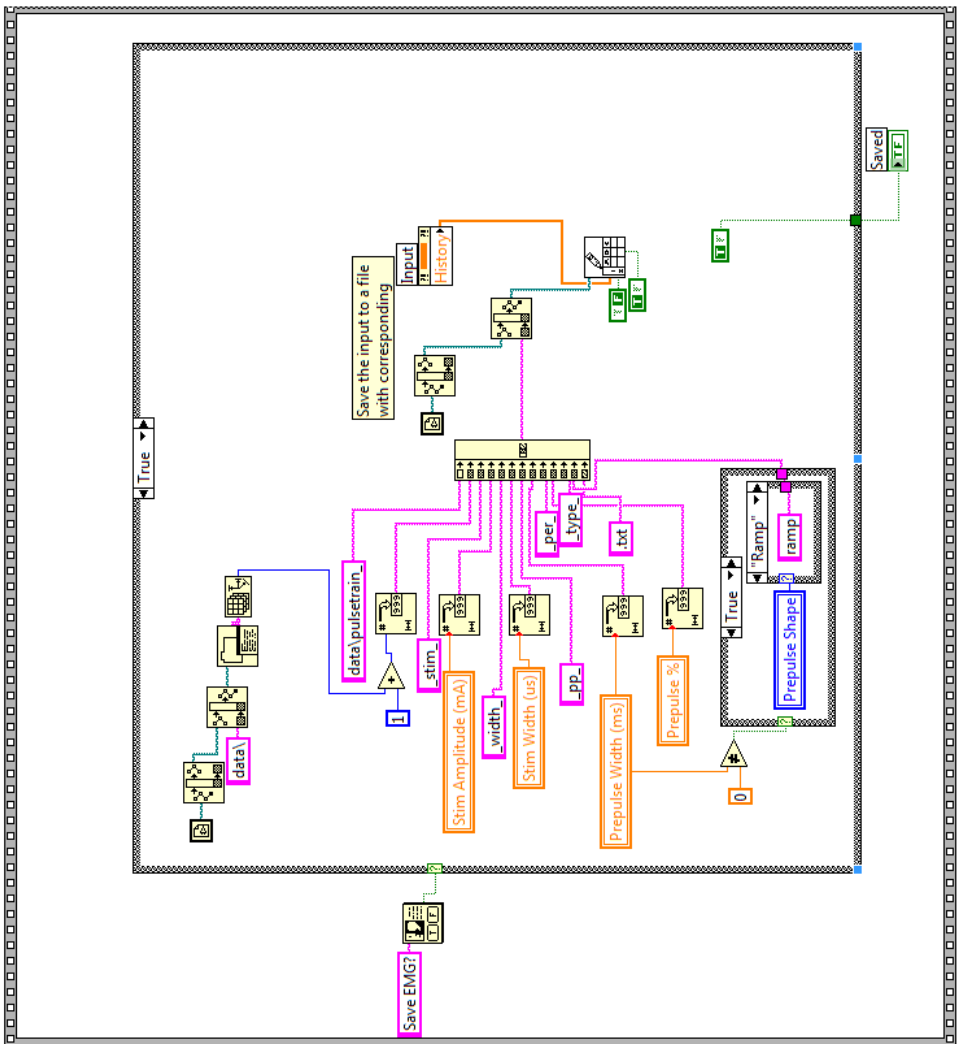

Figure A- 16 – Pulse train wiring diagram showing file saving stage

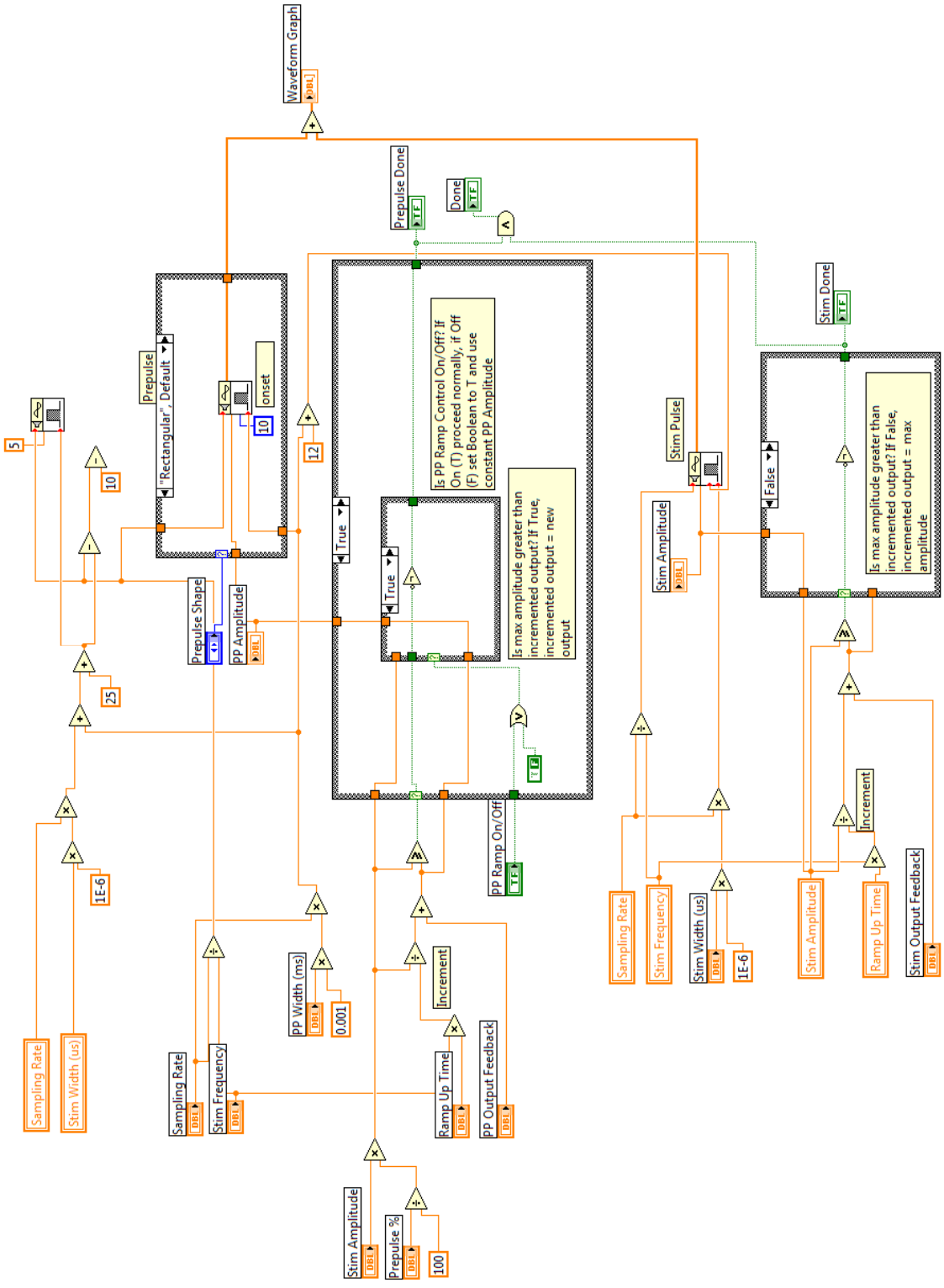

Figure A- 17 – Ramp up VI wiring diagram